

# Frequency and cardinality recovery from sketched data: a novel approach bridging Bayesian and frequentist views

Mario Beraha<sup>1</sup>, Stefano Favaro<sup>2</sup>, and Matteo Sesia<sup>3</sup>

<sup>1</sup>Department of Economics and Statistics, University of Torino

<sup>2</sup>Department of Economics and Statistics, University of Torino and  
Collegio Carlo Alberto

<sup>3</sup>Department of Data Sciences and Operations, University of Southern  
California

September 28, 2023

## Abstract

We study how to recover the frequency of a symbol in a large discrete data set, using only a compressed representation, or sketch, of those data obtained via random hashing. This is a classical problem in computer science, with various algorithms available, such as the count-min sketch. However, these algorithms often assume that the data are fixed, leading to overly conservative and potentially inaccurate estimates when dealing with randomly sampled data. In this paper, we consider the sketched data as a random sample from an unknown distribution, and then we introduce novel estimators that improve upon existing approaches. Our method combines Bayesian nonparametric and classical (frequentist) perspectives, addressing their unique limitations to provide a principled and practical solution. Additionally, we extend our method to address the related but distinct problem of cardinality recovery, which consists of estimating the total number of distinct objects in the data set. We validate our method on synthetic and real data, comparing its performance to state-of-the-art alternatives.

**Keywords:** cardinality recovery; frequency recovery; multi-view learning; nonparametric estimation; normalized random measures; random hashing; smoothed estimation; worst-case analysis.

# 1 Introduction

## 1.1 Background and motivations

A classical problem at the crossroad of computer science and information theory is to recover the empirical frequency of a given object in a large discrete data set, looking at those data only through the lenses of a (lossy) compressed representation with reduced memory footprint, or *sketch* (Misra and Gries, 1982; Alon et al., 1999; Manku and Motwani, 2002; Karp et al., 2003; Charikar et al., 2004; Cormode and Muthukrishnan, 2005). Sketches have been playing an important role in large-scale data science, with applications including: i) real-time analyses of massive data streams, ii) fast query processing based on large databases, iii) privacy preserving analyses, and iv) scalable machine learning. We refer to the monographs by Blum et al. (2020), Cormode and Yi (2020) and Medjedovic et al. (2022), for comprehensive reviews on sketching and its applications.

To give a formal definition of the frequency recovery problem, consider a sample  $(x_1, \dots, x_n)$ , for some  $n \geq 1$ , with each  $x_i$  taking a value in a (possibly infinite) alphabet  $\mathbb{S}$  of symbols. If  $n$  is very large, direct computations with the full data set may be unfeasible. Therefore, one may instead prefer to analyze a sketch of the data, which is typically obtained through random hashing (Mitzenmacher and Upfal, 2017, Chapter 5 and Chapter 15). A random hash function  $h : \mathbb{S} \rightarrow \{1, \dots, J\}$  with width  $J \geq 1$  maps each data point into one of  $J$  buckets, defining a sketch  $\mathbf{C}_J = (C_1, \dots, C_J)$  whose  $j$ -th element  $C_j$  is the number of  $x_i$ 's mapped into the  $j$ -th bucket:  $C_j = \sum_{1 \leq i \leq n} I[h(x_i) = j]$ , for all  $j \in [J] = \{1, \dots, J\}$ , where  $I[\cdot]$  is the indicator function. The problem is to estimate the number of occurrences of a symbol  $x_{n+1}$  (the *query*) in the sample, i.e.,

$$f_{x_{n+1}} = \sum_{i=1}^n I[x_i = x_{n+1}],$$

while looking only at  $\mathbf{C}_J$ . This task is challenging because distinct objects may be mapped into the same bucket, an event known as a *hash collision*. If  $n$  and the cardinality of  $\mathbb{S}$  are both larger than  $J$ , as it is typically the case in practice, then the hash collisions must be numerous, making exact recovery of the empirical frequency  $f_{x_{n+1}}$  impossible. Fortunately, though, it is possible to obtain useful estimates of  $f_{x_{n+1}}$  given  $\mathbf{C}_J$ .

A well-known algorithm to estimate  $f_{x_{n+1}}$  from  $\mathbf{C}_J$  is the count-min sketch (CMS) of Cormode and Muthukrishnan (2005), which provides a deterministic upper bound for  $f_{x_{n+1}}$  (Cormode and Yi, 2020, Chapter 3). In truth, the CMS allows the data to be sketched through multiple independent hash functions, but for simplicity we begin by focusing on a single hash function  $h$  and postpone the discussion of the more general problem. The CMS upper bound for  $f_{x_{n+1}}$  is remarkable for its simplicity and robustness, as it is valid for any sketched data set and for any query. However, this bound becomes loose if hash collisions are frequent. While it is also possible to bound  $f_{x_{n+1}}$  from below by using concentration inequalities that leverage the randomness in the hash function (Cormode and Yi, 2020, Chapter 3), the

problem remains that these classical techniques often lead to relatively uninformative confidence intervals because they pessimistically assume the data are fixed by an adversary (Ting, 2018). This challenge has recently motivated statistical approaches to the frequency recovery problem, under both the classical (frequentist) and Bayesian framework, by relying on the assumption that the data are a random sample from an unknown discrete distribution  $P$  on  $\mathbb{S}$ .

## 1.2 Strengths and limitations of the Bayesian approach

The work of Cai et al. (2018) was the first to develop a Bayesian nonparametric (BNP) approach to frequency recovery from the sketch  $\mathbf{C}_J$ . By modeling the data as a random sample  $(X_1, \dots, X_n)$  from the unknown  $P$ , they assumed a Dirichlet process prior for  $P$  (Ferguson, 1973). This approach leads to a learning-augmented version of the CMS endowed with a posterior distribution for  $f_{X_{n+1}}$ , given  $\mathbf{C}_J$  and the bucket  $h(X_{n+1})$  into which the query is hashed, which allows one to easily extract either a point estimate, e.g. posterior mean, mode and median, or a credible interval. See also Beraha and Favaro (2023). Unsurprisingly, the estimates tend to be more informative than the CMS upper bound if the modeling assumptions fit the data well. Unfortunately, though, this solution is not always applicable because the Dirichlet process cannot describe some essential patterns encountered in realistic data, including for example data with power-law tail behaviour, which are often observed in applications (Ferrer i Cancho and Solé, 2001; Zipf, 2016). This limitation has inspired further advancements in the BNP approach. In particular, Dolera et al. (2021, 2023) extended the approach of Cai et al. (2018) to accommodate more general prior distributions, while Beraha and Favaro (2023) investigated how to apply BNP techniques to deal with more general types of sketched data, such as feature and trait allocations. A difficulty encountered in those works is that the evaluation of posterior distributions, and hence of BNP estimators, is computationally expensive for priors other than the Dirichlet process.

## 1.3 Main contributions and organization of the paper

We develop a novel statistical approach to frequency recovery from sketched data that can be interpreted as a bridge between the current BNP view and a nonparametric classical (frequentist) view. Our approach borrows strength from both views to provide a principled and practical solution overcoming their distinct limitations. Modeling the data as a random sample  $(X_1, \dots, X_n)$  from an unknown distribution  $P$  on  $\mathbb{S}$ , we propose and study an estimator of  $f_{X_{n+1}}$  that relies on the conditional expectation of  $f_{X_{n+1}}$  given  $\mathbf{C}_J$  and  $h(X_{n+1})$ , here denoted by  $\varepsilon_f(P)$ . Section 2 begins by stating the problem, setting up the notation, and establishing a closed-form expression for  $\varepsilon_f(P)$ , as a function of the unknown  $P$ . Then, Section 2.3 proceeds to shed some new light on the fundamental difficulty of the estimation of  $f_{x_{n+1}}$  in a (fully) nonparametric setting, namely without any assumption on  $P$ . In particular, we prove that minimizing a suitable worst-case upper bound of the quadratic risk of  $\varepsilon_f(P)$ , with the minimization being taken over discrete distributions on  $\mathbb{S}$ , leads us back to the CMS upper bound, under some conditions on the support  $\mathbb{S}$  of  $P$ . As we

already know that the CMS estimator is often unsatisfactory in practice, our worst-case analysis suggests that making the sole assumption that the sketched data are a random sample from  $P$  is not sufficient in itself to effectively solve the frequency recovery problem. Stronger assumptions on  $P$  are therefore needed to overcome the limitation of the CMS.

While the BNP approach encodes these additional assumptions through the prior distribution for  $P$ , we propose in Section 3 a *smoothed estimation* approach leading to flexible estimators of  $f_{X_{n+1}}$ , which are much easier to compute compared to BNP estimators. In particular, we assume  $P$  to be a random element on the space of distributions on  $\mathbb{S}$ , whose distribution  $\mathcal{P}$  may depend on a low-dimensional “smoothing” parameter, and obtain an estimator of  $f_{X_{n+1}}$  by averaging the conditional expectation  $\varepsilon_f(P)$  with respect to  $\mathcal{P}$ . If  $P$  belongs to the broad class of normalized random measures (NRMs) (James, 2002; Prünster, 2002; Regazzini et al., 2003), the estimator is the expected value of a mixture of Binomial distributions, providing simple expressions under some special cases of  $\mathcal{P}$ , for which smoothing parameters can be fitted empirically from  $\mathbf{C}_J$ . Concretely, we focus on  $\mathcal{P}$  corresponding to the law of the Dirichlet process and the normalized generalized Gamma process (James, 2002; Pitman, 2003; Lijoi et al., 2007), which allow the tail behaviour of  $P$  to range from exponential tails to heavy power-law tails. Further, these smoothing distributions facilitate the comparison with the existing estimators in the BNP framework. In fact, our estimator is equivalent to the BNP estimator of Cai et al. (2018) under the Dirichlet process, whereas it enjoys significant computational advantages compared to the BNP estimators in Beraha and Favaro (2023) under the normalized generalized Gamma process.

Section 4 explains how to extend our approach to estimate the total number of distinct objects in the data set using the same sketch. This is the well-known *cardinality recovery* problem, for which there exist algorithmic solutions (Flajolet and Martin, 1983, 1985; Flajolet et al., 2007), but it has so far received relatively little attention in statistics compared to frequency recovery. To the best of our knowledge, the only work in this direction is that of Favaro and Sesia (2022), which proposed a BNP approach, encountering however some computational difficulties when dealing with priors other than the Dirichlet process. By contrast, our approach of smoothed estimation provides practical estimators under flexible modeling assumptions. Section 5 discusses how to extend our approach to combine information from sketches produced by multiple independent hash functions, as in the general setting of the CMS. After discussing some technical challenges arising from this extension, we propose a heuristic solution based on multi-view learning (Xu et al., 2013; Shankar et al., 2018; Li et al., 2018b). This works well in practice and shares some similarities with the BNP approach of Cai et al. (2018). Section 6 validates our methods empirically on both synthetic and real data, comparing their performance to that of algorithmic and BNP solutions. Finally, Section ?? concludes with a discussion. The Supplementary Material contains all appendices, which include proofs, additional methodological details, further comparisons with the related literature, and numerical results.

## 1.4 Related work

The CMS treats the data as fixed, computing estimates by leveraging the randomness in the hash functions. This approach can provide theoretical guarantees under minimal assumptions, but it tends to produce very conservative inferences when the data are randomly sampled from some distribution (Ting, 2018; Sesia et al., 2023). Indeed, the CMS can be recovered within our approach through a worst-case analysis over all possible discrete distributions on  $\mathbb{S}$ . Our work is more closely related to the BNP approach, which treats the data as a random sample from  $P$ , places a prior distribution on  $P$ , and obtain estimates from the posterior distribution of  $f_{X_{n+1}}$  given  $\mathbf{C}_J$ . Unfortunately, BNP estimators lead to nontrivial computational challenges for priors beyond the Dirichlet process, which limits their applicability (Beraha and Favaro, 2023). Our approach of smoothed estimation shares some similarities with the BNP approach, as it also specifies some assumptions for  $P$ , but it has the advantage of allowing practical estimators under flexible assumptions on  $P$ . More recently, Sesia and Favaro (2022) and Sesia et al. (2023) proposed a statistical approach to frequency recovery from  $\mathbf{C}_J$  based on conformal inference (Vovk, 2005). In particular, their goal is to provide uncertainty estimates, in the form of confidence intervals satisfying certain coverage guarantees, for frequency estimates computed by any *black-box* model or algorithm. As such, their work is orthogonal to ours. In fact, we can apply their techniques to endow our method with reliable uncertainty estimates, as demonstrated in Section 6.

## 2 Modeling assumptions and preliminary results

As previewed in Section 1, we consider a sample of  $\mathbb{S}$ -valued data points  $(x_1, \dots, x_n)$ , where  $\mathbb{S}$  indicates a (measurable) space of discrete objects. Data can only be observed through a sketch obtained by applying a  $J$ -wide random hash function  $h$ , for an integer  $J \geq 1$ . The hash function is assumed to be random and distributed according to a pairwise independent hash family  $\mathcal{H}_J$ . That is,  $h : \mathbb{S} \rightarrow \{1, \dots, J\}$  such that  $\Pr[h(x_1) = j_1, h(x_2) = j_2] = J^{-2}$  for any  $j_1, j_2 \in \{1, \dots, J\}$  and fixed  $x_1, x_2 \in \mathbb{S}$  such that  $x_1 \neq x_2$ . The pairwise independence of  $\mathcal{H}_J$ , also known as strong universality, implies uniformity, meaning that  $\Pr[h(x) = j] = J^{-1}$  for  $j = 1, \dots, J$ ; see Mitzenmacher and Upfal (2017, Chapter 5 and Chapter 15). Strong universality is a common and mathematically convenient assumption, although different settings may also be considered (Chung et al., 2013). Hashing the data through  $h$  produces a random vector  $\mathbf{C}_J \in \mathbb{N}_0^J$ , referred to as the sketch, whose  $j$ -th bucket is equal to

$$C_j = \sum_{i=1}^n I[h(x_i) = j],$$

for all  $j = 1, \dots, J$ , and such that  $\sum_{1 \leq j \leq J} C_j = n$ . The sketch  $\mathbf{C}_J$  is generally intended to have a (much) smaller memory footprint compared to the sample  $(x_1, \dots, x_n)$ , so it is expected that different data points may be mapped into the same bucket, resulting in a collision.

## 2.1 Modeling assumptions

Throughout the paper, we rely on the following modeling assumptions. Firstly,  $(x_1, \dots, x_n)$  is modeled as a random sample  $\mathbf{X}_n = (X_1, \dots, X_n)$  from an unknown discrete distribution  $P = \sum_{s \in \mathbb{S}} p_s \delta_s$  on  $\mathbb{S}$ , with  $p_s$  being the (unknown) probability of an object  $s \in \mathbb{S}$ . Secondly, the strong universal hash family  $\mathcal{H}_J$ , from which the function  $h$  is drawn, is independent of  $\mathbf{X}_n$ . Formally, for any  $n \geq 1$ ,

$$\begin{aligned} X_1, \dots, X_n &\stackrel{\text{iid}}{\sim} P, \\ h &\stackrel{\text{ind}}{\sim} \mathcal{H}_J, \\ C_j &= \sum_{i=1}^n I(h(X_i) = j), \quad \forall j \in [J]. \end{aligned} \tag{1}$$

Because of the independence between  $\mathcal{H}_J$  and  $\mathbf{X}_n$ , the model (1) implies that

$$\Pr[\mathbf{C}_J = \mathbf{c}] = \binom{n}{c_1, \dots, c_J} \prod_{j=1}^J q_j^{c_j}, \tag{2}$$

where  $q_j := \Pr[h(X_i) = j]$ , for any  $j \in [J]$ , and  $\sum_{1 \leq j \leq J} q_j = 1$ . That is,  $\mathbf{C}_J$  follows a Multinomial distribution with parameter  $(n, q_1, \dots, q_J)$ .

## 2.2 Preliminary results

Under the model defined in (1), the next theorem provides the conditional distribution of  $f_{X_{n+1}}$ , given the sketch  $\mathbf{C}_J$  and the bucket  $h(X_{n+1})$  in which  $X_{n+1}$  is hashed. This distribution will be the main building block of our approach for estimating the empirical frequency  $f_{X_{n+1}}$ .

**Theorem 1.** *For  $n \geq 1$ , let  $(x_1, \dots, x_n)$  be a sample modeled according to (1), and let  $\mathbf{C}_J = \mathbf{c}$  be the corresponding sketch. If  $\mathbb{S}_j := \{s \in \mathbb{S} : h(s) = j\}$ , for any  $j \in [J]$ , then the  $X_i$ 's that are hashed into the  $j$ -th bucket form a random sample from the unknown discrete distribution  $P_j = \sum_{s \in \mathbb{S}_j} \frac{p_s}{q_j} \delta_s$ . Furthermore, for any  $j \in [J]$  and any  $r \in \{0, 1, \dots, c_j\}$*

$$\pi_j(r; P) := \Pr[f_{X_{n+1}} = r \mid \mathbf{C}_J = \mathbf{c}, h(X_{n+1}) = j] = \binom{c_j}{r} \sum_{s \in \mathbb{S}_j} \left(\frac{p_s}{q_j}\right)^{r+1} \left(1 - \frac{p_s}{q_j}\right)^{c_j-r}. \tag{3}$$

See Appendix B.1.1 for the proof of Theorem 1. We consider estimating  $f_{X_{n+1}}$  through a suitable mean functional of the distribution (3). Because of the form of (3), the mean is the easiest functional to handle, as it involves computing the expected value of a Binomial distribution with parameter  $(c_j, p_s/q_j)$ . That is, we write

$$\varepsilon_f(P) := \mathbb{E}[f_{X_{n+1}} \mid \mathbf{C}_J = \mathbf{c}, h(X_{n+1}) = j] = \sum_{r=0}^{c_j} r \pi_j(r; P) = c_j \sum_{s \in \mathbb{S}_j} \left(\frac{p_s}{q_j}\right)^2, \tag{4}$$

which is a function of the unknown distribution  $P_j$ , induced from the distribution  $P$  through random hashing. According to (4), the size  $C_j$  of the bucket in which  $X_{n+1}$  is hashed provides a sufficient statistic to estimate  $f_{X_{n+1}}$ . Since  $\sum_{s \in \mathbb{S}_j} (p_s/q_j)^2$  is the probability that two elements taken at random from the  $j$ -th bucket are of the same symbol,  $\varepsilon_f(P)$  may be interpreted as a measure of the diversity in the composition of the  $j$ -th bucket. In particular, let  $M_{r,c_j}$  be the number of distinct symbols with frequency  $r$  in the  $j$ -th bucket, for any  $r \in [c_j]$ , such that  $K_{c_j} = \sum_{1 \leq r \leq c_j} M_{r,c_j}$  is the (total) number of distinct symbols in the  $j$ -th bucket and  $c_j = \sum_{1 \leq r \leq c_j} r M_{r,c_j}$ . Then, it is easy to show that

$$\varepsilon_f(P) = 1 + \frac{1}{c_j + 1} \sum_{r=1}^{c_j} r^2 \mathbb{E}_{P_j}[M_{r+1,c_j+1}], \quad (5)$$

providing  $\varepsilon_f(P)$  as a function of the  $M_{r,c_j}$ 's. See Appendix B.1.2 for the proof of Equation (5).

### 2.3 The difficulty of nonparametric estimation

The expressions for  $\varepsilon_f(P)$  allow us to highlight the difficulty of nonparametric estimation of the empirical frequency  $f_{X_{n+1}}$  from the sketch  $\mathbf{C}_J$ , showing how this is a nontrivial problem. From the expression for  $\varepsilon_f(P)$  in (5), the most classical moment-based strategy would consist in replacing  $\mathbb{E}_{P_j}[M_{r+1,c_j+1}]$  with its empirical counterpart, namely the number of distinct symbols with frequency  $r$  in the  $j$ -th bucket (Good, 1953; Robbins, 1956, 1968). However, such an empirical quantity is not available from the sketch  $\mathbf{C}_J$ , which only provides the number  $C_j$  of  $X_i$ 's that are hashed into the  $j$ -th bucket. Consequently, one must shift the focus to alternative strategies, possibly centered on minimizing quadratic risk within a well-suited class of estimators. Since  $C_j$  is a sufficient statistics for  $f_{X_{n+1}}$ , for any  $j \in [J]$ , it is intuitive to restrict our attention to estimators that depend on the sketched data only through  $C_j$ . Further, we focus for simplicity on a class of linear estimators in the form  $\hat{f}_\beta = c_j \beta$ , for  $\beta \geq 0$ . This class is inspired by the expression for  $\varepsilon_f(P)$  in (4), which corresponds to the ideal choice of  $\beta = \sum_{s \in \mathbb{S}_j} (p_s/q_j)^2$ . In general, the quadratic risk associated with the estimators in our class is

$$R(\hat{f}_\beta; P) = \mathbb{E}_P[(\beta C_{h(X_{n+1})} - f_{X_{n+1}})^2]. \quad (6)$$

The challenge is that (6) depends on the distribution  $P$ , which is unknown. There are two strategies for addressing this problem: a classical *minimax* analysis, and a *worst-case* analysis. We discuss both strategies below, starting from the more tractable worst-case analysis.

In a worst-case analysis, the goal is to minimize an upper bound  $\tilde{R}(\hat{f}_\beta) \geq R(\hat{f}_\beta; P)$  for all distributions  $P$  within a suitable family  $\mathcal{P}$ , which leads to a *worst-case optimal* estimator  $\beta$  solving  $\min_\beta \tilde{R}(\hat{f}_\beta)$ . This approach draws inspiration from works by Painsky (2022a,b,c), which applied similar techniques to address a different problem. We focus on a broad class of distributions with a bounded number of support points:  $\mathcal{P}_L := \{P : P \text{ has at most } L \text{ support points}\}$ . While the technical details of this analysis are somewhat involved, and therefore deferred to Appendix B.2, the final result is intuitive to explain.

**Theorem 2** (Informal statement). For  $n \geq 1$ , let  $(x_1, \dots, x_n)$  be a sample modeled according to (1), and let  $\mathbf{C}_J = \mathbf{c}$  be the corresponding sketch. For  $L$  large enough, the worst-case optimal estimator of  $f_{X_{n+1}}$ , over the class  $\mathcal{P}_L$  for the risk defined in (6), is  $\hat{f}_\beta \equiv C_{h(X_{n+1})}$ . Moreover, the upper bound  $\tilde{R}(\hat{f}_\beta)$  is tight and it is achieved by  $P \equiv P^*$ , where  $P^*$  is a degenerate distribution that places all probability mass on a single symbol  $s^* \in \mathbb{S}$ .

A more rigorous statement of Theorem 2 is presented in Appendix B.2, along with its proof. At first sight, this result may seem disappointing because it gives a worst-case optimal estimator identical to the original CMS upper bound (see Appendix A.2), and that is already known to be often unsatisfactory in practice. However, Theorem 2 is interesting because the tightness of the analysis highlights the inherent complexity of our nonparametric estimation problem—it is not possible to obtain a more informative worst-case estimator.

The classical minimax analysis consists of solving  $\inf_\beta \sup_{P \in \mathcal{P}} R(\hat{f}_\beta; P)$ , where  $\mathcal{P}$  is an appropriate family of discrete distributions that will be specified below. Estimators  $\hat{f}_\beta$  solving this minimax problem are termed *minimax optimal*, and the corresponding  $\hat{P}$  is the *minimax worst* distribution. Unfortunately, a minimax analysis poses substantial challenges in our case, resulting in the absence of analytical results. Specifically, the main difficulty is that verifying whether a given pair  $(\beta, P)$  solves the minimax problem is NP-hard (Daskalakis et al., 2021). Therefore, we present instead in Appendix B.3 a detailed numerical investigation of the minimax analysis over the class  $\mathcal{P}_L$  previously considered. The results of this study suggest that the minimax optimal estimator is  $\hat{f}_\beta = c_j J/L$ , which is associated with the (minimax-worst) uniform distribution.

In summary, the worst-case analysis and the classical minimax analysis yield antithetical estimators that seem however both equally unsatisfactory in practice: the former mirrors the original CMS upper bound, while the latter tends to trivially estimate  $f_{X_{n+1}}$  as 0 as the latent support size  $L$  of the data distribution is allowed to grow, irrespective of the information contained in the data sketch. This conclusion suggests that additional assumptions regarding the unknown distribution  $P$  are necessary in order to attain more meaningful estimates. Therefore, we propose in the following section the approach of *smoothed estimation*. This approach is based on the idea of averaging the expressions found in Section 2.2 across a family of “plausible” nonparametric distributions, which are characterized by a low-dimensional parameter.

## 3 Smoothed frequency estimation

### 3.1 Outline of our approach

Smoothed estimation can lead to more informative approximations of the empirical frequency  $f_{X_{n+1}}$ , leveraging some assumptions about the unknown distribution  $P$  on  $\mathbb{S}$ . What makes this task nontrivial is that the expression for  $\varepsilon_f(P)$  in (4) depends on the distribution  $P_j$  on  $\mathbb{S}_j$  induced through random hashing, not on the distribution  $P$  of interest. Therefore, our approach requires one to specify  $P$  carefully, in such a



way as to ensure that the bucket-restricted distributions  $P_j$ 's induced from  $P$  are also well-defined and mathematically tractable. This is not an easy problem to address by placing parametric assumptions on  $P$  directly, but it can be solved via a suitable nonparametric assumption. In particular, we propose to treat the distribution  $P$  as a random element from the space of discrete probability distributions on  $\mathbb{S}$ , modeling instead its distribution  $\mathcal{P}$  through a low-dimensional smoothing parameter. Among the many possible ways to specify a distribution for  $P$ , we consider the broad class of normalized random measures (NRMs) (James, 2002; Prünster, 2002; Pitman, 2003; Regazzini et al., 2003; Lijoi and Prünster, 2010). This choice was inspired by related prior work on BNP estimators for  $f_{X_{n+1}}$  (Cai et al., 2018; Dolera et al., 2021, 2023), and it is useful because it leads to an explicit expression for the expected value of  $\varepsilon_f(P)$  with respect to the smoothing distribution  $\mathcal{P}$ , which gives us a practical estimator of  $f_{X_{n+1}}$ . Further, NRMs make it possible to estimate empirically the smoothing parameters from the sketch  $\mathbf{C}_J$ , as explained in Section 3.7. Until then, we will assume that the smoothing parameters are known.

### 3.2 Background on normalized random measures

Consider a completely random measure (CRM)  $\tilde{\mu}$  on  $\mathbb{S}$ , which is defined as a random measure, with values on the space of bounded discrete measures on  $(\mathbb{S}, \mathcal{S})$ , such that for  $k \geq 1$  and for a collection of disjoint Borel sets  $A_1, \dots, A_k \in \mathcal{S}$  the random variables  $\tilde{\mu}(A_1), \dots, \tilde{\mu}(A_k)$  are independent (Kingman, 1967). We focus on CRMs of the form

$$\tilde{\mu}(\cdot) = \int_{\mathbb{R}_+} x \tilde{N}(dx, \cdot) = \sum_{k \geq 1} J_k \delta_{S_k}(\cdot),$$

where  $\tilde{N} = \sum_{k \geq 1} \delta_{(J_k, S_k)}$  is a Poisson random measure on  $\mathbb{R}_+ \times \mathbb{S}$  with Lévy intensity  $\nu(dx, ds)$ , which characterizes the distribution of  $\tilde{\mu}$  (Kingman, 1967, 1993). We consider in particular Lévy intensities of the form  $\nu(dx, ds) = \theta G_0(ds) \rho(x) dx$  where  $\theta > 0$  is a parameter,  $G_0$  is a non-atomic probability measure on  $\mathbb{S}$ , and  $\rho(x) dx$  is a measure on  $\mathbb{R}_+$  such that  $\int_{\mathbb{R}_+} \rho(x) dx = +\infty$  and  $\psi(u) = \int_{\mathbb{R}_+} (1 - e^{-ux}) \rho(x) dx < +\infty$  for all  $u > 0$ , ensuring the total mass  $T = \tilde{\mu}(\mathbb{S})$  of  $\tilde{\mu}$  is positive and almost-surely finite (Pitman, 2003; Regazzini et al., 2003). Then, an NRM on  $\mathbb{S}$  with parameter  $(\theta, G_0, \rho)$  is defined as follows:

$$P(\cdot) = \frac{\tilde{\mu}(\cdot)}{T} = \sum_{k \geq 1} \frac{J_k}{T} \delta_{S_k}(\cdot),$$

where the distribution of the probabilities  $(J_k/T)_{k \geq 1}$  is directed by  $\rho$ , and the locations  $(S_k)_{k \geq 1}$  are i.i.d. from  $G_0$ , independent of  $(J_k/T)_{k \geq 1}$ . In short, we write  $P \sim \text{NRM}(\theta, G_0, \rho)$ .

### 3.3 Smoothed estimation with normalized random measures

Returning to the problem of estimating  $f_{X_{n+1}}$  from the sketch  $\mathbf{C}_J$ , we leverage smoothing assumptions for the distribution  $P$  as follows. We consider the smoothing assumption  $P \sim \text{NRM}(\theta, G_0, \rho)$ , and estimate  $f_{X_{n+1}}$  by taking the expected value

of  $\varepsilon_f(P)$  with respect to the law of  $P$ . It follows from (4) that, in order to compute  $\varepsilon_f(P)$ , it suffices to evaluate

$$\pi_j(r) := \mathbb{E}_{P \sim \text{NRM}(\theta, G_0, \rho)}[\pi_j(r; P)],$$

for all  $j \in [J]$ . Each  $\pi_j(r)$  can be computed by exploiting the Poisson process representation of NRMs and the Poisson coloring theorem (Kingman, 1993, Chapter 5). In particular, this can be achieved by applying the following *restriction property* of NRMs. Suppose  $P$  is a NRM and, for any Borel set  $A \in \mathcal{S}$ , let  $P_A$  denote the random probability measure on  $A$  induced by  $P \sim \text{NRM}(\theta, G_0, \rho)$ ; i.e., the renormalized restriction of  $P$  to the set  $A$ . Then,  $P_A \sim \text{NRM}(\theta G_0(A), G_{0,A}/G_0(A), \rho)$ , where  $G_{0,A}$  is the restriction of the probability measure  $G_0$  to  $A$ . Combined with the strong universality of the hash family  $\mathcal{H}_J$  and the independence of  $\mathcal{H}_J$  from  $P$ , the restriction property of  $P$  implies that

$$P_j \sim \text{NRM}\left(\frac{\theta}{J}, JG_{0, \mathbb{S}_j}, \rho\right). \quad (7)$$

That is, for any  $j \in [J]$ , if  $P \sim \text{NRM}(\theta, G_0, \rho)$ , then the distribution  $P_j$  on  $\mathbb{S}_j$  induced by the random hashing still belongs to the same class of NRMs, and its parameter  $\theta$  is rescaled by the total number of buckets  $J$ . This peculiar property of NRMs is critical to compute  $\pi_j(r)$ .

**Theorem 3.** *For  $n \geq 1$ , let  $(x_1, \dots, x_n)$  be a sample modeled according to (1), and let  $\mathbf{C}_J = \mathbf{c}$  be the corresponding sketch. If  $P \sim \text{NRM}(\theta, G_0, \rho)$ , then for any  $j \in [J]$  and  $r \in \{0, 1, \dots, c_j\}$ ,*

$$\pi_j(r) = \int_0^1 \text{Binomial}(r; c_j, v) f_{V_j}(v) dv, \quad (8)$$

where

$$f_{V_j}(v) = \frac{\theta}{J} v \int_0^{+\infty} t \rho(tv) f_{T_j}(t(1-v)) dt. \quad (9)$$

Above,  $f_{T_j}$  is the density function of the total mass of a CRM with Lévy intensity  $\theta G_{0, \mathbb{S}_j}(ds) \rho(x) dx$ .

See Appendix B.4.1 for the proof of Theorem 3. We will take this result as a starting point to derive explicit estimators for some special examples of NRMs. In particular, Section 3.4 will focus on the Dirichlet process (DP) (Ferguson, 1973) and Section 3.5 on the normalized generalized Gamma process (NGGP) (James, 2002; Prünster, 2002; Pitman, 2003; Lijoi et al., 2007). These smoothing assumptions are interesting because they allow for modeling distributions  $P$  with a flexible tail behaviour, ranging from geometric tails to heavy power-law tails, and they lead to simple expressions for estimators that can be directly related to existing approaches in the BNP framework.

### 3.4 Smoothing with the Dirichlet process

The DP is arguably the most popular NRM, and it is obtained by normalizing the Gamma process (Ferguson, 1973). The latter is a CRM with Lévy intensity

$$\nu(dx, ds) = \theta G_0(ds) \frac{e^{-x}}{x} dx. \quad (10)$$

By assuming the law of the DP as a smoothing distribution, here denoted as  $P \sim \text{DP}(\theta, G_0)$ , it follows from Theorem 3 that  $\pi_j(r)$  is the probability mass in (8) corresponding to the distribution of  $V_j$  obtained by combining (9) with (10). In particular, this leads to

$$V_j = V_\theta := B_{1, \theta/J}, \quad (11)$$

where  $B_{1, \theta/J}$  is a beta random variable with parameters  $(1, \theta/J)$ . Then, for any  $j \in [J]$  and  $r \in \{0, 1, \dots, c_j\}$ ,

$$\pi_j(r) = \int_0^1 \binom{c_j}{r} v^r (1-v)^{c_j-r} f_{V_\theta}(v) dv = \binom{c_j}{r} \frac{\theta}{J} \frac{\Gamma(r+1) \Gamma(\theta/J + c_j - r)}{\Gamma(\theta/J + c_j + 1)}, \quad (12)$$

which corresponds to a Beta-Binomial distribution with parameter  $(c_j, 1, \theta/J)$ . See Appendix B.4.2 for the proof of Equation (11). By applying the result in (12), the next proposition gives an explicit and simple estimator of  $f_{X_{n+1}}$  under the DP smoothing assumption.

**Proposition 4.** *For  $n \geq 1$ , let  $(x_1, \dots, x_n)$  be a sample modeled according to (1), and let  $\mathbf{C}_J = \mathbf{c}$  be the corresponding sketch. If  $P \sim \text{DP}(\theta, G_0)$ , for some  $\theta$ , it follows that*

$$\hat{f}_{X_{n+1}}^{(\text{DP})} := \mathbb{E}_{P \sim \text{DP}(\theta, G_0)}[\varepsilon_f(P)] = c_j \frac{J}{\theta + J}. \quad (13)$$

See Appendix B.4.3 for the proof of Proposition 4. The smoothed frequency estimator in (13) is a linear function of  $c_j$ . In particular, it multiplies  $c_j$  by a weight inversely proportional to the smoothing parameter  $\theta$ , which can be understood as follows. Higher values of  $\theta$  correspond to a larger number of distinct symbols in the random sample  $\mathbf{X}_n$  (Ferguson, 1973). In turn, that results in a larger number of expected hash collisions, which inflates  $c_j$  relative to the true frequency  $f_{X_{n+1}}$ .

Interestingly, the estimator in (13) converges to the CMS estimator as  $\theta \rightarrow 0$ . This behaviour is consistent with the worst-case analysis presented in Section 2.3. Indeed, if  $\theta$  is small,  $P \sim \text{DP}(\theta, G_0)$  becomes close to a degenerate distribution with only one support point, that is, the distribution identified in Theorem 2.

Further, the estimator in (13) coincides with the BNP estimator obtained under the DP prior by Cai et al. (2018), which we denote as  $\varepsilon_f(\text{DP}(\theta, G_0))$  for convenience, despite having been derived through a different approach. That is, it holds true that

$$\hat{f}_{X_{n+1}}^{(\text{DP})} = \varepsilon_f(\text{DP}(\theta, G_0)). \quad (14)$$

This identity follows from the fact that the Beta-Binomial distribution (12) coincides with the posterior distribution of  $f_{X_{n+1}}$ , given  $\mathbf{C}_n$  and  $h(X_{n+1})$ ; see Cai et al. (2018, Proposition 1). The next theorem characterizes the DP as the sole NRM for which smoothed estimation and the BNP approach lead to the same estimator for  $f_{X_{n+1}}$ .

**Theorem 5.** Let  $\hat{f}_{X_{n+1}}^{(NRM)}$  be the smoothed estimator under the model (1) obtained with  $P \sim NRM(\theta, G_0, \rho)$ , and let  $\varepsilon_f(NRM(\theta, G_0, \rho))$  be the BNP estimator under the model (32) with  $P \sim NRM(\theta, G_0, \rho)$ . Then,  $\hat{f}_{X_{n+1}}^{(NRM)} = \varepsilon_f(NRM(\theta, G_0, \rho))$  if and only if the NRM is the DP.

See Appendix B.4.4 for a proof of Theorem 5. We also refer to Appendix A.1 for a detailed review of the relevant BNP framework, and for a more careful discussion of the relation between smoothed estimation and the BNP approach.

We conclude this section by remarking that Theorem 5 motivates the work presented in the next section, which derives an explicit expression for  $\pi_j(r)$  by using a smoothing distribution that is not the law of the DP. Theorem 5 suggests that such an approach should lead to a novel estimator of  $f_{X_{n+1}}$  compared to the existing BNP literature, and indeed that turns out to be the case.

### 3.5 Smoothing with the normalized generalized Gamma process

The NGGP is one of the most popular generalization of the DP. Recall that the NGGP is obtained by normalizing the generalized Gamma process (Brix, 1999), which is a CRM with Lévy intensity

$$\nu(dx, ds) = \theta G_0(ds) \frac{1}{\Gamma(1-\alpha)} x^{-1-\alpha} e^{-\tau x} dx, \quad (15)$$

for any  $\alpha \in [0, 1)$  and  $\tau > 0$ . Under the parameterization  $\alpha = 0$  and  $\tau = 1$ , the NGGP reduces to the DP as the Lévy intensities in (15) and in (10) become equivalent.

By assuming the law of the NGGP as a smoothing distribution, here denoted as  $P \sim NGGP(\theta, G_0, \alpha, \tau)$ , Theorem 3 implies that  $\pi_j(r)$  is the probability mass in (8) corresponding to the distribution of  $V_j$  obtained by combining (9) with (15). In particular, this leads to

$$V_j = V_{\theta, \alpha, \tau} := B_{1-\alpha, \alpha} \left( 1 - \left( \frac{\frac{\theta \tau^\alpha}{J\alpha}}{\frac{\theta \tau^\alpha}{J\alpha} + E} \right)^{1/\alpha} \right) \quad (16)$$

where  $B_{1-\alpha, \alpha}$  is a Beta random variable with parameter  $(1-\alpha, \alpha)$ , and  $E$  is an independent negative Exponential random variable with parameter 1. Therefore, for any  $j \in [J]$  and  $r \in \{0, 1, \dots, c_j\}$ ,

$$\pi_j(r) = \int_0^1 \binom{c_j}{r} v^r (1-v)^{c_j-r} f_{V_{\theta, \alpha, \tau}}(v) dv, \quad (17)$$

which is a generalization of the Beta-Binomial distribution introduced in (12). See Appendix B.4.5 for the proof of Equation (16). By applying the result in (17), the next proposition gives an explicit and simple estimator of  $f_{X_{n+1}}$  under the NGG smoothing assumption.

**Proposition 6.** For  $n \geq 1$ , let  $(x_1, \dots, x_n)$  be a sample modeled according to (1), and let  $\mathbf{C}_J = \mathbf{c}$  be the corresponding sketch. If  $P \sim \text{NGGP}(\theta, G_0, \alpha, \tau)$ , for some  $(\theta, \alpha, \tau)$  it follows that

$$\hat{f}_{X_{n+1}}^{(\text{NGGP})} := \mathbb{E}_{P \sim \text{NGGP}(\theta, G_0, \alpha, \tau)}[\varepsilon_f(P)] = c_j(1 - \alpha) \left( 1 - \frac{\theta\tau^\alpha}{J\alpha} e^{\frac{\theta\tau^\alpha}{J\alpha}} E_{1/\alpha} \left( \frac{\theta\tau^\alpha}{J\alpha} \right) \right), \quad (18)$$

where  $E_{1/\alpha}(z) = \int_1^{+\infty} x^{-1/\alpha} e^{-zx} dx$  denotes the exponential integral function of index  $1/\alpha$ .

See Appendix B.4.6 for the proof of Proposition 6. Similar to the estimator obtained in Proposition 4, the smoothed frequency estimator in (18) also applies a linear shrinkage to  $c_j$ . In particular, the expression in (18) is decreasing in the smoothing parameters  $\theta$ ,  $\tau$ , and  $\alpha$ . This is again intuitive because the expected number of distinct symbols in the random sample  $\mathbf{X}_n$  is an increasing function of these parameters (Lijoi et al., 2007).

In the special case of  $\alpha = 0$  and  $\tau = 1$ , Proposition 6 reduces to Proposition 4, as the NGGP reduces to the DP. This equivalence also can be seen by looking at the random variable  $V_{\theta, \alpha, \tau}$  in (16), since

$$\lim_{\alpha \rightarrow 0} V_{\theta, \alpha, 1} = 1 - e^{-\frac{J}{\theta} E} \stackrel{d}{=} B_{1, \theta/J},$$

where  $B_{1, \theta/J}$  is the beta random variable in (11).

A more interesting case is that of  $\alpha = 1/2$ , which corresponds to a special NGGP known as the normalized inverse Gaussian process (NIGP) (Lijoi et al., 2005, 2007; Favaro et al., 2012). In general, the smoothing parameter  $\alpha \in [0, 1)$  controls the tail behaviour of the distribution  $P$ : the larger  $\alpha$ , the heavier the tail (Pitman, 2003; Lijoi et al., 2007). Therefore, the NGGP allows us to capture flexible tail behaviours for the distribution of the data, ranging from the geometric tails of the DP to the heavy power-law tails, which are often observed in applications.

We conclude this section with some remarks about the connection between the smoothed frequency estimators obtained in Proposition 4 and Proposition 6, and the estimators obtained with the BNP approach (Cai et al., 2018; Beraha and Favaro, 2023). As noted by Beraha and Favaro (2023), the use of prior distributions other than the DP, including for example other NRMs, leads to computationally challenging BNP estimators for the empirical frequency  $f_{X_{n+1}}$ . In particular, the computational cost associated with the BNP estimator under an NGGP scales exponentially in both  $J$  and in  $n$ ; we refer to Beraha and Favaro (2023, Section 2.3) for a detailed discussion on these computational issues. This is a critical limitation of the BNP approach to frequency recovery, whose practical relevance thus remains more limited to the special case of the DP prior. By contrast, the advantage of the approach of smoothed estimation is that it allows one to leverage much more flexible models from the broader class of NRMs and still obtain tractable estimators that can be written in terms of expectations of mixtures of binomial distributions.

### 3.6 Smoothing distributions beyond the normalized generalized Gamma process

It is natural at this point to wonder whether it might be worth to also seek alternative smoothing distributions beyond those studied in Sections 3.4 and 3.5, specifically by applying Theorem 3 with other NRMs. See Lijoi and Prünster (2010) and references therein for some concrete examples of NRMs beyond the NGGP. To address this question, we point out that the use of other NRMs may lead to less explicit distributions for the random variable  $V_j$  in Theorem 3, which is likely to significantly complicate the estimation of  $f_{X_{n+1}}$  in practice. Fortunately, though, the NGGP already offers a reasonable trade-off between the flexibility of the smoothing assumption, in terms of enabling a flexible tail behaviour, and its tractability, in terms of leading to a distribution for  $V_j$  that can be evaluated easily.

To highlight visually the advantages of the NGGP, we plot in Figure 1 the probability  $\pi_j(r)$  computed under different choices of the smoothing parameters  $\theta$  and  $\alpha$ , assuming  $\tau = 1$ . The power of the NGGP smoothing assumption can be evinced by comparing the relatively flexible behaviour of  $\pi_j(r)$ , for different choices of  $\theta$  and  $\alpha$ , to the much more constrained behaviour corresponding to the DP smoothing assumption, which limits  $\pi_j(r)$  to be either monotonically increasing or decreasing.

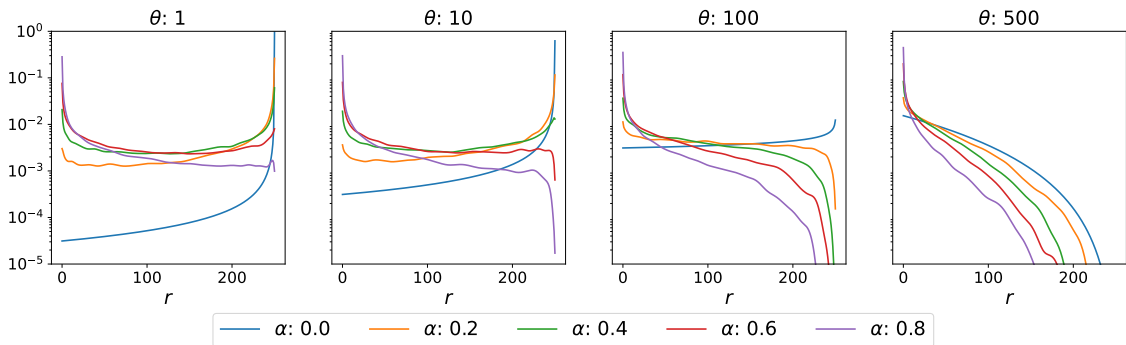


Figure 1: Visualization of the modelling flexibility of the NGGP. The probabilities  $\pi_j(r)$  are plotted as a function of  $r$  for  $c_j = 250$ , for different values of the NGGP smoothing parameters. Different panels focus on different values of  $\theta$ , while the curves drawn in different colors correspond to alternative values of  $\alpha$ . In all cases,  $\tau = 1$ .

### 3.7 Empirical estimation of smoothing parameters

We turn now to the problem of estimating the smoothing parameters from the sketch  $\mathbf{C}_J$ . The NRM smoothing assumption requires specifying the parameter  $\theta > 0$  and a collection of parameters, here denoted by  $\xi$ , introduced by the specification of  $\rho$  in the Lévy intensity of the NRM. For instance, the specification of the Lévy intensity of the NGGP implies that  $\xi = (\alpha, \tau)$ . An intuitive strategy, previously also adopted by Cai et al. (2018) within the BNP approach, consists to maximize the marginal likelihood of the sketch. In particular, one could seek to optimize, with respect to

$(\theta, xi)$ , the marginal likelihood

$$L(\theta, \xi; \xi) = \mathbb{E}_{P \sim \text{NRM}(\theta, G_0, \rho)}[\text{Pr}[\mathbf{C}_J = \mathbf{c}; P]], \quad (19)$$

where  $\text{Pr}[\mathbf{C}_J = \mathbf{c}; P]$  is defined as in (2), with the dependence on the distribution  $P$  now made explicit.

A tractable closed-form expression of (19) is available in the special case of the DP smoothing assumption (Cai et al., 2018), as detailed in Appendix E. To the best of our knowledge, it is not possible to compute a closed-form expression of (19) for more general NGGP smoothing assumptions (Pitman, 2003; Lijoi and Prünster, 2010). The only exception may be when  $\alpha = 1/2$ , which corresponds to the NIGP. In that case, (19) can be computed by relying on the definition of the NIGP presented in Lijoi et al. (2005, Section 3.1), although such an approach results in a complicated expression involving Bessel functions (Dolera et al., 2021). For these reasons, we propose two alternative strategies to estimate smoothing parameters.

The first strategy is relatively efficient from a computational perspective, but it can only be applied if one has direct access to a subset of the original (un-sketched) data. This approach is inspired by the work of Sesia and Favaro (2022), which utilized a similar solution for a somewhat different purpose. The key idea is that, if one can store the first  $m < n$  samples in memory before sketching the rest of the data, which is an assumption that is sometimes realistic, then the smoothing parameter  $(\theta, \xi)$  can be estimated by maximizing the marginal likelihood of the observed data, which tends to be a more tractable quantity compared to the marginal likelihood of the sketch. We refer to Appendix E.2 for further details on this approach.

The second strategy to estimate  $(\theta, \xi)$  was originally proposed by Dolera et al. (2023) and it is more widely applicable, because it only requires access to the sketched data, but it is also more computationally expensive. The key idea is to simulate synthetic data based on a smoothing distribution given the smoothing parameter  $(\theta, \xi)$ , apply the hash function to produce a sketch of them, and then optimize the choice of  $(\theta, \xi)$  in such a way as to minimize the 1-Wasserstein distance between the empirical distribution of the synthetic sketch and the observed sketch. This minimum-distance approach is explained more carefully in Appendix E.2, where we provide some implementation details for the special case of NGGP smoothing assumption, and also outline some convenient computational shortcuts.

## 4 Cardinality estimation

The results presented in Sections 2 and 3 can be extended to also address the distinct problem of cardinality recovery. To describe this problem, consider the usual sample of  $\mathbb{S}$ -valued data points  $(x_1, \dots, x_n)$ , for  $n \geq 1$ , and let  $\mathbf{C}_j$  be a sketch of the  $x_i$ 's obtained through a random hash function  $h$  from the strong universal family  $\mathcal{H}_j$ . The goal is then to estimate the number of distinct symbols in the sample, i.e.,

$$k_n := |\{x_1, \dots, x_n\}|,$$

where  $|\cdot|$  denotes the cardinality of a set. This problem may be considered to be complementary to that of frequency estimation but, as we shall see, it can be addressed using the same data sketch.

Cardinality recovery has already received considerable attention in diverse applications, including spam detection (Becchetti et al., 2006), text mining (Broder, 2000), genomics (Breitwieser et al., 2018), and database management (Halevy et al., 2016). A classical approach is based on the hyperloglog algorithm (Flajolet and Martin, 1983, 1985; Flajolet et al., 2007), which may be described as an analogous of the CMS for frequency recovery. While the hyperloglog uses random hashing to sketch the data differently compared to the CMS (Cormode and Yi, 2020), we will show that many of the concepts and techniques developed in Sections 2 and 3 can be adapted quite naturally to address the cardinality recovery problem. At the same time, however, we will see that cardinality recovery raises some additional technical challenges.

## 4.1 Preliminary results

We assume  $(x_1, \dots, x_n)$  to be a random sample from the model defined in (1), and we consider estimating the number  $K_n$  of distinct symbols in  $\mathbf{X}_n$  through the conditional expectation of  $K_n$  given the sketch  $\mathbf{C}_J$ . Let  $M_{r,n}$  be the number of distinct symbols with frequency  $r$  in  $\mathbf{X}_n$ , for  $r = 1, \dots, n$ , such that  $K_n = \sum_{1 \leq r \leq n} M_{r,n}$  and  $n = \sum_{1 \leq r \leq n} r M_{r,n}$ . If  $\mathcal{M}_{n,J}$  is the domain (support) of the conditional distribution of  $\mathbf{M}_n = (M_{1,n}, \dots, M_{n,n})$  given  $\mathbf{C}_J$ , then by the law of total probability, for any  $r \in \{0, 1, \dots, c_j\}$ ,

$$\Pr[f_{X_{n+1}} = r \mid \mathbf{C}_J = \mathbf{c}] = \sum_{\mathbf{m} \in \mathcal{M}_{n,J}} \Pr[f_{X_{n+1}} = r \mid \mathbf{M}_n = \mathbf{m}] \Pr[\mathbf{M}_n = \mathbf{m} \mid \mathbf{C}_J = \mathbf{c}], \quad (20)$$

where  $\mathbf{p}_{r,n} := \Pr[f_{X_{n+1}} = r \mid \mathbf{M}_n = \mathbf{m}]$  is the conditional probability that  $X_{n+1}$  is a symbol with frequency  $r$  in  $\mathbf{X}_n$ . This is known as the  $r$ -order coverage of  $\mathbf{X}_n$  (Good, 1953). Furthermore, writing the conditional expectation of  $K_n$  given the sketch as

$$\varepsilon_k(P) := \mathbb{E}_P[K_n \mid \mathbf{C}_J = \mathbf{c}] = \sum_{r=0}^{n-1} \mathbb{E}_P[M_{r+1,n} \mid \mathbf{C}_J = \mathbf{c}] \quad (21)$$

and replacing  $\mathbf{p}_{r,n}$  in (20) with any estimate that is linear in  $m_{r+1}$ , we have that  $\varepsilon_k(P)$  can be expressed as a linear function of  $\Pr[f_{X_{n+1}} = r \mid \mathbf{C}_J = \mathbf{c}]$ . The latter probability is available from Theorem 1 by marginalizing (3) over  $h_{X_{n+1}}$ . See Appendix C.1.1 for further details.

The next proposition gives  $\varepsilon_k(P)$  in (21) by making use of the Good-Turing estimate of  $\mathbf{p}_{r,n}$  (Good, 1953), which arguably is the sole nonparametric estimate of  $\mathbf{p}_{r,n}$  to be a linear function of  $m_{r+1}$ .

**Proposition 7.** *For  $n \geq 1$ , let  $(x_1, \dots, x_n)$  be a sample modeled according to (1), and let  $\mathbf{C}_J = \mathbf{c}$  be the corresponding sketch. If  $\hat{\mathbf{p}}_{r,n}$  is the Good-Turing estimate of  $\mathbf{p}_{r,n}$ , i.e.,*

$$\hat{\mathbf{p}}_{r,n} = (r+1) \frac{m_{r+1}}{n},$$

then

$$\varepsilon_k(P) = n \sum_{j=1}^J q_j \sum_{r=0}^{c_j} \frac{1}{r+1} \pi_j(r; P) = n \sum_{j=1}^J \frac{q_j}{c_j+1} \sum_{s \in \mathbb{S}_j} \left( 1 - \left( 1 - \frac{p_s}{q_j} \right)^{c_j+1} \right). \quad (22)$$



See Appendix C.1.2 for the proof of Proposition 7. Similarly to  $\varepsilon_f(P)$  in the context of frequency recovery, the conditional expectation  $\varepsilon_k(P)$  is a functional of the unknown distribution  $P_j$  on  $\mathbb{S}_j := \{s \in \mathbb{S} : h(s) = j\}$ , induced from the distribution  $P$  through random hashing. However, a notable difference between  $\varepsilon_f(P)$  and  $\varepsilon_k(P)$  is that the latter involves all  $C_j$ 's, and it also depends on the unknown probability  $q_j := \Pr[h(X_i) = j]$ , which must be estimated from  $\mathbf{C}_J$ .

An intuitive plug-in estimate of  $q_j$  may be obtained by exploiting the fact that  $\mathbf{C}_J$  is distributed as a Multinomial distribution with parameter  $(n, q_1, \dots, q_J)$ . Then, for each  $j \in [J]$ , the maximum likelihood estimator of  $q_j$  is

$$\hat{q}_j = \frac{c_j}{n}.$$

Therefore, we propose to approximate (22) by replacing  $q_j$  with the estimate  $\hat{q}_j$ . This will form the cornerstone of our approach of smoothed cardinality estimation, presented in Section 4.2.

## 4.2 Smoothed cardinality estimation

Our approach of smoothed estimation is motivated by the general difficulty of obtaining nontrivial cardinality estimates in a (fully) nonparametric setting, namely without any assumption on  $P$ . This is demonstrated in Appendix C.2 by presenting worst-case analysis of this problem analogous to those previously discussed in Section 2.3 in the context of frequency estimation. Following in the footsteps of Section 3, we take the results of Theorem 3 as a starting point to derive estimators of  $K_n$  as the expected value of  $\varepsilon_k(P)$  with respect to the smoothing distribution in the class of NRMs. We focus on the DP (ref. Section 3.4) and the NGGP (ref. Section 3.5). By applying (12), the next proposition gives an explicit and simple estimator of  $K_n$  under the DP smoothing assumption.

**Proposition 8.** *For  $n \geq 1$ , let  $(x_1, \dots, x_n)$  be a sample modeled according to (1), and let  $\mathbf{C}_J = \mathbf{c}$  be the corresponding sketch. If  $P \sim DP(\theta, G_0)$ , for some  $\theta$ , it follows that*

$$\hat{K}_n^{(DP)} := \mathbb{E}_{P \sim DP(\theta, G_0)}[\varepsilon_k(P)] = n \frac{\theta}{J} \sum_{j=1}^J \frac{q_j}{1 + c_j} \left( \psi \left( 1 + c_j + \frac{\theta}{J} \right) - \psi \left( \frac{\theta}{J} \right) \right), \quad (23)$$

where  $\psi$  is the digamma function, defined as the derivative of the logarithm of the Gamma function.

See Appendix C.3.1 for a proof of Proposition 8. The smoothed cardinality estimator  $\hat{K}_n^{(DP)}$  takes an explicit form that can be evaluated easily, besides from the issue that it still depends on the unknown probabilities  $q_j$ 's. As anticipated above, we rely on a plug-in approach and substitute  $q_j$  with  $\hat{q}_j = c_j/n$ .

Finally, by applying (17), the next proposition gives an explicit and simple estimator of  $K_n$  under the NGGP smoothing assumption.

**Proposition 9.** For  $n \geq 1$ , let  $(x_1, \dots, x_n)$  be a sample modeled according to (1), and let  $\mathbf{C}_J = \mathbf{c}$  be the corresponding sketch. If  $P \sim \text{NGGP}(\theta, G_0, \alpha, \tau)$ , for some  $(\theta, \alpha, \tau)$  it follows that

$$\hat{K}_n^{(\text{NGGP})} := \mathbb{E}_{P \sim \text{NGGP}(\theta, G_0, \alpha, \tau)}[\varepsilon_k(P)] = n \sum_{j=1}^J \frac{q_j}{1 + c_j} \int_0^1 \frac{1 - (1 - v)^{c_j+1}}{v} f_{V_{\theta, \alpha, \tau}}(v) (dv), \quad (24)$$

where  $f_{V_{\theta, \alpha, \tau}}$  is the probability density function of the random variable  $V_{\theta, \alpha, \tau}$  in (16).

See Appendix C.3.2 for a proof of Proposition 9. Similar to the estimator obtained in Proposition 8, the smoothed cardinality estimator  $\hat{K}_n^{(\text{NGGP})}$  in (24) also involves the unknown probabilities  $q_j$ 's, which we propose to replace in practice with their the maximum likelihood estimates  $\hat{q}_j = c_j/n$ . Note that the expression of the estimator in Proposition 9 is slightly more involved compared to that in Proposition 8 because it entails an integral with respect to the probability density function of the random variable  $V_{\theta, \alpha, \tau}$  in (16). However, this integral is not difficult to evaluate in practice because it can be approximated via standard Monte Carlo methods. Indeed from (16) it straightforward to generate independent samples for  $V_{\theta, \alpha, \tau}$ . Note that we will simulate these values only once and reuse them for all the  $J$  integrals in (24), in order to reduce the variance of the estimator.

## 5 Estimation from sketches with multiple hash functions

We now discuss how to extend our approach to combine information from sketches produced by multiple independent hash functions, as in the general setting of the CMS of Cormode and Muthukrishnan (2005). This extension strengthens the connection between our approach and the algorithmic approach of the CMS, reviewed in Appendix A.2. In fact, the latter is typically applied using multiple independent hash functions, in order to improve the efficiency of the data compression (Cormode and Yi, 2020, Chapter 2). For simplicity, we focus on the problem of frequency recovery and do not discuss cardinality recovery using multiple hash functions, though similar approaches could also be utilized for that purpose.

To introduce the more general sketch, for  $M \geq 1$  let  $h_1, \dots, h_M$  be  $J$ -wide random hash functions, with  $h_l : \mathbb{S} \rightarrow \{1, \dots, J\}$  for  $l = 1, \dots, M$ , that are i.i.d. from a pairwise independent hash family  $\mathcal{H}_J$ . Hashing  $(x_1, \dots, x_n)$  through  $h_1, \dots, h_M$  produces a random matrix  $\mathbf{C}_{M, J} \in \mathbb{N}_0^{M \times J}$ , referred to as the sketch, whose  $(l, j)$ -th bucket is

$$C_{l, j} = \sum_{i=1}^n I(h_l(x_i) = j),$$

for each  $l \in [M]$  and  $j \in [J]$ , such that  $\sum_{1 \leq j \leq J} C_{l, j} = n$ . More precisely, each hash function  $h_l$  maps each data point  $x_i$  into one of the  $J$  buckets, thus defining the sketch  $\mathbf{C}_{M, J}$  whose  $(l, j)$ -th element  $C_{l, j}$  is the number of  $x_i$ 's that are hashed by  $h_l$  in the  $j$ -th bucket.

## 5.1 Modeling assumptions and preliminary results

We rely on the following modeling assumptions for the sample  $(x_1, \dots, x_n)$ , which naturally extend the setup of Section 2.1 to the case of multiple hash functions. Firstly,  $(x_1, \dots, x_n)$  is modeled as a random sample  $\mathbf{X}_n = (X_1, \dots, X_n)$  from an unknown discrete distribution  $P = \sum_{s \in \mathbb{S}} p_s \delta_s$  on  $\mathbb{S}$ , with  $p_s$  being the (unknown) probability of an object  $s \in \mathbb{S}$ . Secondly, the strong universal hash family, from which the functions  $h_1, \dots, h_M$  are drawn (independently), is independent of  $\mathbf{X}_n$ . Formally, for any  $n \geq 1$ , we consider the model:

$$\begin{aligned} X_1, \dots, X_n &\stackrel{\text{iid}}{\sim} P & (25) \\ h_1, \dots, h_M &\stackrel{\text{iid}}{\sim} \mathcal{H}_J \\ C_{l,j} &= \sum_{i=1}^n I(h_l(X_i) = j), \quad \forall l \in [M], \forall j \in [J]. \end{aligned}$$

Under this model, we consider the problem of estimating the empirical frequency  $f_{X_{n+1}}$  from the sketch  $\mathbf{C}_{M,J}$ . In particular, following the approach developed in Section 2 for  $M = 1$ , this problem requires to compute the conditional distribution of  $f_{X_{n+1}}$  given  $\mathbf{C}_{M,D}$  and the buckets  $\mathbf{h}_M(X_{n+1}) := (h_1(X_{n+1}), \dots, h_M(X_{n+1}))$  into which  $X_{n+1}$  is hashed.

It is possible to derive explicit, though cumbersome, expressions for the distribution of  $\mathbf{C}_{M,J}$  and for the conditional distribution of  $f_{X_{n+1}}$  given  $\mathbf{C}_{M,D}$  and  $\mathbf{h}_M(X_{n+1})$ , as shown in Appendix D.1. Here, we present a simplified version of these distributions under the following two additional assumptions.

A1) Independence from random hashing. For any  $(j_1, \dots, j_M) \in \{1, \dots, J\}^{M \times n}$ ,

$$\Pr[h_1(X_i) = j_1, \dots, h_M(X_i) = j_M] = \prod_{l=1}^M \Pr[h_l(X_i) = j_l].$$

A2) Identity in distribution with respect to hashing. For any pair of indices  $i_1 \neq i_2$ ,

$$\Pr[h_l(X_{i_1}) = j_l] = \Pr[h_l(X_{i_2}) = j_l].$$

Under the model in (25), assuming that Assumptions A1) and A2) also hold, we can write

$$\Pr[\mathbf{C}_{M,J} = \mathbf{c}] = \mathcal{C}(n, \mathbf{c}) \prod_{l=1}^M \prod_{j=1}^J q_{l,j}^{c_{l,j}}, \quad (26)$$

where the  $q_{l,j}$ 's are probabilities defined as  $q_{l,j} := \Pr[h_{X_i} = j]$ , for any  $l \in [M]$  and  $j \in [J]$ , and  $\mathcal{C}(n, \mathbf{c})$  is a (combinatorial) coefficient, defined in Appendix D.2, that reduces to the Multinomial coefficient if  $M = 1$ . See Appendix D.2 for the proof of Equation (26).

**Theorem 10.** *For  $n \geq 1$  let  $(x_1, \dots, x_n)$  be a random sample modeled according to (25), and  $\mathbf{C}_{M,J} = \mathbf{c}$  the corresponding sketch. Assume that Assumptions A1) and*

A2) also hold. If  $\mathbb{S}_{j_l} := \{s \in \mathbb{S} : h_l(s) = j_l\}$ , for any  $j_l \in [J]$  and  $l \in [M]$ , then for any  $r \in \{0, 1, \dots, n\}$ ,

$$\begin{aligned} \pi_{\mathbf{j}}(r, P) &:= \Pr[f_{X_{n+1}} = r \mid \mathbf{C}_{M,J} = \mathbf{c}, \mathbf{h}_M(X_{n+1}) = \mathbf{j}] \\ &= \binom{n}{r} \frac{\mathcal{C}(n-r, \mathbf{c})}{\mathcal{C}(n, \mathbf{c})} \prod_{l=1}^M q_{l,j_l}^{\left(\frac{1}{M}-1\right)(r+1)} \sum_{s \in \mathbb{S}_{j_l}} \left(\frac{p_s}{q_{l,j_l}}\right)^{\frac{r+1}{M}} \left(1 - \frac{p_s}{q_{l,j_l}}\right)^{c_{l,j_l}-r} I(r \leq c_{l,j_l}). \end{aligned} \quad (27)$$

See Appendix D.3 for the proof of Theorem 10. If  $M = 1$ , then Theorem 10 reduces to Theorem 1, as  $\mathcal{C}(n, \mathbf{c})$  reduces to the Multinomial coefficient. From here, an intuitive approach to estimate the empirical frequency  $f_{X_{n+1}}$  from the sketch  $\mathbf{C}_{M,J}$  is to follow in the footsteps of Sections 2 and 3, considering the means of the distribution (27), i.e.,

$$\varepsilon_f(P) := \sum_{r=0}^n r \pi_{\mathbf{j}}(r, P).$$

However, the expression in (27) anticipates that the resulting estimator of  $f_{X_{n+1}}$  is not practical because it depends on the combinatorial coefficients  $\mathcal{C}(n-r, \mathbf{c})$ , for  $r \in \{0, 1, \dots, n\}$ , which are computationally expensive to evaluate if  $n-r$  is large.

In the following section, we propose to circumvent this computational challenge by taking an alternative approach, which is inspired by the recent literature on *multi-view* (or multimodal) learning (Xu et al., 2013; Shankar et al., 2018; Li et al., 2018b). In general, multi-view learning is concerned with aggregating distinct inferences obtained from different views or representations of the same data set. In particular, here, we focus on analyzing separately the sketches obtained with each hash function, and then combining the corresponding inferences through suitable rules, such as the product of experts (Hinton, 2002) and its generalizations (Cao and Fleet, 2014; Joshi et al., 2022; Jung et al., 2023).

## 5.2 Multi-view learning

We consider the sketch  $\mathbf{C}_{M,J}$  as a collection of  $M$  distinct sketches, say  $\mathbf{C}_{1,J}, \dots, \mathbf{C}_{M,J}$ , where each  $\mathbf{C}_{l,J}$  for  $l \in [M]$  is obtained by applying the corresponding hash function  $h_l$  to the sample  $(x_1, \dots, x_n)$ . Following the general multi-view learning approach, we can interpret  $\mathbf{C}_{1,J}, \dots, \mathbf{C}_{M,J}$  as  $M$  different views of the data set, and then apply Theorem 1 to each of them separately. This gives a distinct conditional distribution for the empirical frequency  $f_{X_{n+1}}$ , given the sketch  $\mathbf{C}_{l,J}$  and the bucket  $h_l(X_{n+1})$  in which  $X_{n+1}$  is hashed, for each  $l \in [M]$ . That is, for each  $r \in \{0, 1, \dots, c_{l,j}\}$ , we compute the probability

$$\begin{aligned} \pi_{j_l}(r; P) &:= \Pr[f_{X_{n+1}} = r \mid \mathbf{C}_{l,J} = \mathbf{c}_l, h_l(X_{n+1}) = j_l] \\ &= \binom{c_{l,j}}{r} \sum_{s \in \mathbb{S}_{j_l}} \left(\frac{p_s}{q_{j_l}}\right)^{r+1} \left(1 - \frac{p_s}{q_{j_l}}\right)^{c_{l,j}-r}. \end{aligned} \quad (28)$$

Then, we consider two alternative multi-view rules to aggregate the probabilities  $\pi_{j_l}(r; P)$  in (28) corresponding to different views  $l \in [M]$  of the data set, as explained

below. We find these rules intuitive and relatively easy to deal with, though other options are also possible.

The first multi-view rule that we consider is known as the *product of experts* (Hinton, 2002). This consists of defining, for each  $r \in \{0, 1, \dots, n\}$ , the cumulative distribution function

$$\tilde{\pi}_{\mathbf{j}}(r; P) := \frac{1}{Z} \prod_{l=1}^M \pi_{j_l}(r, P), \quad (29)$$

with  $Z$  being the normalizing constant, and using such a distribution as a computationally efficient approximation of (27). Intuitively, the distribution function (29) assigns high mass to values of  $r$  for which none of the individual “single-view” distributions  $\pi_{j_l}(r)$  is too small and are well supported by most of these distributions. This is interpreted as a consensus among “experts”, i.e. distributions, that find a region of values on which they can agree. We refer to Hinton (2002) for further intuitions on the product of experts.

The second multi-view rule is called *minimum of experts* and it is inspired by the CMS. This rule considers the distribution of the minimum of  $M$  independent random variables distributed according to (28). That is, if  $\Pi_{j_l}(\cdot; P)$  denotes the cumulative distribution function corresponding to (28), for each  $r \in \{0, 1, \dots, n\}$  we consider an approximation of (27) by means of a distribution  $\mathring{\pi}_{\mathbf{j}}(\cdot; P)$  whose cumulative distribution function is

$$\mathring{\Pi}_{\mathbf{j}}(r; P) := 1 - \prod_{l=1}^M (1 - \Pi_{j_l}(r, P)). \quad (30)$$

Based on the approximations in (29) and (30) of the conditional distribution (27), we propose to utilize the corresponding expected values as practical estimators of the empirical frequency  $f_{X_{n+1}}$  from the sketch  $\mathbf{C}_{M,J}$ , following the same arguments developed in Sections 2 and 3. Under the (fully) nonparametric approach of Section 2.3, it can be seen that the application of the worst-case analysis to each single view leads to recovering the classical CMS algorithm (34) from (30). Indeed, from Theorem 2 it is straightforward to see that  $\pi_{j_l}(r) = \delta_{c_{l,j_l}}(r)$  and (30) reduces to  $\min\{c_{1,j_1}, \dots, c_{M,j_M}\}$ . Under the approach of smoothed estimation of Section 3, the DP smoothing assumption on (29) leads to

$$\tilde{\pi}_{\mathbf{j}}(r) \propto \prod_{l=1}^M \binom{c_{l,j}}{r} \frac{\theta}{J} \frac{\Gamma(r+1)\Gamma(\theta/J + c_{l,j} - r)}{\Gamma(\theta/J + c_{l,j} + 1)}, \quad (31)$$

and

$$\tilde{f}_{X_{n+1}}^{(\text{DP})} = \sum_{r=0}^n r \tilde{\pi}_{\mathbf{j}}(r),$$

for all  $r \in \{0, 1, \dots, n\}$ . It is easy to see that the distribution (31) coincides with the posterior distribution of  $f_{X_{n+1}}$ , given  $\mathbf{C}_{M,J}$  and  $\mathbf{h}(X_{n+1})$ , under a DP prior, obtained in Cai et al. (2018, Theorem 2). See also Equation (8) in Dolera et al. (2023). Therefore, the smoothed frequency estimator  $\tilde{f}_{X_{n+1}}^{(\text{DP})}$  coincides with the BNP estimator proposed by Cai et al. (2018) as the posterior mean. See also Dolera et al.

(2023) for further details. Along the same lines, one may also obtain a generalization of (31) by applying the NGGP smoothing assumption to (29). These smoothing assumptions could also be applied to (30), leading to estimators that have not been previously considered in the literature.

## 6 Numerical illustrations

### 6.1 Setup and performance metrics

We present several simulation studies to assess the performance of our methods. In particular, we consider two data generating processes: i) we sample data  $X_1, \dots, X_n$  using the generative process (generalized Pólya urn) induced by the Pitman-Yor process (PYP) (Pitman and Yor, 1997) with parameter  $\gamma$  (strength) and  $\sigma$  (discount) to be specified case-by-case; ii) we sample data following a Zipfian distribution with tail parameter  $c$ . Both data generating processes display a power law behaviour. As the evaluation metric, for the cardinality estimator we report the absolute error between the true number of distinct symbols and the estimated one. For the frequency estimators, we consider the mean absolute error between true frequency and estimated, stratified by the true frequency (Dolera et al., 2023). That is, we consider non-overlapping frequency bins  $(l_m, u_m]_{m \geq 1}$  and report

$$\text{MAE}_m = \frac{1}{\sum_{s \in \mathcal{S}} I(f_s \in (l_m, u_m])} \sum_{s \in \mathcal{S}} |f_s - \hat{f}_s| I(N_s \in (l_m, u_m]),$$

where  $f_s = \sum_{i=1}^n I(X_i = s)$  is empirical frequency, and  $\hat{f}_s$  denotes its corresponding estimate.

### 6.2 Synthetic data: smoothed estimators with a single hash function

We consider the two smoothing distributions discussed in Section 3, namely the Dirichlet process and the NGGP. To estimate the parameters in the DP, we maximize the integrated likelihood of the observed sketch as discussed in Appendix E. While considering the NGGP, we store in memory the first  $m$  observations  $X_1, \dots, X_m$ , with  $m \approx n/20$ , and choose the parameters that maximize the integrated likelihood of  $X_1, \dots, X_m$ . See Appendix E for further details on the associated algorithms. As far as the computational cost is concerned, optimizing under the DP smoothing is almost instantaneous (less than 1 second) while for the NGGP the optimization takes is between 30 seconds and 5 minutes.

We generate  $n = 100,000$  observations from  $\text{PYP}(\gamma, \sigma)$  for  $\gamma \in \{1, 10, 100, 1000\}$  and  $\sigma \in \{0, 0.25, 0.5, 0.75\}$  and from a Zipfian distribution with parameter  $c = 1.3, 1.6, 1.9, 2.2$ . The data are hashed by a random hash function of with  $J = 128$ . Figures 2 and 3 report the MAEs of the frequency estimators stratified across 5 frequency bins [when data are generated from  \$\text{PYP}\(\gamma, 0.75\)\$  and from the Zipf distribution, respectively](#), while Table 1 in the Appendix reports all the remaining numerical values. Results are averaged across 50 independent repetitions. It is clear

that the NGGP smoothing outperforms the DP smoothing for both data generating processes, and across all values of their parameters.

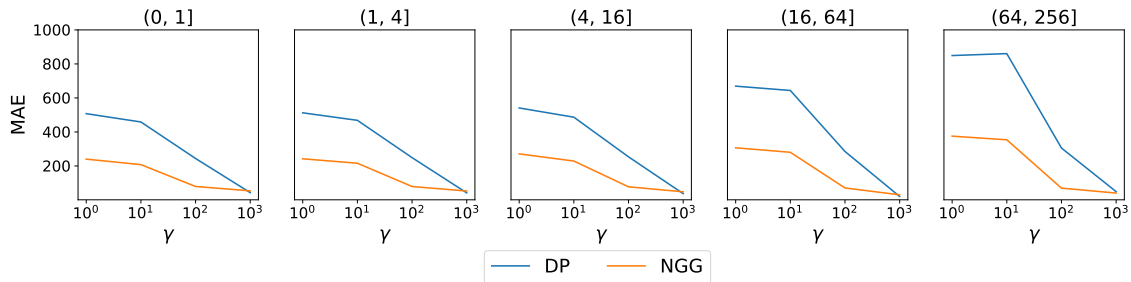


Figure 2: MAEs for the frequency estimators with DP and NGG smoothing, in experiments involving synthetic data generated from a Pitman-Yor process with parameters  $\gamma$  (varies across the  $x$ -axis) and  $\sigma = 0.75$  (see Section 6.2). Different plots correspond to different frequency bins.

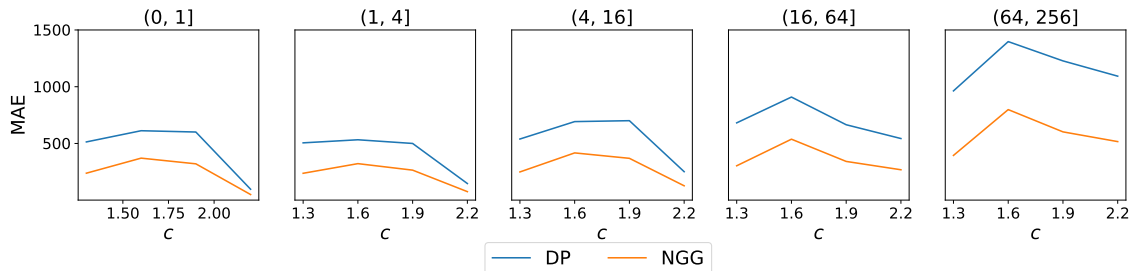


Figure 3: MAEs for the frequency estimators with DP and NGG smoothing in experiments involving synthetic data generated from a Zipf distribution (see Section 6.2). In each plot, the parameter  $c$  of the Zipf distribution varies across the  $x$ -axis. Different plots correspond to different frequency bins.

We now consider the cardinality estimation problem, assuming the same data generating processes as above. We set  $n \in \{100, 1000, 10000, 100000\}$ . The data are hashed by a random hash function of with  $J = 128$ . Figure 4 reports the true and estimated cardinalities for a simulated setting, while Tables 2 and 3 report the errors achieved by the different smoothing distributions, averaging across 50 independent repetitions. The NGGP smoothing generally outperforms the DP when the discount parameter of the Pitman-Yor process is greater than zero. Conversely, the DP yields slightly better performances when the discount is equal to zero. Similarly, the NGGP performs better when the parameter of the Zipf distribution is closer to one (i.e., heavier tails of the distribution), while the DP gives better estimates if  $c = 2.2$ .

In Appendix F.1, we discuss the impact of the parameter  $J$  on both frequency and cardinality recovery.

### 6.3 Synthetic data: multiple hash functions

We now move to the case of multiple hash functions. In the following, we fix a total memory budget for the sketch  $\mathbf{C}_{M,J}$  so that  $M \times J = 1,000$ . We consider

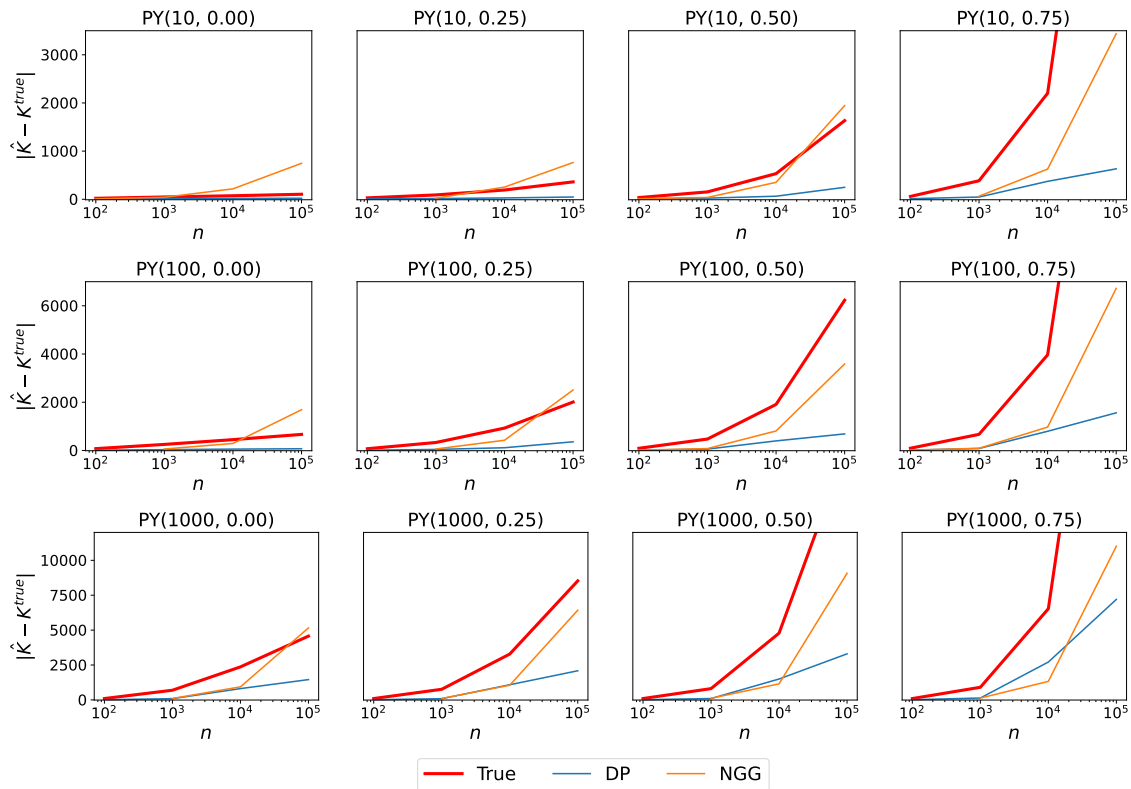


Figure 4: True and estimated cardinalities for the simulation setup in Section 6.2.

data generated from a PYP( $\gamma, \sigma$ ), letting  $\gamma \in \{10, 100, 1000\}$  and  $\sigma \in \{0.25, 0.75\}$ , and simulate  $n = 500,000$  observations for each possible combination of the parameters. In analogy with the multiview literature, we analyze each view separately (in parallel) and estimate one set of parameters for each view.

We consider the frequency estimators based on the product of expert (PoE) aggregation (29) and the minimum of expert (min) aggregation (30) rules, under the DP and NGG smoothing assumption. We also compare their performance with the original count-min sketch algorithm. Figure 5 reports the MAEs for two choices of the parameters of the data generating process, and Tables 4 - 5 in the Appendix report all the remaining numerical values.

Several interesting insights can be noticed. First, the min aggregation rule usually outperforms the PoE rule. Moreover, in accordance to what the simulations in the previous sections found, the NGGP smoothing is preferable to the DP. When the data has a moderate power-law behaviour (i.e., when the discount parameter of the Pitman-Yor process generating the data is  $\sigma = 0.25$ ), the CMS is competitive with the product of experts aggregation with DP smoothing, but falls short of all the remaining methods. Instead, when data exhibits heavy power-laws, the CMS yields much larger errors especially at low frequencies. For all data sets, it seems that the smoothed estimators benefit from a moderate (e.g., 10) number of hash functions. This is also the case of the CMS but only for moderate power laws. With heavier power laws instead, the CMS performs better by having only one or two hash functions.



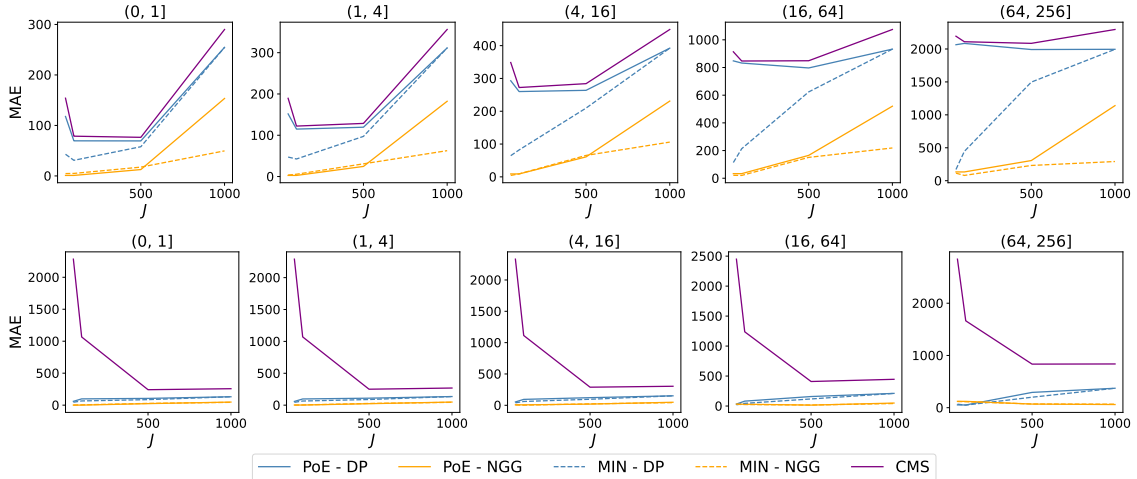


Figure 5: MAEs for the frequency estimators in Section 6.3, stratified by true frequency bins. Top row, data generated from a Pitman-Yor process with parameters  $(100, 0.25)$ . Bottom row, data from a Pitman-Yor process with parameters  $(100, 0.75)$ . In the bottom row, the PoE-NGG and MIN-NGG lines are overlapping.

## 6.4 Calibration of multi-hash aggregation rules

In addition to obtaining point estimates for  $f_{X_{n+1}}$ , our machinery can produce prediction intervals. For instance, a 95% prediction interval can be constructed by looking at the 2.5% and 97.5% quantile of (29) or (30). Then, it is important to assess whether such predictions are calibrated and the width of the intervals. Sesia and Favaro (2022) showed empirically how the BNP posterior distribution for  $f_{X_{n+1}}$  under a DP prior obtained in Cai et al. (2018), which coincides with our PoE rule with DP smoothing, is typically miscalibrated and produces intervals that are too wide.

The following empirical results will show that miscalibration is not unique to the Bayesian setting, but it is rather a common problem, one that affects both of the aggregation rules that we proposed regardless of whether the smoothing is based on the DP or NGGP assumptions. We will call the intervals obtained using (29) and (30) the “smoothed-PoE” and “smoothed-min” intervals, respectively. We propose to overcome this pitfall using the conformal inference approach proposed by Sesia and Favaro (2022). In particular, we show that using the point estimators considered previously (i.e., obtained as the expected value of (29) or (30)) to produce intervals as in Sesia and Favaro (2022) leads to shorter prediction intervals with valid coverage. We will call such intervals the “conformal-PoE” and “conformal-min” intervals, respectively. Observe that both the smoothed and conformal intervals depend on the choice of smoothing distribution.

We consider data generated from a Pitman-Yor process with parameter  $(10, 0.25)$  and  $(100, 0.25)$  and simulate  $n = 250,000$  observations. For the “conformalized” approach, we follow the guidelines in Sesia and Favaro (2022) and use their default values to tune our intervals. In particular, we store the first  $m = 25,000$  observations to calibrate the intervals and evaluate the coverage and length of the prediction intervals over an additional 2,500 data points. Figure 6 reports the results averaged

over 50 independent replications. We can see that all the intervals have coverage above the nominal level (0.9). As far as the interval lengths is concerned, the behaviour changes significantly in the different settings, as explained next.

The plots on the left of Figure 6 focus on the case where the data are generated from PYP(10, 0.25). In that case, if we apply the DP smoothing, the smoothed-min intervals are extremely wide, while the conformal-min intervals are slightly shorter but still appear quite uninformative. By contrast, both the smoothed-PoE and conformal-PoE intervals are much shorter, although the smoothed-PoE have a coverage below the nominal level if  $J = 50$  or  $J = 100$ . Instead, when using the NGGP smoothing, the smoothed-PoE and smoothed-min intervals are large, while the conformal-PoE and conformal-min are much shorter with a similar length.

The plots on the right of Figure 6 focus on the case where the data are from a PYP(100, 0.25). In that case, the smoothed and conformal interval lengths are in the same order of magnitude, but we can still acknowledge how conformal intervals are generally shorter. In particular, under the DP smoothing, the conformal-PoE intervals are the shortest, followed by the conformal-min intervals and smoothed-PoE. Under the NGGP smoothing, the min and PoE rule yield essentially the same intervals, while the conformal approach improves rather significantly over the smoothed approach.

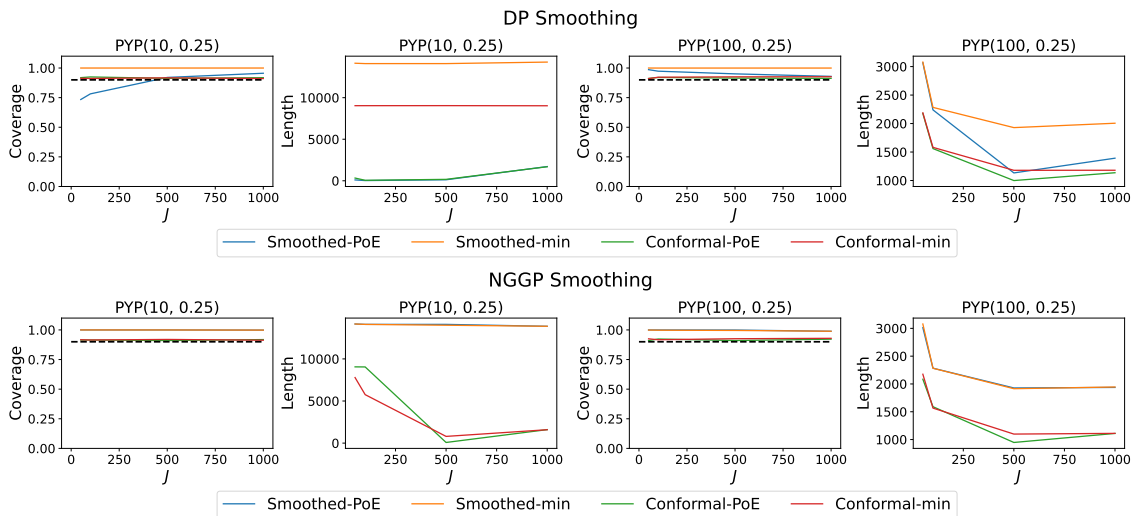


Figure 6: Calibration and average lengths of the intervals derived from the product of expert and the min aggregation rule using a Dirichlet process smoothing (top row) and an NGGP smoothing (bottom row), for two different data generating processes.

## 6.5 Real data sets

We consider two real data sets, displaying remarkably different behaviours in terms of their frequency distribution, that were also analyzed in Sesia and Favaro (2022). The first data set consists of the texts of 18 open-domain classic pieces of English literature from the Gutenberg Corpus. The frequency distribution here has a clear power-law behaviour, as shown in Figure 7. We subsample 600,000 bigrams from

the corpus, displaying approximately 120,000 distinct combinations. The second data set contains nucleotide sequences from SARS-CoV-2 viruses, made publicly available by the National Center for Biotechnology Information (Hatcher et al., 2017). These data include 43,196 sequences, each consisting of approximately 30,000 nucleotides. The goal is to estimate the empirical frequency of each possible 16-mer, a distinct sequence of 16 DNA bases found in contiguous nucleotides. Given that each nucleotide has one of 4 bases, there are  $4^{16} \approx 4.3$  billion possible 16-mers. The frequency distribution of the DNA sequences is reported in Figure 7. Its behaviour is rather unusual: there are no “common” sequences, and most of the sequences appear approximately 1,000 times in the data set. There are also a handful of more common sequences that appear 2000 times and some rare sequences that appear only a few times. We subsample 2,000,000 data points from the data set, displaying approximately 20,000 unique sequences.

First, we focus on the recovery of the number of distinct symbols in the data. To this end, we sketch the data with a random hash function of size 100,000. We consider the estimators based on the DP and NGGP smoothing and estimate the parameters as discussed above. Figure 7 shows the true end estimated  $K_n$  for different values of  $n$ . For the bigrams data set, the NGGP smoothed estimator clearly outperforms the DP alternative and neatly resembles the true  $K_n$ . Instead, for the Covid-DNA data, both estimators overestimate  $K_n$  and it is the DP that performs slightly better.

As far as the frequency recovery is concerned, we follow the same setup of Section 6.3 and fix a total memory budget of  $M \times J = 10,000$ , letting  $M = 10, 4, 2, 1$ . We sketch the data and evaluate the four different estimators based on the DP and NGGP smoothing combined via the product of experts and the “min” rule. Figure 8 shows the MAES stratified by frequency. For the English bigrams data set, the behaviour is as expected: the NGGP typically achieves the best performance, although the estimators are similar. For the Covid-DNA data set instead, all estimators yield very similar performances. This is to be expected since the data does not have a power-law behaviour, and shows that the NGGP smoothing can be used for a wide range of data sets. For a comparison, for both data sets, the CMS algorithms error are at least one order of magnitude larger than with our smoothed estimators.

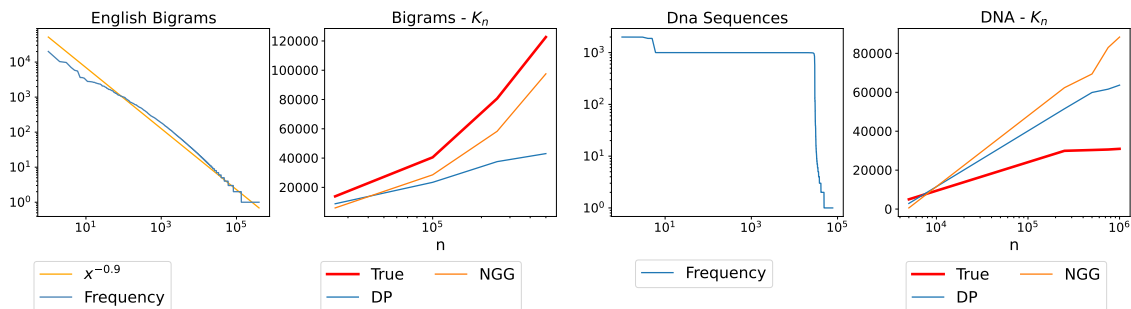


Figure 7: From left to right: frequency distribution for the Gutenberg corpus bigrams, true and estimated  $K_n$  for the bigrams dataset, frequency distribution for the Covid-DNA dataset, true and estimated  $K_n$  for the Covid-DNA dataset.

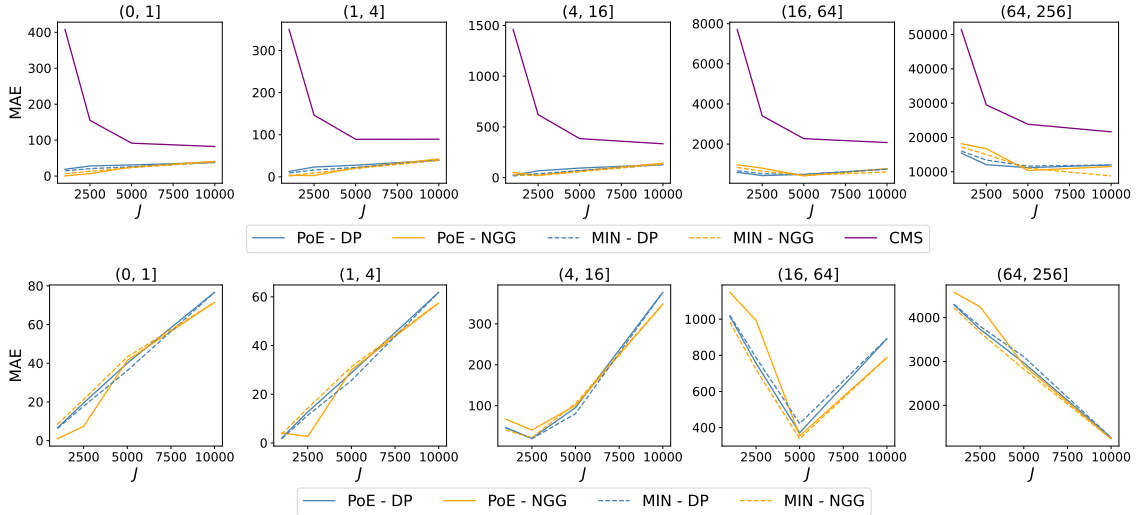


Figure 8: MAEs for the frequency estimators on the Gutenberg corpus bigrams (top row), and Covid-DNA sequences (bottom row), stratified by true frequency bins.

## 7 Discussion

We proposed a novel statistical approach to frequency and cardinality recovery from sketched data, showing that it provides a principled, and practical, solution that overcomes some of the limitations of current approaches. This work opens several opportunities for further research. In particular, in the future one may consider developing an in-depth analysis for the problem of endowing our method with uncertainty estimates, which here has been addressed only empirically by relying on recent works of Sesia and Favaro (2022) and Sesia et al. (2023). Further, one may consider the more general setting in which data belong to more than one symbol, referred to as traits, and exhibit nonnegative integer levels of associations with each trait; e.g., single cell data contain multiple genes with their expression levels, members of a social networks have friends to which they send multiple messages, documents contain different topics with their words. In the trait allocation setting, a BNP approach to frequency recovery has been developed in Cai et al. (2018) and Beraha and Favaro (2023), showing some computational issues in the evaluation of posterior distributions, in analogy with the classical setting. Our work suggests that extending the idea of smoothed estimation to the trait allocation setting may lead to frequency estimators that are much easier to compute compared to BNP estimators, under flexible modeling assumptions.

As further directions for future works, it would be interesting to explore the relevance of our approach for large-scale streaming and distributed problems. This may require adapting our method to allow for a sequential estimation of smoothing parameters and extending our multi-view formulation to account for the cost of aggregating inference across different servers under communication constraints. Moreover, we plan to extend our framework to other statistical problems involving more complex data streams such as graphs (Cormode and Yi, 2020, Chapter 7) for which several Bayesian nonparametric models have been recently proposed (see, e.g.,

Caron and Fox, 2017; Ricci et al., 2022).

## Acknowledgements

M.B. and S.F. received funding from the European Research Council (ERC) under the European Union’s Horizon 2020 research and innovation programme under grant agreement No 817257. S.F. also gratefully acknowledges the Italian Ministry of Education, University and Research (MIUR), “Dipartimenti di Eccellenza” grant 2018-2022. S.F. is also affiliated to IMATI-CNR “Enrico Magenes” (Milan, Italy). M.S. was supported in part by NSF grant DMS 2210637 and by an Amazon Research Award. M.S. is also affiliated with the Department of Computer Science at the University of Southern California.

## References

- AAMAND, A., INDYK, P. AND VAKILIAN, A. (2019). Frequency estimation algorithms under Zipfian distribution. *Preprint arXiv:1908.05198*.
- ALON, N., MATIAS, Y. AND SZEGEDY, M. (1999). The space complexity of approximating the frequency moments. *Journal of Computer and System Sciences* **58**, 137–147.
- BECCHETTI, L, CASTILLO, C., DONATO, D., LEONARDI, S., AND BAEZA-YATES, R. (2006) Using rank propagation and probabilistic counting for link-based spam detection. In *Proceedings of the Workshop on Web Mining and Web Usage Analysis*.
- BERAHA, M. AND FAVARO, S. (2023). Random measure priors in Bayesian frequency recovery from sketches. *Preprint arXiv:2303.15029*.
- BLUM, A., HOPCROFT, J. AND KANNAN, R. (2020). Foundations of data science. *Cambridge University Press*.
- BRIX, A. (1999). Generalized Gamma measures and shot-noise Cox processes. *Advances in Applied Probability* **31**, 929–953.
- BREITWIESER, F. P., BAKER, D. N., SALZBERG, S. L. (2018) KrakenUniq: confident and fast metagenomics classification using unique k-mer counts. *Genome Biology* **19**, 1–10.
- BRODER, A. Z. (2000). Identifying and filtering near-duplicate documents. In *Annual symposium on combinatorial pattern matching*.
- CAI, D., MITZENMACHER, M. AND ADAMS, R.P. (2018). A Bayesian nonparametric view on count–min sketch. In *Advances in Neural Information Processing Systems*.

- CAO, Y. AND FLEET, D. J. (2014). Generalized product of experts for automatic and principled fusion of Gaussian process predictions. *Preprint arXiv:1410.7827*.
- CARON, F., AND FOX, E. B. (2017). Sparse graphs using exchangeable random measures. *Journal of the Royal Statistical Society Series B: Statistical Methodology*, **79**, 1295–1366.
- CHARIKAR, M., CHEN, K. AND FARACH-COLTON, M. (2002) Finding frequent items in data streams. *Theoretical Computer Science* **312**, 3–15
- CHUNG, K., MITZENMACHER, M. AND VADHAN, S.P. (2013). Why simple hash functions work: exploiting the entropy in a data stream. *Theory of Computing* **9**, 897–945.
- CORMODE, G. (2023). *Applications of sketching and pathways to impact*. In *International Conference on Management of Data*.
- CORMODE, G. AND MUTHUKRISHNAN, S. (2005). An improved data stream summary: the count-min sketch and its applications. *Journal of Algorithms* **55**, 58–75.
- CORMODE, G. AND YI, K. (2020). *Small summaries for big data*. Cambridge University Press.
- DASKALAKIS, C., STRATIS S., AND MANOLIS Z. (2021). The complexity of constrained min-max optimization. In *Proceedings of the 53rd Annual ACM SIGACT Symposium on Theory of Computing*.
- DESFONTAINES, D., LOCHBIHLER, A., AND BASIN, D. (2019). Cardinality estimators do not preserve privacy In *Proceedings on Privacy Enhancing Technologies*.
- DICK, T., WONG, E., AND DANN, C. (2014). How many random restarts are enough? *Technical report, Carnegie Mellon University*.
- DOLERA, E., FAVARO, S. AND PELUCHETTI, S. (2021). A Bayesian nonparametric approach to count-min sketch under power-law data stream. In *International Conference on Artificial Intelligence and Statistics*.
- DOLERA, E., FAVARO, S. AND PELUCHETTI, S. (2023). Learning-augmented count-min sketches via Bayesian nonparametrics. *Journal of Machine Learning Research* **24**, 1–60.
- DURAND, M. AND FLAJOLET, F. (2003). Loglog counting of large cardinalities. In *European Symposium on Algorithms*.
- FAVARO, S., LIJOI AND PRÜNSTER (2012). On the stick-breaking representation of normalized inverse Gaussian priors. *Biometrika* **99**, 663–674.
- FAVARO, S. AND SESIA, M. (2022). Bayesian nonparametric estimation of coverage probabilities and distinct counts from sketched data. *Preprint arXiv:2209.02135*.
- FERGUSON, T.S. (1973). A Bayesian analysis of some nonparametric problems. *The Annals of Statistics* **1**, 209–230.

- FERGUSON, T.S. (1974). Prior distributions on spaces of probability measures. *The Annals of Statistics* **2**, 615–629.
- FERRER I CANCHO, R. AND SOLÉ, R. V.. Two regimes in the frequency of words and the origins of complex lexicons: Zipf’s law revisited. *Journal of Quantitative Linguistics*, 8(3):, 165–173.
- FLAJOLET, P., FUSY, E., GANDOUET, O. AND MEUNIER, F. (2007). Hyperloglog: the analysis of a near-optimal cardinality estimation algorithm. In *Analysis of Algorithms*.
- FLAJOLET, P. AND MARTIN, G.N. (1983). Probabilistic counting. In *IEEE Conference on Foundations of Computer Science*.
- FLAJOLET, P. AND MARTIN, G.N. (1985). Probabilistic counting algorithms for database applications. *Journal of Computer and System Sciences* **31**, 182–209.
- GILKS, W. R. AND PASCAL W. (1992). Adaptive rejection sampling for Gibbs sampling. *Journal of the Royal Statistical Society: Series C (Applied Statistics)*, **41** 337–348.
- GNEDIN, A., HANSEN, H., AND PITMAN, J. (2007). Notes on the occupancy problem with infinitely many boxes: general asymptotics and power laws. *Probability Surveys*, **4** 146–171.
- GOOD, I.J.(1953). The population frequencies of species and the estimation of population parameters. *Biometrika* **40**, 237–264.
- GOOD, I.J. AND TOULMIN, G.H. (1956). The number of new species, and the increase in population coverage, when a sample is increased. *Biometrika* **43**, 45–63.
- HALEVY, A., KORN, F., NOY, N. F., OLSTON, C., POLYZOTIS, N., ROY, S., AND WHANG, S. E. (2016). Goods: Organizing Google’s datasets. In *Proceedings of the 2016 International Conference on Management of Data*.
- HATCHER, E. L., ZHDANOV, S. A., BAO, Y., BLINKOVA, O., NAWROCKI, E. P., OSTAPCHUCK, Y., SCHAFFER, A.A., AND BRISTER, J. R. (2017). Virus Variation Resource—improved response to emergent viral outbreaks. *Nucleic acids research*, **45**, D482–D490.
- HINTON, G. E. (2002). Training products of experts by minimizing contrastive divergence. *Neural Computing*, **14** 1771–1800.
- HSU, C., INDYK, P., KATABI, D. AND VAKILIAN, A. (2019) Learning-based frequency estimation algorithms. In *International Conference on Learning Representations*.
- JAMES, L.F. (2002). Poisson process partition calculus with applications to exchangeable models and Bayesian nonparametrics. *Preprint arXiv:math/0205093*.

- JAMES, L. F., LIJOI, A., AND PRÜNSTER, I. (2009). Posterior analysis for normalized random measures with independent increments. *Scandinavian Journal of Statistics*, **36**, 76–97.
- JOSHI, A., GUPTA, N., SHAH, J., BHATTARAI, B., MODI, A., AND STOYANOV, D. (2022). Generalized product-of-experts for learning multimodal representations in noisy environments. In *International Conference on Multimodal Interaction*.
- JUNG, M. C., ZHAO, H., DIPNALL, J., GABBE, B., AND DU, L. (2023) Uncertainty estimation for multi-view data: the power of seeing the whole picture. In *Advances in Neural Information Processing Systems*.
- KARP, R., SHENKER, S. AND PAPADIMITRIOU, C.H. (2003). A simple algorithm for finding frequent elements in streams and bags. *ACM Transactions on Database Systems* **28**, 51–53.
- KINGMAN, J.F.C (1967). Completely random measures. *Pacific Journal of Mathematics* **21**, 59–78.
- KINGMAN, J.F.C (1993). *Poisson processes*. Oxford University Press, Oxford.
- LI, Y., YANG, M., AND ZHANG, Z. (2018). A survey of multi-view representation learning. In *IEEE Transactions on Knowledge and Data Engineering*, **31**, 1863–1883.
- LIJOI, A., MENA, R. H., AND PRÜNSTER, I. (2005). Hierarchical mixture modeling with normalized inverse-Gaussian priors. *Journal of the American Statistical Association* **100**, 1278–1291.
- LIJOI, A., MENA, R. H. AND PRÜNSTER, I. (2007). Controlling the reinforcement in Bayesian non-parametric mixture models. *Journal of the Royal Statistical Society Series B* **69**, 715–740.
- LIJOI, A. AND PRÜNSTER, I. (2010). Models beyond the Dirichlet process. In *Bayesian Nonparametrics*, Hjort, N.L., Holmes, C.C. Müller, P. and Walker, S.G. Eds. Cambridge University Press.
- MEDJEDOVIC, D., TAHIROVIC, E. AND DEDOVIC, I. (2022). Algorithms and data structures for massive datasets. *Manning*
- MANKU, G.S. AND MOTWANI, R. (2002). Approximate frequency counts over data streams. In *Proceedings of the International Conference on Very Large Data Bases*.
- MISRA, J. AND GRIES D. (1982). Finding repeated elements. *Science of computer programming* **2**, 143–152.
- MITZENMACHER, M. AND UPFAL, E. (2017). *Probability and computing: randomization and probabilistic techniques in algorithms and data analysis*. Cambridge University Press.



- PAINSKY, A. (2022). Generalized Good-Turing improves missing mass estimation. *Journal of the American Statistical Association*. In press.
- PAINSKY, A. (2022). Confidence intervals for unobserved events. *Preprint arXiv:2211.03052*.
- PAINSKY, A. (2022). Convergence guarantees for the Good-Turing estimator. *Journal of Machine Learning Research* **23**, 1–37
- PITMAN, J. (2003). Poisson-Kingman partitions. In *Science and Statistics: A Festschrift for Terry Speed*, Goldstein, D.R. Eds. Institute of Mathematical Statistics.
- PITMAN, J., AND YOR, M. (1997). The two-parameter Poisson-Dirichlet distribution derived from a stable subordinator. *The Annals of Probability*, **25**, 855–900.
- PRÜNSTER, I. (2002). *Random probability measures derived from increasing additive processes and their application to Bayesian statistics*. PhD Thesis, University of Pavia.
- REGAZZINI, E., LIJOI, A. AND PRÜNSTER, I. (2003). Distributional results for means of normalized random measures with independent increments. *The Annals of Statistics*. **31**, 560–585.
- RICCI, F. Z., GUINDANI, M., AND SUDDERTH, E. (2022). Thinned random measures for sparse graphs with overlapping communities. In *Advances in Neural Information Processing Systems*.
- ROBBINS, H.E. (1956). An empirical Bayes approach to statistics. In *Proceedings of the Berkeley Symposium* **1**, 157–163.
- ROBBINS, H.E. (1968). Estimating the total probability of the unobserved outcomes of an experiment. *The Annals of Mathematical Statistics* **39**, 256–257.
- SEZIA, M. AND FAVARO, S. (2022). *Conformalized frequency estimation from sketched data*. In *Advances in Neural Information Processing Systems*.
- SEZIA, M., FAVARO, S. AND DOBRIBAN, E. (2023). *Conformal Frequency Estimation using Discrete Sketched Data with Coverage for Distinct Queries*. In *Preprint arXiv:2211.04612*.
- SHANKAR, S.K., PRIETO, L. P., RODRIGUEZ-TRIANA M. J., RUIZ-CALLEJA, A. (2018). A Review of Multimodal Learning Analytics Architectures. In *International Conference on Advanced Learning Technologies*.
- TEC, MAURICIO (2018). AdaptiveRejectionSampling.jl. URL: <https://github.com/mauriciogtec/AdaptiveRejectionSampling.jl>
- TING, D. (2018). Count-min: Optimal estimation and tight error bounds using empirical error distributions. In *Proceedings of the 24th ACM SIGKDD International Conference on Knowledge Discovery & Data Mining*, 2319–2328.

VOVK, V., GAMMERMAN, A., AND SHAFER, G. (2005) Algorithmic learning in a random world. Springer.

XU, C. AND TAO, D. AND XU, C. (2013). A survey on multi-view learning. *Preprint arXiv:1304.5634*.

ZIPF, G. K. (2016) *Human behavior and the principle of least effort: An introduction to human ecology*. Ravenio Books.

## A Further details about related prior work

### A.1 Review of the BNP approach

This section reviews the BNP approach of Cai et al. (2018), which proposed first to address our frequency estimation problem by assuming a Dirichlet process prior for the data distribution. This BNP framework was later extended by Dolera et al. (2021), Dolera et al. (2023), and Beraha and Favaro (2023) to accommodate a broader class of prior distributions belonging to the NRM class. In this section, we present a unified summary of the BNP approach by following the notation of Beraha and Favaro (2023).

The BNP framework rests on the two key assumptions. Firstly, the data  $(x_1, \dots, x_n)$  are modeled as a random sample  $\mathbf{X}_n = (X_1, \dots, X_n)$  from an unknown distribution  $P = \sum_{s \in \mathbb{S}} p_s \delta_s$  on  $\mathbb{S}$ , endowed by a nonparametric prior  $\mathcal{P}$ . Secondly, the hash family  $\mathcal{H}_J$  is independent of  $\mathbf{X}_n$ . That is, for any  $n \geq 1$ ,

$$\begin{aligned} P &\sim \mathcal{P}, \\ X_1, \dots, X_n &| P \stackrel{\text{iid}}{\sim} P, \\ h &\sim \mathcal{H}_J, \\ C_j &= \sum_{i=1}^n I(h(X_i) = j), \quad \forall j \in \{1, \dots, J\}. \end{aligned} \tag{32}$$

Beraha and Favaro (2023) studied the estimation of the empirical frequency  $f_{X_{n+1}}$  under the model in (32) with  $P \sim \text{NRM}(\theta, G_0, \rho)$ , extending the prior work of Cai et al. (2018) which focused on the sub-family of DP priors. In particular, Theorem 2.2 in Beraha and Favaro (2023) provides the posterior distribution of  $f_{X_{n+1}}$ , given the sketch  $\mathbf{C}_J$  and the bucket  $h(X_{n+1})$  in which  $X_{n+1}$  is hashed, whose expected value,

$$\varepsilon_f(\text{NRM}(\theta, G_0, \rho)) = \mathbb{E}_{P \sim \text{NRM}(\theta, G_0, \rho)}[f_{X_{n+1}} | \mathbf{C}_J = \mathbf{c}, h(X_{n+1}) = j] \tag{33}$$

is a BNP estimator  $f_{X_{n+1}}$  under a squared loss function. Moreover, it is shown in Beraha and Favaro (2023) that: i) the BNP estimator  $\varepsilon_f(\text{DP}(\theta, G_0))$  coincides with the learning-augmented CMS of Cai et al. (2018); ii) the DP prior is the sole NRMs for which the BNP estimator (33) depends on the sketch  $\mathbf{C}_J$  only through  $C_{h(X_{n+1})}$ , namely the size of the bucket in which  $X_{n+1}$  is hashed.

The interplay between our approach and the BNP approach emerges through the framework of smoothed estimation in Section 3, which also relies on distributional assumptions on  $P$ . In the BNP framework, the (prior) assumption on  $P$  is applied to obtain estimators as expected values under the posterior of  $P$  given  $\mathbf{X}_n$ . Instead, in the framework of smoothed estimation, the (smoothing) assumption on  $P$  is applied to obtain estimators as expected values under the distribution of  $P$ . From Beraha and Favaro (2023) it emerges how priors beyond the DP, such as NRM priors, lead to BNP estimators that involve non-trivial computational challenges. By contrast, smoothed estimation leads to simple estimators for any smoothing assumption in the class of NRMs.

It is interesting that our smoothed estimator in (13) coincides exactly with the BNP estimator obtained under the DP prior by Cai et al. (2018), as explained in Section 3.4. Further, the DP as the sole NRM for which the BNP approach and the framework of smoothed estimation lead to the same estimator for  $f_{X_{n+1}}$ ; see Theorem 5.

## A.2 Review of the CMS algorithm

Unlike the BNP framework reviewed in Appendix A.1 or the framework discussed in this paper, the classical CMS algorithm (Cormode and Muthukrishnan, 2005) treats the data  $(x_1, \dots, x_n)$  as arbitrarily fixed. Therefore, one may say that the CMS is not, strictly speaking, a statistical approach. Instead, the CMS computes frequency estimates by leveraging only the randomness in the hash functions, as reviewed below.

For  $M \geq 1$  let  $h_1, \dots, h_M$  be  $J$ -wide random hash functions, with  $h_l : \mathbb{S} \rightarrow \{1, \dots, J\}$  for  $l \in [M]$ , that are i.i.d. from the pairwise independent hash family  $\mathcal{H}_J$  (Mitzenmacher and Upfal, 2017, Chapter 5 and Chapter 15). Sketching  $(x_1, \dots, x_n)$  through  $h_1, \dots, h_M$  produces a random matrix  $\mathbf{C}_{M,J} \in \mathbb{N}_0^{M \times J}$  whose  $(l, j)$ -th bucket is

$$C_{l,j} = \sum_{i=1}^n I(h_l(x_i) = j),$$

for each  $l \in [M]$  and  $j \in [J]$ , such that  $\sum_{1 \leq j \leq J} C_{l,j} = n$ . More precisely, each  $h_l$  maps each  $x_i$  into one of the  $J$  buckets, defining the sketch  $\mathbf{C}_{M,J}$  whose  $(l, j)$ -th element  $C_{l,j}$  is the number of  $x_i$ 's hashed by  $h_l$  in the  $j$ -th bucket.

Based on  $\mathbf{C}_{M,J}$ , the CMS estimates  $f_{x_{n+1}}$  by taking the smallest count among the  $M$  buckets into which  $x_{n+1}$  is hashed,

$$\hat{f}_{x_{n+1}}^{(\text{CMS})} = \min\{C_{1,h_1(x_{n+1})}, \dots, C_{M,h_M(x_{n+1})}\}. \quad (34)$$

As  $\hat{f}_v^{(\text{CMS})}$  is the count  $C_{l,h_k(x_{n+1})}$  associated with the hash function with the fewest collisions, it provides a deterministic upper bound on the true  $f_{x_{n+1}}$ :

$$\hat{f}_{x_{n+1}}^{(\text{CMS})} \geq f_{x_{n+1}}.$$

Further, if  $J = \lceil e/\varepsilon \rceil$  and  $M = \lceil \log 1/\delta \rceil$ , for any  $\varepsilon > 0$  and  $\delta > 0$ , then  $\hat{f}_{x_{n+1}}^{(\text{CMS})}$  also satisfies

$$\hat{f}_{x_{n+1}}^{(\text{CMS})} \leq f_{x_{n+1}} + \varepsilon m,$$

with probability at least  $1 - \delta$  over the randomness in the hash functions. These results provide a theoretical guarantee for  $\hat{f}_{x_{n+1}}^{(\text{CMS})}$  in terms of a confidence interval, but they often tend to be too conservative to be useful in practice if the data are randomly sampled from some distribution instead of fixed arbitrarily (Ting, 2018; Sesia et al., 2023). We refer to Cormode and Yi (2020, Chapter 3) for a more comprehensive account on the CMS, and generalizations thereof.

The interplay between our approach and the CMS algorithm emerges through our nonparametric analysis. In particular, we find that the worst-case estimator of  $f_{X_{n+1}}$  derived in Section 2.3 coincides exactly with the original CMS upper bound.

## B Further details on frequency recovery

### B.1 Proofs for Section 2

#### B.1.1 Proof of Theorem 1

Recall that under the statistical model (1),  $\mathbf{X}_n$  is a random sample from the distribution  $P = \sum_{s \in \mathbb{S}} p_s \delta_s$ , with  $p_s \in (0, 1)$  being the probability of  $s \in \mathbb{S}$ , and the random hash function  $h : \mathbb{S} \rightarrow \{1, \dots, J\}$  is independent of  $\mathbf{X}_n$ . Under these assumptions, for any  $s \in \mathbb{S}$

$$\Pr[X_i = s \mid h(X_i) = j] = \frac{p_s}{q_j}.$$

That is, if  $\mathbb{S}_j = \{s \in \mathbb{S} : h(s) = j\}$ , with  $j = 1, \dots, J$ , then the random variables  $X_i$ 's that are hashed into the  $j$ -th bucket form a random sample from the following distribution:

$$P_j = \sum_{s \in \mathbb{S}_j} \frac{p_s}{q_j} \delta_s.$$

Now, we evaluate the conditional distribution of  $f_{X_{n+1}}$ , given  $\mathbf{C}_J$  and  $h(X_{n+1})$ , i.e., for  $r = 0, 1, \dots, c_j$

$$\Pr[f_{X_{n+1}} = r \mid \mathbf{C}_J = \mathbf{c}, h(X_{n+1}) = j] = \frac{\Pr[f_{X_{n+1}} = r, \mathbf{C}_J = \mathbf{c}, h(X_{n+1}) = j]}{\Pr[\mathbf{C}_J = \mathbf{c}, h(X_{n+1}) = j]}. \quad (35)$$

We first evaluate the denominator of (35), which is trivial, and then consider the numerator. Since  $\mathbf{X}_n$  is a random sample from  $P$ , the sketch  $\mathbf{C}_J$  is distributed as a Multinomial distribution with parameter  $(n, q_1, \dots, q_J)$ , where  $q_j := \Pr[h(X_i) = j]$  for  $j = 1, \dots, J$ . Then,

$$\Pr[\mathbf{C}_J = \mathbf{c}, h(X_{n+1}) = j] = \binom{n}{c_1, \dots, c_J} q_1^{c_1} \cdots q_{j-1}^{c_{j-1}} q_j^{c_j+1} q_{j+1}^{c_{j+1}} \cdots q_J^{c_J}. \quad (36)$$

Now, we evaluate the numerator of (35). To such a purpose, it is useful to define the following event:  $B(n, r) = \{X_1 = \dots = X_r = X_{n+1}, \{X_{r+1}, \dots, X_n\} \cap \{X_{n+1}\} = \emptyset\}$ . Then,

$$\begin{aligned} & \Pr[f_{X_{n+1}} = r, \mathbf{C}_J = \mathbf{c}, h(X_{n+1}) = j] \\ &= \Pr \left[ f_{X_{n+1}} = r, \sum_{i=1}^n I(h(X_i) = 1) = c_1, \dots, \sum_{i=1}^n I(h(X_i) = J) = c_J, h(X_{n+1}) = j \right] \\ &= \binom{n}{r} \sum_{s \in \mathbb{S}} \Pr \left[ B(n, r), X_{n+1} = s, \sum_{i=1}^n I(h(X_i) = 1) = c_1, \dots \right. \\ & \quad \left. \dots, \sum_{i=1}^n I(h(X_i) = J) = c_J, h(X_{n+1}) = j \right] \\ &= \binom{n}{r} \sum_{s \in \mathbb{S}} \Pr \left[ B(n, r), X_{n+1} = s, \sum_{i=r+1}^n I(h(X_i) = 1) = c_1, \dots \right] \end{aligned}$$

$$\begin{aligned} & \dots, \sum_{i=r+1}^n I(h(X_i) = j) = c_j - r, \dots \\ & \dots, \sum_{i=r+1}^n I(h(X_i) = J) = c_J, h(X_{n+1}) = j \Big]. \end{aligned}$$

Accordingly, the distribution of  $(f_{X_{n+1}}, \mathbf{C}_J, h(X_{n+1}))$  is completely determined by the distribution of  $(X_1, \dots, X_n, X_{n+1})$ . Therefore, from the last equation, we can write the following

$$\begin{aligned} & \Pr[f_{X_{n+1}} = r, \mathbf{C}_J = \mathbf{c}, h(X_{n+1}) = j] \\ &= \binom{n}{r} \sum_{s \in \mathbb{S}} \Pr[X_1 = \dots = X_r = X_{n+1} = s, X_{r+1} \neq s, \dots, X_n \neq s] \\ & \times \Pr \left[ \sum_{i=r+1}^n I(h(X_i) = 1) = c_1, \dots, \sum_{i=r+1}^n I(h(X_i) = j) = c_j - r, \dots \right. \\ & \quad \left. \dots, \sum_{i=r+1}^n I(h(X_i) = J) = c_J, h(X_{n+1}) = j \mid X_{r+1} \neq s, \dots, X_n \neq s, X_{n+1} = s \right] \\ &= \binom{n}{r} \sum_{s \in \mathbb{S}} p_s^{r+1} (1 - p_s)^{n-r} I(s \in \mathbb{S} : h(s) = j) \\ & \times \Pr \left[ \sum_{i=r+1}^n I(h(X_i) = 1) = c_1, \dots, \sum_{i=r+1}^n I(h(X_i) = j) = c_j - r, \dots \right. \\ & \quad \left. \dots, \sum_{i=r+1}^n I(h(X_i) = J) = c_J \mid X_{r+1} \neq s, \dots, X_n \neq s, X_{n+1} = s \right]. \end{aligned}$$

Based on the last identity, we can write the conditional probability of  $f_{X_{n+1}}$ , given  $\mathbf{C}_J$  and  $h(X_{n+1})$ , with respect to the distribution  $P_j$  on  $\mathbb{S}_j$ . In particular, we can write the following:

$$\begin{aligned} & \Pr[f_{X_{n+1}} = r, \mathbf{C}_J = \mathbf{c}, h(X_{n+1}) = j] \\ &= \binom{n}{r} \sum_{s \in \mathbb{S}_j} p_s^{r+1} (1 - p_s)^{n-r} \\ & \quad \times \binom{n-r}{c_1, \dots, c_j - r, \dots, c_J} \left( \frac{q_1}{1 - p_s} \right)^{c_1} \dots \left( \frac{q_j - p_s}{1 - p_s} \right)^{c_j - r} \dots \left( \frac{q_J}{1 - p_s} \right)^{c_J} \\ &= \binom{n}{r} \sum_{s \in \mathbb{S}_j} p_s^{r+1} \\ & \quad \times \binom{n-r}{c_1, \dots, c_j - r, \dots, c_J} q_1^{c_1} \dots (q_j - p_s)^{c_j - r} \dots q_J^{c_J} \\ &= \binom{n}{r} \sum_{s \in \mathbb{S}_j} q_j^{c_j - r} p_s^{r+1} \\ & \quad \times \binom{n-r}{c_1, \dots, c_j - r, \dots, c_J} q_1^{c_1} \dots \left( 1 - \frac{p_s}{q_j} \right)^{c_j - r} \dots q_J^{c_J} \end{aligned}$$

$$\begin{aligned}
&= \binom{n}{r} \sum_{s \in \mathbb{S}_j} q_j^{c_j+1} \left( \frac{p_s}{q_j} \right)^{r+1} \\
&\quad \times \binom{n-r}{c_1, \dots, c_j-r, \dots, c_J} q_1^{c_1} \cdots \left( 1 - \frac{p_s}{q_j} \right)^{c_j-r} \cdots q_J^{c_J} \\
&= \binom{n}{r} \frac{\binom{n-r}{c_1, \dots, c_j-r, \dots, c_J}}{\binom{c_j}{r}} q_j^{c_j+1} \prod_{1 \leq i \neq j \leq J} q_i^{c_i} \sum_{s \in \mathbb{S}_j} \binom{c_j}{r} \left( \frac{p_s}{q_j} \right)^{r+1} \left( 1 - \frac{p_s}{q_j} \right)^{c_j-r} \\
&= \binom{n}{c_1, \dots, c_J} q_j^{c_j+1} \prod_{1 \leq i \neq j \leq J} q_i^{c_i} \sum_{s \in \mathbb{S}_j} \binom{c_j}{r} \left( \frac{p_s}{q_j} \right)^{r+1} \left( 1 - \frac{p_s}{q_j} \right)^{c_j-r}. \tag{37}
\end{aligned}$$

Therefore, according to (35), which is combined with (36) and (37), we obtain the following:

$$\begin{aligned}
&\Pr[f_{X_{n+1}} = r \mid \mathbf{C}_J = \mathbf{c}, h(X_{n+1}) = j] \\
&= \frac{\binom{n}{c_1, \dots, c_J} q_j^{c_j+1} \prod_{1 \leq i \neq j \leq J} q_i^{c_i} \sum_{s \in \mathbb{S}_j} \binom{c_j}{r} \left( \frac{p_s}{q_j} \right)^{r+1} \left( 1 - \frac{p_s}{q_j} \right)^{c_j-r}}{\binom{n}{c_1, \dots, c_J} q_1 \cdots q_{j-1}^{c_{j-1}} q_j^{c_j+1} q_{j+1}^{c_{j+1}} \cdots q_J^{c_J}} \\
&= \sum_{s \in \mathbb{S}_j} \binom{c_j}{r} \left( \frac{p_s}{q_j} \right)^{r+1} \left( 1 - \frac{p_s}{q_j} \right)^{c_j-r} \\
&= \binom{c_j}{r} \sum_{s \in \mathbb{S}_j} \left( \frac{p_s}{q_j} \right)^{r+1} \left( 1 - \frac{p_s}{q_j} \right)^{c_j-r},
\end{aligned}$$

which is a functional of  $P_j = \sum_{s \in \mathbb{S}_j} (p_s/q_j) \delta_s$  on  $\mathbb{S}_j$ , for  $j = 1, \dots, J$ . This completes the proof.

### B.1.2 Proof of Equation (5)

Under the statistical model (1), the  $X_i$ 's that are hashed into the  $j$ -th bucket form a random sample from  $P_j = \sum_{s \in \mathbb{S}_j} (p_s/q_j) \delta_s$ . We assume that such a random sample features  $K_{c_j} \leq c_j$  distinct symbols, and for any  $s \in \mathbb{S}_j$  we denote by  $N_{s,c_j} = \sum_{1 \leq i \leq c_j} I(X_i = s)$  the frequency of the symbol  $s$ , such that  $0 \leq N_{s,c_j} \leq c_j$  and  $\sum_{s \in \mathbb{S}_j} N_{s,c_j} = c_j$ . Then, for  $r = 1, \dots, c_j$

$$M_{r,c_j} = \sum_{s \in \mathbb{S}_j} I(N_{s,c_j} = r)$$

such that  $K_{c_j} = \sum_{1 \leq r \leq c_j} M_{r,c_j}$  and  $c_j = \sum_{1 \leq r \leq c_j} r M_{r,c_j}$ . Accordingly, we can write that

$$\begin{aligned}
\mathbb{E}_{P_j}[M_{r,c_j}] &= \mathbb{E} \left[ \sum_{s \in \mathbb{S}_j} I(N_{s,c_j} = r) \right] \\
&= \sum_{s \in \mathbb{S}_j} \Pr[N_{s,c_j} = r]
\end{aligned}$$

$$\begin{aligned}
&= \sum_{s \in \mathbb{S}_j} \binom{c_j}{r} \left( \frac{p_s}{q_j} \right)^r \left( 1 - \frac{p_s}{q_j} \right)^{c_j - r} \\
&= \sum_{s \in \mathbb{S}_j} \binom{c_j}{r} \left( \frac{p_s}{q_j} \right)^r \left( 1 - \frac{p_s}{q_j} \right)^{c_j - r},
\end{aligned}$$

i.e.

$$\begin{aligned}
\mathbb{E}_{P_j}[M_{r+1, c_j+1}] &= \sum_{s \in \mathbb{S}_j} \binom{c_j + 1}{r + 1} \left( \frac{p_s}{q_j} \right)^{r+1} \left( 1 - \frac{p_s}{q_j} \right)^{c_j+1-r-1} \\
&= \frac{c_j + 1}{r + 1} \sum_{s \in \mathbb{S}_j} \binom{c_j}{r} \left( \frac{p_s}{q_j} \right)^{r+1} \left( 1 - \frac{p_s}{q_j} \right)^{c_j - r}. \tag{38}
\end{aligned}$$

The proof is completed by comparing (38) with the expression of  $\pi_j(r, P)$  in Equation (3).

## B.2 Worst case analysis

For notation's sake, we define a slightly different class of distributions for our worst-case analysis, that allows us to take into account the number of support points of each  $P_j$ . Let

$$\mathcal{P}_{J,K} := \{P \text{ such that } P_j \text{ has at most } K \text{ support points for each } j = 1, \dots, J\}.$$

Of course,  $\mathcal{P}_L \subseteq \mathcal{P}_{J,K}$ . The main technical result to prove Theorem 2 is the following lemma.

**Lemma 1.** *Let  $K > 0$ . For any  $P \in \mathcal{P}_{J,K}$  we have*

$$R(\hat{f}_\beta; P) \leq \max_{A_J, B_J, C, D \in \Omega} \beta^2 n A_J + n(n-1) \left( \beta^2 - \frac{2\beta}{K} \right) B_J + nC + n(n-1)D, \tag{39}$$

where the maximum is taken over the set  $\Omega := \{(a, b, c, d) \in [0, 1]^4 : a \geq b, a \geq c, b \geq d, c \geq d\}$ , such that  $A_J := \sum_{1 \leq j \leq J} q_j^2$ ,  $B_J := \sum_{1 \leq j \leq J} q_j^3$ ,  $C := \sum_{s \in \mathbb{S}} p_s^2$  and  $D := \sum_{s \in \mathbb{S}} p_s^3$ .

*Proof.* As a first step, we write the quadratic risk  $R(f_\beta, P) = \mathbb{E}_P[(\beta C_{h(X_{n+1})} - f_{X_{n+1}})^2]$  as follows:

$$R(f_\beta, P) = \mathbb{E}_P \left[ \left( \sum_{i=1}^n \beta I(h(X_{n+1}) = h(X_i)) - I(X_i = X_{n+1}) \right)^2 \right],$$

where

$$\begin{aligned}
&\left( \sum_{i=1}^n \beta I(h(X_{n+1}) = h(X_i)) - I(X_i = X_{n+1}) \right)^2 \\
&= \beta^2 \sum_{i,l=1}^n I(h(X_{n+1}) = h(X_i)) I(h(X_{n+1}) = h(X_l)) \\
&\quad - 2\beta \sum_{i,l=1}^n I(h(X_{n+1}) = h(X_i)) I(X_{n+1} = X_l) + \sum_{i,l=1}^n I(X_{n+1} = X_i) I(X_{n+1} = X_l).
\end{aligned}$$



Hence,

$$R(f_\beta, P) = \beta^2 \sum_{i,l=1}^n \Pr[h(X_{n+1}) = h(X_i) = h(X_l)] \\ - 2\beta \sum_{i,l=1}^n \Pr[h(X_{n+1}) = h(X_i), X_{n+1} = X_l] + \sum_{i,l=1}^n \Pr[X_i = X_l = X_{n+1}]$$

Now, we consider each term separately. In particular, by separating the cases  $i = l$  and  $i \neq l$  we get

$$\sum_{i,l=1}^n \Pr[h(X_{n+1}) = h(X_i) = h(X_l)] = n \sum_{j=1}^J q_j^2 + n(n-1) \sum_{j=1}^J q_j^3, \\ \sum_{i,l=1}^n \Pr[h(X_{n+1}) = h(X_i), X_{n+1} = X_l] = n \sum_{s \in \mathbb{S}} p_s^2 + n(n-1) \sum_{j=1}^J q_j \sum_{s \in \mathbb{S}_j} p_s^2$$

and

$$\sum_{i,l=1}^n \Pr[X_i = X_l = X_{n+1}] = n \sum_{s \in \mathbb{S}} p_s^2 + n(n-1) \sum_{s \in \mathbb{S}} p_s^3,$$

i.e.,

$$R(f_\beta, P) = \beta^2 \left( n \sum_{j=1}^J q_j^2 + n(n-1) \sum_{j=1}^J q_j^3 \right) \\ - 2\beta \left( n \sum_{s \in \mathbb{S}} p_s^2 + n(n-1) \sum_{j=1}^J q_j \sum_{s \in \mathbb{S}_j} p_s^2 \right) + n \sum_{s \in \mathbb{S}} p_s^2 + n(n-1) \sum_{s \in \mathbb{S}} p_s^3.$$

Now, let us focus on the set of distributions with at most  $K \times J$  support points, such that each the distribution  $P_j$  has at most  $K$  support points. Under this assumption it holds that  $\sum_{s \in \mathbb{S}} p_s^2 \geq \frac{1}{KJ}$ , where equality is achieved for  $p_s = (KJ)^{-1}$ . Moreover, we can write

$$\sum_{j=1}^J q_j \sum_{s \in \mathbb{S}_j} p_s^2 = \sum_{j=1}^J q_j^3 \sum_{s \in \mathbb{S}_j} \left( \frac{p_s}{\pi_j} \right)^2 \geq \sum_{j=1}^J \frac{q_j^3}{K}.$$

Hence

$$R(f_\beta, P) \leq \beta^2 \left( n \sum_{j=1}^J q_j^2 + n(n-1) \sum_{j=1}^J q_j^3 \right) \\ - 2\beta \left( \frac{n}{KJ} + \sum_{j=1}^J \frac{q_j^3}{K} \right) + n \sum_{s \in \mathbb{S}} p_s^2 + n(n-1) \sum_{s \in \mathbb{S}} p_s^3,$$

which completes the proof.  $\square$

Then, the proof of Theorem 2 follows by noticing that for  $K$  large enough, in such a way that  $\beta^2 - \frac{2\beta}{K} > 0$ , then the maximum on the right-hand side of (39) is obtained by setting  $A_J = B_J = C = D = 1$ , which entails  $P \equiv P^*$ , with  $P^*$  being a degenerate distribution on  $s^* \in \mathbb{S}$ . By minimizing, with respect to  $\beta$ , the risk function associated with the degenerate distribution  $P^*$ , we get  $\beta = 1$ . That is, the resulting estimator for  $f_{X_{n+1}}$  is

$$\hat{f}_1 = C_{h(X_{n+1})}.$$

### B.3 An algorithmic solution to the minimax risk for frequency estimation

In the minimax framework, we look for  $\beta$  and  $P$  that solve the following optimization problem

$$\inf_{\beta \in \mathbb{R}} \sup_{P \in \Delta_{K,J}} R(f_\beta, P), \quad (40)$$

where  $\Delta_{K,J}$  is the set of distributions on  $\mathbb{S}$  such that, when restricted on each  $\mathbb{S}_j$ ,  $P$  gives positive mass to at most  $K$  elements. The problem (40) is convex in  $\beta$  but is not concave in  $P$ . Then, looking for an analytic solution, or checking that a particular  $(\beta, P)$  is a solution, is a non-trivial task (this might be impossible or, at least, NP-Hard). Here, we rely on numerical software in order to approximate (40). By using the epigraph representation of the minimax problem, we consider the constrained (equivalent) optimization

$$\begin{aligned} & \inf_{\beta \in \mathbb{R}} Z \\ & \text{sub. } Z \geq R(f_\beta, P) \\ & P \in \Delta_{K,J}, \end{aligned}$$

which is amenable to numerical optimization. We make use the Python package Pyomo as an interface to the IpoptSolver, which is the state of the art solver for constrained optimization. Since the problem is not concave in  $P$ , there will be locally-optimal solutions to (40). We run the algorithm several times with different starting points for  $P$  and  $\beta$ , using the high-confidence criterion for the number of restarts (Dick et al., 2014). We set  $n = 10,000$  and let  $J = 10, 25, 50$ ,  $K = 10, 25, 50, 100$ . For all such values, we find that the numerical solution to (40) identifies as optimal parameters  $\beta^* = 1/K$  and  $P^*$  being the uniform distribution over the  $K \times J$  support points. Figure 9 summarizes these findings.

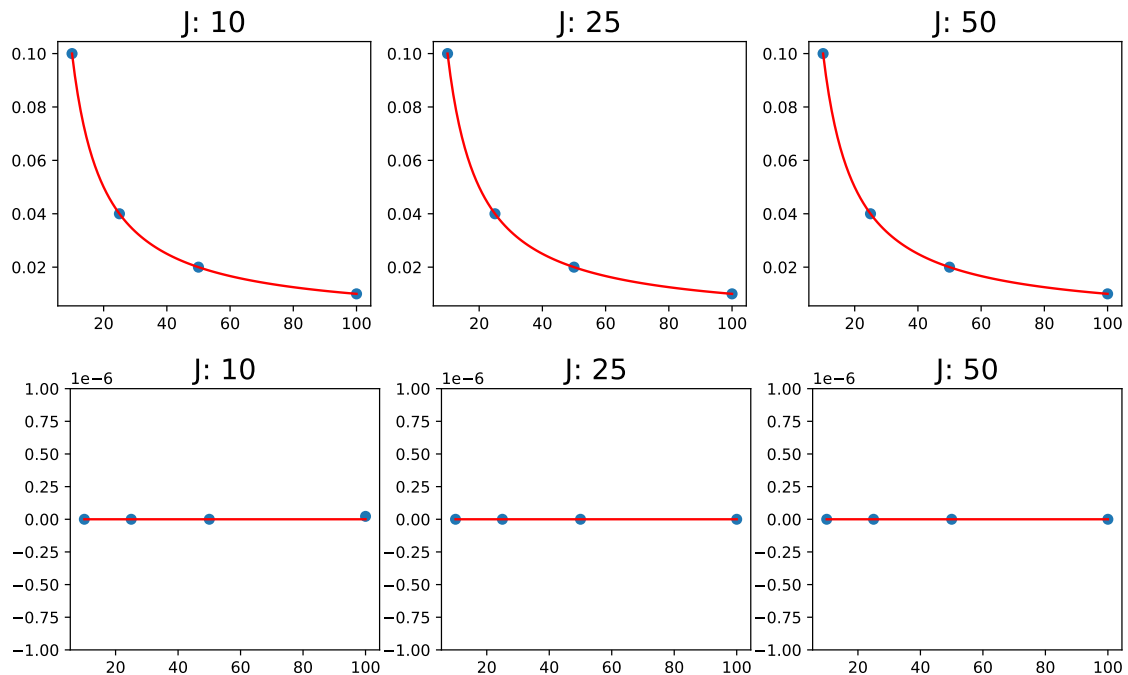


Figure 9: Top row: the coefficients  $\beta^*$  found numerically (blue dots) as  $K$  varies on the x-axis. The red line is  $1/K$ . Bottom row: total variation distance between  $P^*$  found numerically and the uniform distribution.

## B.4 Proofs for Section 3

### B.4.1 Proof of Theorem 3

The proof combines the restriction property of NRMs with some identities for functionals of NRMs. In particular, from the restriction property,  $P_j \sim \text{NRM}(\theta/J, JG_{0, \mathbb{S}_j}, \rho)$  such that

$$\pi_j(r) = \mathbb{E}_{P_j \sim \text{NRM}(\theta/J, JG_{0, \mathbb{S}_j}, \rho)} \left[ \binom{c_j}{r} \sum_{s \in \mathbb{S}_j} \left( \frac{p_s}{q_j} \right)^{r+1} \left( 1 - \frac{p_s}{q_j} \right)^{c_j - r} \right], \quad (41)$$

for  $j = 1, \dots, J$ . Let  $\tilde{\mu}_j$  be a CRM on  $\mathbb{S}_j$  with Lévy intensity  $\nu(dx, ds) = \theta G_{0, \mathbb{S}_j}(ds)\rho(dx)$ , such that

$$P_j(\cdot) = \frac{\tilde{\mu}_j(\cdot)}{T_j}$$

with  $T_j$  being the total mass of  $\tilde{\mu}_j$ , i.e.  $T_j = \tilde{\mu}_j(\mathbb{S}_j)$ , whose distribution has density function denoted by  $f_{T_j}$ . Then, from Pitman (2003, Equation 11) the right-hand side of (41) is

$$\binom{c_j}{r} \int_0^1 v^r (1-v)^{c_j - r} f_{V_j}(v) dv$$

where

$$f_{V_j}(v) = \frac{\theta}{J} v \int_0^{+\infty} t \rho(tv) f_{T_j}(t(1-v)) dt,$$

follows from Pitman (2003, Lemma 1), i.e. Pitman (2003, Equation 25). This completes the proof.

#### B.4.2 Proof of Equation (11)

The proof follows by combining the general form (9) with the Lévy intensity (10). In particular, if  $P \sim \text{DP}(\theta, G_0)$  then by the restriction property  $P_j \sim \text{DP}(\theta/J, JG_{0, \mathbb{S}_j})$ , for  $j = 1, \dots, J$ . That is,  $P_j$  is a NRM obtained by normalizing a CRM  $\tilde{\mu}_j$  on  $\mathbb{S}_j$  with Lévy intensity

$$\nu(dx, ds) = \theta G_{0, \mathbb{S}_j}(ds) \frac{e^{-x}}{x} dx. \quad (42)$$

From (42), by means of the Lévy-Khintchine formula for the Laplace functional of  $\mu_j$ , one has

$$f_{T_j}(t) = \frac{1}{\Gamma(\theta/J)} t^{\theta/J-1} e^{-t}, \quad (43)$$

(Pitman, 2003, Section 5.1). Then, by combining (9) with (42) and (43) we can write that

$$\begin{aligned} f_{V_j}(v) &= \frac{\theta}{J} v \int_0^{+\infty} t \frac{e^{-tv}}{tv} \frac{1}{\Gamma(\theta/J)} (t(1-v))^{\theta/J-1} e^{-t(1-v)} dt \\ &= \frac{\theta/J}{\Gamma(\theta/J)} \int_0^{+\infty} (t(1-v))^{\theta/J-1} e^{-t} dt \\ &= \frac{\theta/J}{\Gamma(\theta/J)} (1-v)^{\theta/J-1} \int_0^{+\infty} t^{\theta/J-1} e^{-t} dt \\ &= \frac{\theta}{J} (1-v)^{\theta/J-1}, \end{aligned}$$

which is the density function of a Beta distribution with parameter  $(1, \theta/J)$ . The proof is completed.

#### B.4.3 Proof of Proposition 4

It is useful to recall the expression of  $\varepsilon_f(P)$  and  $\varepsilon_k(P)$  in terms of the  $\pi_j(r, P)$ 's, i.e.,

$$\varepsilon_f(P) = \sum_{r=0}^{c_j} r \pi_j(r, P) \quad (44)$$

and

$$\varepsilon_k(P) = \sum_{j=1}^J q_j \sum_{r=0}^{c_j} \frac{n}{r+1} \pi_j(r, P) \quad (45)$$

from (4) and (22), respectively. The estimator of  $f_{X_{n+1}}$  then follows from (44) by replacing the probabilities  $\pi_j(r, P)$ 's with the estimated probabilities  $\pi_j(r)$  in (12):

$$\begin{aligned}\hat{f}_{X_{n+1}}^{(\text{DP})} &= \sum_{r=0}^{c_j} r \int_0^1 \binom{c_j}{r} v^r (1-v)^{c_j-r} f_{V_\theta}(v) dv \\ &= c_j \int_0^1 v f_{V_\theta}(v) dv \\ &= c_j \frac{J}{\theta + J}.\end{aligned}$$

#### B.4.4 Proof of Theorem 5

We start by observing that  $\hat{f}_{X_{n+1}}^{NRM} = \mathbb{E}_{P \sim NRM} [\varepsilon_f(P)] = \sum_{r=0}^{c_j} r \pi_j(r)$ , where  $\pi_j$  is defined in Theorem 3, depends on the sketch  $\mathbf{C}_J$  only through  $C_{h(X_{n+1})}$  by definition. On the other hand, the Bayesian posterior in Theorem 2.2 in Beraha and Favaro (2023) depends, in general, on the whole sketch. Furthermore, Theorem 2.3 in Beraha and Favaro (2023) characterizes the DP as the sole Poisson-Kingman (a fortiori, the only NRM) for which the posterior of  $f_{X_{n+1}}$  depends on  $\mathbf{C}$  only through  $C_{h(X_{n+1})}$ . The proof is concluded by noting the equality between the posterior under the DP prior (Cai et al., 2018; Dolera et al., 2023) and  $\hat{f}_{X_{n+1}}^{DP}$  in Proposition 4.

#### B.4.5 Proof of Equation (16)

As for the case of the DP, with respect to Equation (11), the proof follows by combining the general form (9) with the Lévy intensity (15). In particular, if  $P \sim \text{NGGP}(\theta, G_0, \alpha, \tau)$  then by the restriction property  $P_j \sim \text{NGGP}(\theta/J, JG_{0, \mathbb{S}_j}, \alpha, \tau)$ , for  $j = 1, \dots, J$ . That is,  $P_j$  is a NRM obtained by normalizing a CRM  $\tilde{\mu}_j$  on  $\mathbb{S}_j$  with Lévy intensity

$$\nu(dx, ds) = \theta G_{0, \mathbb{S}_j}(ds) \frac{1}{\Gamma(1-\alpha)} x^{-1-\alpha} e^{-\tau x}. \quad (46)$$

From (46), by means of the Lévy-Khintchine formula for the Laplace functional of  $\mu_j$ , one has

$$f_{T_j}(t) = e^{\frac{(\theta/J)\tau\alpha}{\alpha}} e^{-\tau t} f_\alpha(t), \quad (47)$$

where  $f_\alpha$  is a density function such that  $\int_0^{+\infty} \exp\{-\lambda t\} f_\alpha(t) dt = \exp\{-(\theta/\alpha J)\lambda^\alpha\}$  (Pitman, 2003, Section 5.4). Then, by combining (9) with (46) and (47) we can write that

$$\begin{aligned}f_{V_j}(v) &= \frac{\theta}{J} v \int_0^{+\infty} t \frac{1}{\Gamma(1-\alpha)} (tv)^{-1-\alpha} e^{-\tau tv} e^{\frac{(\theta/J)\tau\alpha}{\alpha}} e^{-\tau t(1-v)} f_\alpha(t(1-v)) dt \\ &= \frac{\theta/J}{\Gamma(1-\alpha)} e^{\frac{(\theta/J)\tau\alpha}{\alpha}} v^{-\alpha} \int_0^{+\infty} t^{-\alpha} e^{-\tau t} f_\alpha(t(1-v)) dt \\ &= \frac{\theta/J}{\Gamma(1-\alpha)} e^{\frac{(\theta/J)\tau\alpha}{\alpha}} v^{-\alpha} (1-v)^{\alpha-1} \int_0^{+\infty} z^{-\alpha} e^{-\tau \frac{z}{1-v}} f_\alpha(z) dz\end{aligned}$$

$$\begin{aligned}
& [\text{by using } z^{-\alpha} = \frac{1}{\Gamma(\alpha)} \int_0^{+\infty} y^{\alpha-1} e^{-yz} dy] \\
&= \frac{\theta/J}{\Gamma(1-\alpha)} e^{\frac{(\theta/J)\tau^\alpha}{\alpha}} v^{-\alpha} (1-v)^{\alpha-1} \int_0^{+\infty} \left( \frac{1}{\Gamma(\alpha)} \int_0^{+\infty} y^{\alpha-1} e^{-yz} dy \right) e^{-\tau \frac{z}{1-v}} f_\alpha(z) dz \\
&= \frac{\theta/J}{\Gamma(\alpha)\Gamma(1-\alpha)} e^{\frac{(\theta/J)\tau^\alpha}{\alpha}} v^{-\alpha} (1-v)^{\alpha-1} \int_0^{+\infty} \int_0^{+\infty} y^{\alpha-1} e^{-z(y + \frac{\tau}{1-v})} f_\alpha(z) dz dy \\
&= \frac{\theta/J}{\Gamma(\alpha)\Gamma(1-\alpha)} e^{\frac{(\theta/J)\tau^\alpha}{\alpha}} v^{-\alpha} (1-v)^{\alpha-1} \int_0^{+\infty} y^{\alpha-1} e^{-\frac{\theta/J}{\alpha} (y + \frac{\tau}{1-v})} dy \\
&= \frac{\theta/J}{\Gamma(\alpha)\Gamma(1-\alpha)} e^{\frac{(\theta/J)\tau^\alpha}{\alpha}} v^{-\alpha} (1-v)^{\alpha-1} \int_0^{+\infty} y^{\alpha-1} e^{-\frac{(\theta/J)\tau^\alpha}{\alpha} (\frac{y}{\tau} + \frac{1}{1-v})} dy \\
& [\text{by the change of variable } h = y/\tau] \\
&= \tau^\alpha \frac{\theta/J}{\Gamma(\alpha)\Gamma(1-\alpha)} e^{\frac{(\theta/J)\tau^\alpha}{\alpha}} v^{-\alpha} (1-v)^{\alpha-1} \int_0^{+\infty} h^{\alpha-1} e^{-\frac{(\theta/J)\tau^\alpha}{\alpha} (h + \frac{1}{1-v})} dh \\
& [\text{by the change of variable } y = (h - hp + p)/(h - hp + 1)] \\
&= \tau^\alpha \frac{\theta/J}{\Gamma(\alpha)\Gamma(1-\alpha)} e^{\frac{(\theta/J)\tau^\alpha}{\alpha}} v^{-\alpha} (1-v)^{\alpha-1} \\
&\quad \times \int_0^{+\infty} \frac{1}{(1-y)^2} \left( \frac{y-v}{(1-v)(1-y)} \right)^{\alpha-1} e^{-\frac{(\theta/J)\tau^\alpha}{\alpha} (\frac{y-v}{(1-v)(1-y)} + \frac{1}{1-v})} dy \\
&= \tau^\alpha \frac{\theta/J}{\Gamma(\alpha)\Gamma(1-\alpha)} e^{\frac{(\theta/J)\tau^\alpha}{\alpha}} v^{-\alpha} \\
&\quad \times \int_v^1 (y-v)^{\alpha-1} (1-y)^{-\alpha-1} e^{-\frac{(\theta/J)\tau^\alpha}{\alpha} (1-y)^{-\alpha}} dy \\
&= \tau^\alpha \frac{\theta/J}{\Gamma(\alpha)\Gamma(1-\alpha)} e^{\frac{(\theta/J)\tau^\alpha}{\alpha}} \\
&\quad \times \int_v^1 \frac{1}{y} \left( \frac{v}{y} \right)^{1-\alpha-1} \left( 1 - \frac{v}{y} \right)^{\alpha-1} (1-y)^{-\alpha-1} e^{-\frac{(\theta/J)\tau^\alpha}{\alpha} (1-y)^{-\alpha}} dy,
\end{aligned}$$

which is the density function of the distribution of the product of two independent random variables: i) a Beta random variable with parameter  $(1-\alpha, \alpha)$ ; ii) the random variable

$$1 - \left( \frac{\frac{\theta\tau^\alpha}{J\alpha}}{\frac{\theta\tau^\alpha}{J\alpha} + E} \right)^{1/\alpha},$$

with  $E$  being a negative Exponential random variable with parameter 1. The proof is completed.

#### B.4.6 Proof of Proposition 6

It is useful to recall the expression of  $\varepsilon_f(P)$  and  $\varepsilon_k(P)$  in terms of the  $\pi_j(r, P)$ 's, i.e.,

$$\varepsilon_f(P) = \sum_{r=0}^{c_j} r \pi_j(r, P) \quad (48)$$

and

$$\varepsilon_k(P) = \sum_{j=1}^J q_j \sum_{r=0}^{c_j} \frac{n}{r+1} \pi_j(r, P) \quad (49)$$

from (4) and (22), respectively. Then, the estimator of  $f_{X_{n+1}}$  follows from (48) by replacing the probabilities  $\pi_j(r, P)$ 's with the estimated probabilities  $\pi_j(r)$  in (17):

$$\begin{aligned} \hat{f}_{X_{n+1}}^{(\text{NGGP})} &= \sum_{r=0}^{c_j} r \int_0^1 \binom{c_j}{r} v^r (1-v)^{c_j-r} f_{V_{\theta, \alpha, \tau}}(v) dv \\ &= c_j \int_0^1 v f_{V_{\theta, \alpha, \tau}}(v) dv \\ &= c_j \mathbb{E} \left[ B_{1-\alpha, \alpha} \left( 1 - \left( \frac{\frac{\theta \tau^\alpha}{J\alpha}}{\frac{\theta \tau^\alpha}{J\alpha} + E} \right)^{1/\alpha} \right) \right] \\ &= c_j (1-\alpha) \left( 1 - \mathbb{E} \left[ \left( \frac{\frac{\theta \tau^\alpha}{J\alpha}}{\frac{\theta \tau^\alpha}{J\alpha} + E} \right)^{1/\alpha} \right] \right) \\ &= c_j (1-\alpha) \left( 1 - \frac{\theta \tau^\alpha}{J\alpha} e^{\frac{\theta \tau^\alpha}{J\alpha}} E_{1/\alpha} \left( \frac{\theta \tau^\alpha}{J\alpha} \right) \right), \end{aligned}$$

where  $E$  denotes the exponential integral function, defined as the integral  $E_a(z) = \int_1^{+\infty} x^{-a} \exp\{-zx\} dx$ .

## C Further details on cardinality recovery

### C.1 Proofs for Section 4.1

#### C.1.1 $\varepsilon_k(P)$ as a linear functional of $\mathbf{p}_{r,n}$

For some  $\beta > 0$ , we denote by  $\tilde{\mathbf{p}}_{n,r} = \beta m_{r+1}$  an estimator of the coverage probability  $\mathbf{p}_{n,r}$ , which is a linear function of  $m_{r+1}$ , for  $r = 1, \dots, n$ . Now, we replace the coverage probability  $\mathbf{p}_{n,r}$  in (20) with its estimator  $\tilde{\mathbf{p}}_{n,r}$ . In particular, for any  $r = 0, 1, \dots, c_j$  we can write

$$\Pr[f_{X_{n+1}} = r \mid \mathbf{C}_J = \mathbf{c}] = \sum_{\mathbf{m} \in \mathcal{M}_{n,J}} \beta m_{r+1} \Pr[\mathbf{M}_n = \mathbf{m} \mid \mathbf{C}_J = \mathbf{c}],$$

i.e.

$$\begin{aligned} \mathbb{E}_P[M_{r+1,n} \mid \mathbf{C}_J = \mathbf{c}] &= \sum_{\mathbf{m} \in \mathcal{M}_{n,J}} m_{r+1} \Pr[\mathbf{M}_n = \mathbf{m} \mid \mathbf{C}_J = \mathbf{c}] \\ &= \frac{1}{\beta} \Pr[f_{X_{n+1}} = r \mid \mathbf{C}_J = \mathbf{c}]. \end{aligned}$$

Since  $K_n = \sum_{1 \leq r \leq n} M_{r,n}$ , we can exploit this relation to obtain  $\mathbb{E}_P[K_n \mid \mathbf{C}_J = \mathbf{c}]$ , that is

$$\mathbb{E}_P[K_n \mid \mathbf{C}_J = \mathbf{c}] = \sum_{r=0}^{n-1} \mathbb{E}_P[M_{r+1,n} \mid \mathbf{C}_J = \mathbf{c}]$$

The proof is completed, as we showed that  $\mathbb{E}_P[K_n \mid \mathbf{C}_J = \mathbf{c}]$  can be expressed as a (linear) function of  $\Pr[f_{X_{n+1}} = r \mid \mathbf{C}_J = \mathbf{c}]$ , whose expression is available from Theorem 1.

### C.1.2 Proof of Proposition 7

Along lines similar to the proof of Equation (21), we replace the coverage probability  $\mathbf{p}_{n,r}$  in (20) with the Good-Turing estimate  $\hat{\mathbf{p}}_{n,r}$ . In particular, for any  $r = 0, 1, \dots, c_j$  we can write

$$\Pr[f_{X_{n+1}} = r \mid \mathbf{C}_J = \mathbf{c}] = \sum_{\mathbf{m} \in \mathcal{M}_{n,J}} \frac{r+1}{n} m_{r+1} \Pr[\mathbf{M}_n = \mathbf{m} \mid \mathbf{C}_J = \mathbf{c}],$$

i.e.

$$\begin{aligned} \mathbb{E}_P[M_{r+1,n} \mid \mathbf{C}_J = \mathbf{c}] &= \sum_{\mathbf{m} \in \mathcal{M}_{n,J}} m_{r+1} \Pr[\mathbf{M}_n = \mathbf{m} \mid \mathbf{C}_J = \mathbf{c}] \\ &= \frac{n}{r+1} \Pr[f_{X_{n+1}} = r \mid \mathbf{C}_J = \mathbf{c}]. \end{aligned}$$

According to this expression, we can directly apply Theorem 1, from which it follows that

$$\begin{aligned} \Pr[f_{X_{n+1}} = r \mid \mathbf{C}_J = \mathbf{c}] &= \sum_{j=1}^J \Pr[f_{X_{n+1}} = r \mid \mathbf{C}_J = \mathbf{c}, h(X_{n+1}) = j] \Pr[h(X_{n+1}) = j] \\ &= \sum_{j=1}^J q_j \pi_j(r; P) \end{aligned}$$

i.e.  $\mathbb{E}_P[M_{r+1,n} \mid \mathbf{C}_J = \mathbf{c}] = \frac{n}{r+1} \sum_{1 \leq j \leq J} q_j \pi_j(r; P)$ . Now, since  $K_n = \sum_{1 \leq r \leq n} M_{r,n}$ , we write

$$\begin{aligned} \mathbb{E}_P[K_n \mid \mathbf{C}_J = \mathbf{c}] &= \sum_{r=0}^{n-1} \mathbb{E}_P[M_{r+1,n} \mid \mathbf{C}_J = \mathbf{c}] \\ &= \sum_{r=0}^{n-1} \frac{n}{r+1} \sum_{j=1}^J q_j \pi_j(r; P) \\ &= \sum_{r=0}^{n-1} \frac{n}{r+1} \sum_{j=1}^J q_j \binom{c_j}{r} \sum_{s \in \mathbb{S}_j} \left(\frac{p_s}{q_j}\right)^{r+1} \left(1 - \frac{p_s}{q_j}\right)^{c_j-r} \\ &= n \sum_{j=1}^J q_j \sum_{s \in \mathbb{S}_j} \sum_{r=0}^{n-1} \frac{1}{r+1} \binom{c_j}{r} \left(\frac{p_s}{q_j}\right)^{r+1} \left(1 - \frac{p_s}{q_j}\right)^{c_j-r} \\ &= n \sum_{j=1}^J q_j \sum_{s \in \mathbb{S}_j} \sum_{r=0}^{c_j} \frac{1}{r+1} \binom{c_j}{r} \left(\frac{p_s}{q_j}\right)^{r+1} \left(1 - \frac{p_s}{q_j}\right)^{c_j-r} \\ &= n \sum_{j=1}^J \sum_{s \in \mathbb{S}_j} \frac{q_j}{c_j+1} \left(1 - \left(1 - \frac{p_s}{q_j}\right)^{c_j+1}\right) \end{aligned}$$

with the last identity following by a summation of Binomial probabilities. The proof is completed.



## C.2 Worst-case estimation for nonparametric cardinality recovery

A worst-case analysis is more challenging in the context of estimating  $K_n$ , compared to the frequency recovery problem presented in Section 2.3, because the expression of  $\varepsilon_k(P)$  in (22) does not depend linearly on the counts of a single hash bucket, unlike that for  $\varepsilon_f(P)$  in (4). Therefore, we find it useful to take a slightly different approach in this section. Noting that  $K_n = \sum_{r=1}^n M_{r,n}$ , it is intuitive to consider the problem of nonparametric estimation of  $M_{r,n}$ —the number of distinct symbols with frequency  $r$ .

To construct a class of estimators for  $M_{r,n}$ , we will rely on the following identity.

**Lemma 2.** *The following identity holds*

$$\mathbb{E}_P[M_{r+1,n} \mid \mathbf{C}_J = \mathbf{c}] = \frac{n}{r+1} \sum_{j=1}^J q_j \frac{r+1}{c_j+1} \mathbb{E}_{P_j}[M_{r+1,c_j+1}]. \quad (50)$$

The proof of Equation (50) is similar to the proof of Proposition 7. We report it here for completeness.

*Proof.* Along lines similar to the proof of Proposition 7, we replace the coverage probability  $\mathbf{p}_{n,r}$  in (20) with the Good-Turing estimate  $\hat{\mathbf{p}}_{n,r}$ . In particular, for any  $r = 0, 1, \dots, c_j$  we can write

$$\Pr[f_{X_{n+1}} = r \mid \mathbf{C}_J = \mathbf{c}] = \sum_{\mathbf{m} \in \mathcal{M}_{n,J}} \frac{r+1}{n} m_{r+1} \Pr[\mathbf{M}_n = \mathbf{m} \mid \mathbf{C}_J = \mathbf{c}],$$

i.e.

$$\begin{aligned} \mathbb{E}_P[M_{r+1,n} \mid \mathbf{C}_J = \mathbf{c}] &= \sum_{\mathbf{m} \in \mathcal{M}_{n,J}} m_{r+1} \Pr[\mathbf{M}_n = \mathbf{m} \mid \mathbf{C}_J = \mathbf{c}] \\ &= \frac{n}{r+1} \Pr[f_{X_{n+1}} = r \mid \mathbf{C}_J = \mathbf{c}]. \end{aligned}$$

According to this expression, we can directly apply Theorem 1, from which it follows that

$$\Pr[f_{X_{n+1}} = r \mid \mathbf{C}_J = \mathbf{c}] = \sum_{j=1}^J q_j \binom{c_j}{r} \sum_{s \in \mathbb{S}_j} \left(\frac{p_s}{q_j}\right)^{r+1} \left(1 - \frac{p_s}{q_j}\right)^{c_j-r},$$

i.e.,

$$\begin{aligned} \mathbb{E}_P[M_{r+1,n} \mid \mathbf{C}_J = \mathbf{c}] &= \frac{n}{r+1} \sum_{j=1}^J q_j \binom{c_j}{r} \sum_{s \in \mathbb{S}_j} \left(\frac{p_s}{q_j}\right)^{r+1} \left(1 - \frac{p_s}{q_j}\right)^{c_j-r} \\ &= \frac{n}{r+1} \sum_{j=1}^J q_j \frac{r+1}{c_j+1} \mathbb{E}_{P_j}[M_{r+1,c_j+1}], \end{aligned}$$

which completes the proof.  $\square$

Intuitively, the sole information available from the sketch  $\mathbf{C}_J$  about  $\mathbb{E}_{P_j}[M_{r+1,c_j+1}]$  is that  $M_{r+1,c_j+1} \leq (c_j + 1)/(r + 1)$ . Therefore, it is natural to consider the class of linear estimators  $\hat{M}_{r+1,c_j+1} := \beta_j(c_j + 1)/(r + 1)$ , with parameter  $\beta_j \in [0, 1]$ . This gives rise to the following class of estimators for  $M_{r+1,n}$ :

$$\hat{M}_\beta = \frac{n}{r+1} \sum_{j=1}^J q_j \beta_j = \frac{n}{r+1} \langle \mathbf{q}, \boldsymbol{\beta} \rangle, \quad (51)$$

where  $\langle \mathbf{q}, \boldsymbol{\beta} \rangle$  is the scalar product between  $\mathbf{q} = (q_1, \dots, q_J)$  and the  $\boldsymbol{\beta} = (\beta_1, \dots, \beta_J)$ .

The next theorem provides an upper bound for the quadratic risk  $R(\hat{M}_\beta; P) = \mathbb{E}_P[(\hat{M}_\beta - M_{r+1,n})^2]$  associated with the class of estimators defined above, under some relatively weak assumptions on the scalar product  $\langle \mathbf{q}, \boldsymbol{\beta} \rangle$ .

**Theorem 11.** *For any fixed  $r \geq 0$ , assume that  $\langle \mathbf{q}, \boldsymbol{\beta} \rangle < (r + 1)/2n$ . Then,  $R(\hat{M}_\beta; P) \leq U(\mathbf{q}, \boldsymbol{\beta})$ , where*

$$U(\mathbf{q}, \boldsymbol{\beta}) := \left( \frac{n}{r+1} \right)^2 \langle \mathbf{q}, \boldsymbol{\beta} \rangle^2 + \left( 1 - 2 \frac{n}{r+1} \langle \mathbf{q}, \boldsymbol{\beta} \rangle \right) A_{r,n} + B_{r,n}, \quad (52)$$

for

$$A_{r,n} := \binom{n}{r+1} \left( \frac{r}{n-1} \right)^r \left( 1 - \frac{r}{n-1} \right)^{n-r-1}$$

and

$$B_{r,n} := \binom{n}{r+1} \binom{n}{r+1} \left( \frac{r}{n-2} \right)^{2r} \left( 1 - \frac{2r}{n-2} \right)^{n-2r-2}.$$

*Proof.* As a first step, we write the quadratic risk associated to the estimator (51). In particular, we write

$$\begin{aligned} & \mathbb{E}_P \left[ \left( \hat{M}_{r+1,n} - M_{r+1,n} \right)^2 \right] \\ &= \left( \frac{n}{r+1} \right)^2 \langle \boldsymbol{\pi}, \boldsymbol{\beta} \rangle^2 - 2 \frac{n}{r+1} \langle \boldsymbol{\pi}, \boldsymbol{\beta} \rangle \binom{n}{r+1} \sum_{s \in \mathbb{S}} p_s^{r+1} (1 - p_s)^{n-r-1} \\ & \quad + \binom{n}{r+1} \sum_{s \in \mathbb{S}} p_s^{r+1} (1 - p_s)^{n-r-1} \\ & \quad + \binom{n}{r+1} \binom{n}{r+1} \sum_{s \neq v \in \mathbb{S}} p_s^{r+1} p_v^{r+1} (1 - p_s - p_v)^{n-2r-2}, \end{aligned} \quad (53)$$

where  $\binom{n}{x \ y} = \frac{n!}{x!y!(n-x-y)!}$ . Now, the second term and the third term on the right-hand side of (53) can be handled by using Proposition 3 in Painsky (2022c). In particular, we have

$$\sum_{s \in \mathbb{S}} p_s^{r+1} (1 - p_s)^{n-r-1} \leq \max_{q \in [0,1]} q^r (1 - q)^{n-r} = \left( \frac{r}{n-1} \right)^r \left( 1 - \frac{r}{n-1} \right)^{n-r-1}. \quad (54)$$

As far as the last term of (53) concerned, from Proposition 2 in Painsky (2022c) we can write that

$$\sum_{s \neq v \in \mathcal{S}} p_s^{r+1} p_v^{r+1} (1 - p_s - p_v)^{n-2r-2} \leq \max_{q_1, q_2 \in \Delta_2} q_1^r q_2^r (1 - q_1 - q_2)^{n-2r-2} =: \psi(q_1, q_2), \quad (55)$$

where  $\Delta_2$  is the two-dimensional simplex  $\{x, y \in [0, 1]^2 \text{ s.t. } x + y \leq 1\}$ . Also, for any  $q_1, q_2 \in \Delta_2$ ,

$$r \log q_1 + r \log q_2 = 2r \left( \frac{\log q_1 + \log q_2}{2} \right) \leq 2r \log \left( \frac{q_1 + q_2}{2} \right)$$

such that

$$\psi(q_1, q_2) \leq \psi \left( \frac{q_1 + q_2}{2}, \frac{q_1 + q_2}{2} \right),$$

i.e.,

$$\max_{q_1, q_2 \in \Delta_2} q_1^r q_2^r (1 - q_1 - q_2)^{n-2r} = \max_{q \in [0, 0.5]} q^{2r} (1 - 2q)^{n-2r-2} = \left( \frac{r}{n-2} \right)^{2r} \left( 1 - \frac{2r}{n-2} \right)^{n-2r-2}.$$

Now, if put together the above findings, under the assumption that  $\langle \mathbf{q}, \boldsymbol{\beta} \rangle < (r + 1)/2n$ , we have

$$\begin{aligned} & \mathbb{E}_P \left[ \left( \hat{M}_{r+1, n} - M_{r+1, n} \right)^2 \right] \\ & \leq \left( \frac{n}{r+1} \right)^2 \langle \boldsymbol{\pi}, \boldsymbol{\beta} \rangle^2 \\ & \quad + \left( 1 - 2 \frac{n}{r+1} \langle \boldsymbol{\pi}, \boldsymbol{\beta} \rangle \right) \binom{n}{r+1} \left( \frac{r}{n-1} \right)^r \left( 1 - \frac{r}{n-1} \right)^{n-r-1} \\ & \quad + \left( \frac{r}{n-2} \right)^{2r} \left( 1 - \frac{2r}{n-2} \right)^{n-2r-2}, \end{aligned}$$

which completes the proof.  $\square$

Note that the assumption  $\langle \mathbf{q}, \boldsymbol{\beta} \rangle < (r + 1)/2n$  relates  $\boldsymbol{\beta}$  to the distribution  $P$  through the probabilities  $q_j$ , and it is easy to check.

Since the only unknown quantity in  $U(\mathbf{q}, \boldsymbol{\beta})$  is  $\mathbf{q}$ , it makes sense to substitute the maximum likelihood estimator  $\hat{q}_j = c_j/n$  and then optimize the risk with respect to  $\boldsymbol{\beta}$ . This leads to the conclusion that the worst-case optimal  $\boldsymbol{\beta}$  is any point in  $[0, 1]^J$  satisfying

$$\sum_{j=1}^J c_j \beta_j = n \binom{n-1}{r} \left( \frac{r}{n-1} \right)^r \left( 1 - \frac{r}{n-1} \right)^{n-r}.$$

Therefore, this optimization problem unfortunately does not admit a unique solution. Plugging any of the worst-case optimal  $\boldsymbol{\beta}$  in (51), we can check from Eq. (2) in Gnedin et al. (2007) that the estimator  $\hat{M}_\beta$  coincides with the expected value of the number of symbols with frequency  $r$  in a sample of size  $n$  from a uniform distribution over  $n/r$  symbols. Therefore, as in the case of the frequency estimation

problem, the worst-case estimator is rather unsatisfactory and motivates the use of smoothed estimators also for the cardinality recovery.

Alternatively, instead of substituting the maximum likelihood estimator for  $q_j$ , we can proceed in a “min-max” fashion and study the following optimization problem

$$\min_{\boldsymbol{\beta} \in [0,1]^J} \max_{\mathbf{q} \in \Delta_J} U(\mathbf{q}, \boldsymbol{\beta}),$$

where  $U(\mathbf{q}, \boldsymbol{\beta})$  is the upper bound for the quadratic risk defined in (52) and the  $\Delta_J$  is the  $J$ -th dimensional simplex. By proceeding similarly to Appendix B.3, we assume that  $P$  has at most  $KJ$  support points and that the induced distribution  $P_j$  has at most  $K$  points, for any  $j \in [J]$ . From the discussion above, it should not be surprising that the estimator obtained is not unique and not interesting as well. Indeed, we performed an extensive numerical study (not reported here in the interest of brevity) which confirmed that the solution to minimax problem is  $q_j = 1/J$ , for each  $j \in [J]$ , while the optimal value of  $\boldsymbol{\beta}$  is not unique.

We conclude this section by emphasizing that a limitation of this worst-case analysis is that the upper bound  $U(\mathbf{q}, \boldsymbol{\beta})$  for the quadratic risk that is not tight, in contrast with the analysis of the frequency estimation problem from Section 2.3. However, the analysis presented in this section can still be informative. In fact, if  $P$  is the uniform distribution over  $n/r$  support points such that  $q_j = 1/J$ , then  $|R(\hat{M}_\beta, P) - U(\mathbf{q}, \beta)| \leq K$  where  $K$  is a constant that does not depend on  $\boldsymbol{\beta}$ . Therefore, also in the case of the cardinality recovery problem, we can see that fully nonparametric estimation is challenging and the estimators we obtain using a worst-case framework are essentially trivial. This conclusion suggests that additional modelling assumptions are needed to obtain satisfactory estimators and motivates our framework for smoothed estimation.

## C.3 Proofs for Section 4.2

### C.3.1 Proof of Proposition 8

With an argument similar to that of the proof of Proposition 4, we can see that the estimator of  $K_n$  in (23) follows from (45) by replacing the probabilities  $\pi_j(r, P)$ 's with the estimated probabilities  $\pi_j(r)$  in (12). That is,

$$\begin{aligned} \hat{K}_n^{(\text{DP})} &= \sum_{j=1}^J q_j \sum_{r=0}^{c_j} \frac{n}{r+1} \int_0^1 \binom{c_j}{r} v^r (1-v)^{c_j-r} f_{V_\theta}(v) dv \\ &= n \sum_{j=1}^J \frac{q_j}{c_j+1} \int_0^1 \frac{1 - (1-v)^{c_j+1}}{v} f_{V_\theta}(v) dv \\ &= n \sum_{j=1}^J \frac{q_j}{c_j+1} \left( \frac{\theta}{J} \psi \left( 1 + c_j + \frac{\theta}{J} \right) - \frac{\theta}{J} \psi \left( \frac{\theta}{J} \right) \right), \end{aligned}$$

where  $\psi$  denotes the digamma function, defined as  $\psi(z) = \frac{d}{dz} \log \Gamma(z)$ .

### C.3.2 Proof of Proposition 9

With an argument similar to that of the proof of Proposition 6, we can see that the estimator of  $K_n$  follows from (49) by replacing the probabilities  $\pi_j(r, P)$ 's with the estimated probabilities  $\pi_j(r)$  in (17). That is,

$$\begin{aligned}\hat{K}_n^{(\text{NGGP})} &= \sum_{j=1}^J q_j \sum_{r=0}^{c_j} \frac{n}{r+1} \int_0^1 \binom{c_j}{r} v^r (1-v)^{c_j-r} f_{V_{\theta, \alpha, \tau}}(v) dv \\ &= n \sum_{j=1}^J \frac{q_j}{c_j+1} \int_0^1 \frac{1 - (1-v)^{c_j+1}}{v} f_{V_{\theta, \alpha, \tau}}(v) dv,\end{aligned}$$

and this can not be simplified further by solving the integral in  $v$ .

## D Further details on sketches with multiple hash functions

### D.1 Distributions under the model (25)

We determine the distribution of  $\mathbf{C}_{M,J}$  and the conditional distribution of  $f_{X_{n+1}}$ , given  $\mathbf{C}_{M,J}$  and  $\mathbf{h}(X_{n+1})$ . Note that  $\mathbf{h}(X_{n+1}) \in \{1, \dots, J\}^M$ , such that for any  $\mathbf{j} \in \{1, \dots, J\}^M$ , we set

$$q_{\mathbf{j}} = \Pr[\mathbf{h}(X_{n+1}) = \mathbf{j}]. \quad (56)$$

The distribution of  $\mathbf{C}_{M,J}$  is a generalization of the Multinomial distribution. In particular, because  $\mathbf{X}_n$  is a random sample from the discrete distribution  $P$  on  $\mathbb{S}$ , then we can write,

$$\Pr[\mathbf{C}_{M,J} = \mathbf{c}] = \sum_{(j_1(1), \dots, j_M(1), \dots, (j_1(n), \dots, j_M(n))) \in S_{n, \mathbf{c}}} \prod_{i=1}^n q_{\mathbf{j}(i)} \quad (57)$$

where

$$S_{n, \mathbf{c}} = \left\{ \{1, \dots, J\}^{M \times n} : \sum_{i=1}^n I(j_1(i) = 1) = c_{1,1}, \dots, \sum_{i=1}^n I(j_M(i) = J) = c_{M,J} \right\}.$$

Now, we consider the conditional distribution of  $f_{X_{n+1}}$ , given  $\mathbf{C}_{M,J}$  and  $\mathbf{h}(X_{n+1})$ , that is

$$\Pr[f_{X_{n+1}} = r \mid \mathbf{C}_{M,J} = \mathbf{c}, \mathbf{h}(X_{n+1}) = \mathbf{j}] = \frac{\Pr[f_{X_{n+1}} = r, \mathbf{C}_{M,J} = \mathbf{c}, \mathbf{h}(X_{n+1}) = \mathbf{j}]}{\Pr[\mathbf{C}_{M,J} = \mathbf{c}, \mathbf{h}(X_{n+1}) = \mathbf{j}]} \quad (58)$$

We compute (58) by evaluating (separately) the numerator and the denominator. We start by evaluating the denominator of the conditional probability in (58). From

(57), we write

$$\begin{aligned}
& \Pr[\mathbf{C}_{M,J} = \mathbf{c}, \mathbf{h}(X_{n+1}) = \mathbf{j}] \\
&= q_{\mathbf{j}} \Pr[\mathbf{C}_{M,J} = \mathbf{c}] \\
&= q_{\mathbf{j}} \sum_{(j_1(1), \dots, j_m(1), \dots, (j_1(n), \dots, j_m(n))) \in \mathcal{S}_{n, \mathbf{c}}} \prod_{i=1}^n q_{\mathbf{j}(i)}
\end{aligned} \tag{59}$$

Now, we evaluate the numerator of the conditional probability in (58). Let us define the event  $B(n, r) = \{X_1 = \dots = X_r = X_{n+1}, \{X_{r+1}, \dots, X_n\} \cap \{X_{n+1}\} = \emptyset\}$ . Then, we write

$$\begin{aligned}
& \Pr[f_{X_{n+1}} = r, \mathbf{C}_{M,J} = \mathbf{c}, \mathbf{h}(X_{n+1}) = \mathbf{j}] \\
&= \Pr \left[ f_{X_{n+1}} = r, \sum_{i=1}^n I(h_1(X_i) = 1) = c_{1,1}, \dots, \sum_{i=1}^n I(h_1(X_i) = J) = c_{1,J}, \dots \right. \\
&\quad \dots, \sum_{i=1}^n I(h_l(X_i) = 1) = c_{l,1}, \dots, \sum_{i=1}^n I(h_l(X_i) = J) = c_{l,J}, \dots \\
&\quad \left. \dots, \sum_{i=1}^n I(h_M(X_i) = 1) = c_{M,1}, \dots, \sum_{i=1}^n I(h_M(X_i) = J) = c_{M,J}, \mathbf{h}(X_{n+1}) = \mathbf{j} \right] \\
&= \binom{n}{r} \sum_{s \in \mathbb{S}} \Pr \left[ B(n, r), X_{n+1} = s, \sum_{i=1}^n I(h_1(X_i) = 1) = c_{1,1}, \dots, \sum_{i=1}^n I(h_1(X_i) = J) = c_{1,J}, \dots \right. \\
&\quad \dots, \sum_{i=1}^n I(h_l(X_i) = 1) = c_{l,1}, \dots, \sum_{i=1}^n I(h_l(X_i) = J) = c_{l,J}, \dots \\
&\quad \left. \dots, \sum_{i=1}^n I(h_M(X_i) = 1) = c_{M,1}, \dots, \sum_{i=1}^n I(h_M(X_i) = J) = c_{M,J}, \mathbf{h}(X_{n+1}) = \mathbf{j} \right] \\
&= \binom{n}{r} \sum_{s \in \mathbb{S}} \Pr \left[ B(n, r), X_{n+1} = s, \sum_{i=r+1}^n I(h_1(X_i) = 1) = c_{1,1}, \dots \right. \\
&\quad \dots, \sum_{i=r+1}^n I(h_1(X_i) = j_1) = c_{1,j_1} - r, \dots, \sum_{i=r+1}^n I(h_1(X_i) = J) = c_{1,J}, \dots \\
&\quad \dots, \sum_{i=r+1}^n I(h_l(X_i) = 1) = c_{l,1}, \dots \\
&\quad \dots, \sum_{i=r+1}^n I(h_l(X_i) = j_l) = c_{l,j_l} - r, \dots, \sum_{i=r+1}^n I(h_l(X_i) = J) = c_{l,J}, \dots \\
&\quad \dots, \sum_{i=r+1}^n I(h_M(X_i) = 1) = c_{M,1}, \dots \\
&\quad \left. \dots, \sum_{i=r+1}^n I(h_M(X_i) = j_M) = c_{1,j_M} - r, \dots, \sum_{i=r+1}^n I(h_M(X_i) = J) = c_{M,J}, \mathbf{h}(X_{n+1}) = \mathbf{j} \right].
\end{aligned}$$

Accordingly, the distribution of  $(f_{X_{n+1}}, \mathbf{C}_{M,J}, \mathbf{h}(X_{n+1}))$  is completely determined by the distribution of  $(X_1, \dots, X_n, X_{n+1})$ . Therefore, from the previous equation, we

can write that

$$\begin{aligned}
& \Pr[f_{X_{n+1}} = r, \mathbf{C}_{M,J} = \mathbf{c}, \mathbf{h}(X_{n+1}) = \mathbf{j}] \\
&= \binom{n}{r} \sum_{s \in \mathbb{S}} \Pr[X_1 = \dots = X_r = X_{n+1} = s, X_{r+1} \neq s, \dots, X_n \neq s] \\
&\quad \times \Pr \left[ \sum_{i=r+1}^n I(h_1(X_i) = 1) = c_{1,1}, \dots, \sum_{i=r+1}^n I(h_1(X_i) = j_1) = c_{1,j_1} - r, \dots \right. \\
&\quad \dots, \sum_{i=r+1}^n I(h_1(X_i) = J) = c_{1,J}, \dots \\
&\quad \dots, \sum_{i=r+1}^n I(h_l(X_i) = 1) = c_{l,1}, \dots, \sum_{i=r+1}^n I(h_l(X_i) = j_l) = c_{l,j_l} - r, \dots \\
&\quad \dots, \sum_{i=r+1}^n I(h_l(X_i) = J) = c_{l,J}, \dots \\
&\quad \dots, \sum_{i=r+1}^n I(h_M(X_i) = 1) = c_{M,1}, \dots, \sum_{i=r+1}^n I(h_M(X_i) = j_M) = c_{1,j_M} - r, \dots \\
&\quad \left. \dots, \sum_{i=r+1}^n I(h_M(X_i) = J) = c_{M,J}, \mathbf{h}(X_{n+1}) = \mathbf{j} \mid X_{r+1} \neq s, \dots, X_n \neq s, X_{n+1} = s \right] \\
&= \binom{n}{r} \sum_{s \in \mathbb{S}} p_s^{r+1} (1 - p_s)^{n-r} I(s \in \mathbb{S} : (\mathbf{h}(s) = \mathbf{j})) \\
&\quad \times \Pr \left[ \sum_{i=r+1}^n I(h_1(X_i) = 1) = c_{1,1}, \dots, \sum_{i=r+1}^n I(h_1(X_i) = j_1) = c_{1,j_1} - r, \dots \right. \\
&\quad \dots, \sum_{i=r+1}^n I(h_1(X_i) = J) = c_{1,J}, \dots \\
&\quad \dots, \sum_{i=r+1}^n I(h_l(X_i) = 1) = c_{l,1}, \dots, \sum_{i=r+1}^n I(h_l(X_i) = j_l) = c_{l,j_l} - r, \dots \\
&\quad \dots, \sum_{i=r+1}^n I(h_l(X_i) = J) = c_{l,J}, \dots \\
&\quad \dots, \sum_{i=r+1}^n I(h_M(X_i) = 1) = c_{M,1}, \dots, \sum_{i=r+1}^n I(h_M(X_i) = j_M) = c_{1,j_M} - r, \dots \\
&\quad \left. \dots, \sum_{i=r+1}^n I(h_M(X_i) = J) = c_{M,J} \mid X_{r+1} \neq s, \dots, X_n \neq s, X_{n+1} = s \right].
\end{aligned}$$

Based on the last identity, we can define the set  $\mathbb{S}_{\mathbf{j}} = \{s \in \mathbb{S} : (\mathbf{h}(s) = \mathbf{j})\}$ , and then we write

$$\Pr[f_{X_{n+1}} = r, \mathbf{C}_{M,J} = \mathbf{c}, \mathbf{h}(X_{n+1}) = \mathbf{j}] \tag{60}$$

$$\begin{aligned}
&= \binom{n}{r} \sum_{s \in \mathbb{S}_j} p_s^{r+1} (1-p_s)^{n-r} \\
&\quad \times \sum_{(j_1(1), \dots, j_M(1), \dots, j_1(n-r), \dots, j_M(n-r)) \in S_{n-r, \mathbf{c}}} \prod_{i=1}^{n-r} \frac{(q_{\mathbf{j}(i)} - p_s I(\mathbf{j} = \mathbf{j}(i)))}{(1-p_s)} \\
&= \binom{n}{r} \sum_{s \in \mathbb{S}_j} p_s^{r+1} \sum_{(j_1(1), \dots, j_M(1), \dots, j_1(n-r), \dots, j_M(n-r)) \in S_{n-r, \mathbf{c}}} \prod_{i=1}^{n-r} (q_{\mathbf{j}(i)} - p_s I(\mathbf{j} = \mathbf{j}(i))),
\end{aligned}$$

where

$$S_{n-r, \mathbf{c}} = \left\{ \{1, \dots, J\}^{M \times n} : \sum_{i=r+1}^n I(j_1(i) = 1) = c_{1,1}, \dots, \sum_{i=r+1}^n I(j_M(i) = J) = c_{M,J} \right\}.$$

Therefore, according to (58), which is combined with (59) with and (60), we obtain the following:

$$\begin{aligned}
&\Pr[f_{X_{n+1}} = r \mid \mathbf{C}_{M,J} = \mathbf{c}, \mathbf{h}(X_{n+1}) = \mathbf{j}] \tag{61} \\
&= \binom{n}{r} \sum_{s \in \mathbb{S}_j} p_s^{r+1} \frac{\sum_{(j_1(1), \dots, j_M(1), \dots, j_1(n-r), \dots, j_M(n-r)) \in S_{n-r, \mathbf{c}}} \prod_{i=1}^{n-r} (q_{\mathbf{j}(i)} - p_s I(\mathbf{j} = \mathbf{j}(i)))}{q_{\mathbf{j}} \sum_{(j_1(1), \dots, j_M(1), \dots, j_1(n), \dots, j_M(n)) \in S_{n, \mathbf{c}}} \prod_{i=1}^n q_{\mathbf{j}(i)}}.
\end{aligned}$$

## D.2 Proof of Equation (26)

The proof relies on a direct application of the assumptions A1) and A2) to (57). In particular, used these assumptions, we can factorizes the probabilities  $q_{\mathbf{j}(i)}$ 's, and then we write

$$\prod_{i=1}^n q_{\mathbf{j}(i)} = q_{1,j_1}(1) \cdots q_{M,j_M}(1) \cdots q_{1,j_1}(n) \cdots q_{M,j_M}(n) = \prod_{l=1}^M q_{l,1}^{c_{l,1}} \cdots q_{l,J}^{c_{l,J}},$$

i.e.,

$$\begin{aligned}
\Pr[\mathbf{C}_{M,J} = \mathbf{c}] &= \sum_{(j_1(1), \dots, j_M(1), \dots, j_1(n), \dots, j_M(n)) \in S_{n, \mathbf{c}}} \prod_{i=1}^n q_{\mathbf{j}(i)} \tag{62} \\
&= \left( \sum_{(j_1(1), \dots, j_M(1), \dots, j_1(n), \dots, j_M(n)) \in S_{n, \mathbf{c}}} 1 \right) \prod_{l=1}^M q_{l,1}^{c_{l,1}} \cdots q_{l,J}^{c_{l,J}},
\end{aligned}$$

where

$$\mathcal{C}(n, \mathbf{c}) = \left( \sum_{(j_1(1), \dots, j_M(1), \dots, j_1(n), \dots, j_M(n)) \in S_{n, \mathbf{c}}} 1 \right)$$

is a (combinatorial) coefficient, depending on  $n$ ,  $M$ ,  $J$  and the  $c_{l,j}$ 's. This completes the proof.



### D.3 Proof of Theorem 10

The proof relies on a direct application of the assumptions A1) and A2) to (61). In particular, used these assumptions, we start by rewriting the denominator of (61) as follows:

$$\begin{aligned}
& \Pr[\mathbf{C}_{M,J} = \mathbf{c}, \mathbf{h}(X_{n+1}) = \mathbf{j}] & (63) \\
&= q_{1,j_1} \cdots q_{M,j_M} \\
&\quad \times \mathcal{C}(n, \mathbf{c}) \prod_{l=1}^M q_{l,1}^{c_{l,1}} \cdots q_{l,J}^{c_{l,J}} \\
&= \mathcal{C}(n, \mathbf{c}) \prod_{l=1}^M q_{l,1}^{c_{l,1}+I(j_l=1)} \cdots q_{l,J}^{c_{l,J}+I(j_l=J)} \\
&= \mathcal{C}(n, \mathbf{c}) q_{1,j_1}^{c_{1,j_1}+1} \cdots q_{M,j_M}^{c_{M,j_M}+1} \prod_{l=1}^M \prod_{1 \leq t \neq j_l \leq J} q_{l,t}^{c_{l,t}}.
\end{aligned}$$

Along similar lines, under the assumptions A1) and A2) we rewrite the denominator of (61) as follows:

$$\Pr[f_{X_{n+1}} = r, \mathbf{C}_{M,J} = \mathbf{c}, \mathbf{h}(X_{n+1}) = \mathbf{j}] \quad (64)$$

$$\begin{aligned}
&= \binom{n}{r} \sum_{s \in \mathbb{S}_j} p_s^{r+1} \\
&\quad \times \mathcal{C}(n-r, \mathbf{c}) \\
&\quad \times \prod_{l=1}^M (q_{l,1} - p_s I(j_l=1))^{c_{l,1}-rI(j_l=1)} \cdots (q_{l,J} - p_s I(j_l=J))^{c_{l,J}-rI(j_l=J)} \\
&= \binom{n}{r} \sum_{s \in \mathbb{S}_j} p_s^{r+1} \\
&\quad \times \mathcal{C}(n-r, \mathbf{c}) \\
&\quad \times \prod_{l=1}^M q_{l,1}^{c_{l,1}-rI(j_l=1)} \cdots q_{l,J}^{c_{l,J}-rI(j_l=J)} \\
&\quad \times \left(1 - \frac{p_s}{q_{l,1}} I(j_l=1)\right)^{c_{l,1}-rI(j_l=1)} \cdots \left(1 - \frac{p_s}{q_{l,J}} I(j_l=J)\right)^{c_{l,J}-rI(j_l=J)} \\
&= \binom{n}{r} \sum_{s \in \mathbb{S}_j} p_s^{r+1} & (65)
\end{aligned}$$

$$\begin{aligned}
&\quad \times \mathcal{C}(n-r, \mathbf{c}) & (66) \\
&\quad \times q_{1,j_1}^{c_{1,j_1}-r} \left(1 - \frac{p_s}{q_{1,j_1}}\right)^{c_{1,j_1}-r} \cdots q_{M,j_M}^{c_{M,j_M}-r} \left(1 - \frac{p_s}{q_{M,j_M}}\right)^{c_{M,j_M}-r} \prod_{l=1}^M \prod_{1 \leq t \neq j_l \leq J} q_{l,t}^{c_{l,t}}. & (67)
\end{aligned}$$

Finally, by combining (63) and (63), the conditional probability (61) can be written as

$$\begin{aligned}
& \Pr[f_{X_{n+1}} = r \mid \mathbf{C}_{M,J} = \mathbf{c}, \mathbf{h}(X_{n+1}) = \mathbf{j}] \\
&= \binom{n}{r} \frac{\mathcal{C}(n-r, \mathbf{c})}{\mathcal{C}(n, \mathbf{c})} \\
&\quad \times \sum_{s \in \mathbb{S}_j} p_s^{r+1} \frac{q_{1,j_1}^{c_{1,j_1}-r} \left(1 - \frac{p_s}{q_{1,j_1}}\right)^{c_{1,j_1}-r} \cdots q_{M,j_M}^{c_{M,j_M}-r} \left(1 - \frac{p_s}{q_{M,j_M}}\right)^{c_{M,j_M}-r} \prod_{l=1}^M \prod_{1 \leq t \neq j_l \leq J} q_{l,t}^{c_{l,t}}}{q_{1,j_1}^{c_{1,j_1}+1} \cdots q_{M,j_M}^{c_{M,j_M}+1} \prod_{l=1}^M \prod_{1 \leq t \neq j_l \leq J} q_{l,t}^{c_{l,t}}} \\
&= \binom{n}{r} \frac{\mathcal{C}(n-r, \mathbf{c})}{\mathcal{C}(n, \mathbf{c})} \\
&\quad \times \sum_{s \in \mathbb{S}_j} p_s^{(r+1)(1-M)} \left(\frac{p_s}{q_{1,j_1}}\right)^{r+1} \left(1 - \frac{p_s}{q_{1,j_1}}\right)^{c_{1,j_1}-r} \cdots \left(\frac{p_s}{q_{M,j_M}}\right)^{r+1} \left(1 - \frac{p_s}{q_{M,j_M}}\right)^{c_{M,j_M}-r} \\
&= \binom{n}{r} \frac{\mathcal{C}(n-r, \mathbf{c})}{\mathcal{C}(n, \mathbf{c})} \\
&\quad \times \sum_{s \in \mathbb{S}_{j_1}} \cdots \sum_{s \in \mathbb{S}_{j_M}} p_s^{(r+1)(1-M)} \left(\frac{p_s}{q_{1,j_1}}\right)^{r+1} \left(1 - \frac{p_s}{q_{1,j_1}}\right)^{c_{1,j_1}-r} \cdots \left(\frac{p_s}{q_{M,j_M}}\right)^{r+1} \left(1 - \frac{p_s}{q_{M,j_M}}\right)^{c_{M,j_M}-r} \\
&= \binom{n}{r} \frac{\mathcal{C}(n-r, \mathbf{c})}{\mathcal{C}(n, \mathbf{c})} \\
&\quad \times \sum_{s \in \mathbb{S}_{j_1}} p_s^{\left(\frac{1}{M}-1\right)(r+1)} \left(\frac{p_s}{q_{1,j_1}}\right)^{r+1} \left(1 - \frac{p_s}{q_{1,j_1}}\right)^{c_{1,j_1}-r} \cdots \\
&\quad \cdots \times \sum_{s \in \mathbb{S}_{j_M}} p_s^{\left(\frac{1}{M}-1\right)(r+1)} \left(\frac{p_s}{q_{M,j_M}}\right)^{r+1} \left(1 - \frac{p_s}{q_{M,j_M}}\right)^{c_{M,j_M}-r} \\
&= \binom{n}{r} \frac{\mathcal{C}(n-r, \mathbf{c})}{\mathcal{C}(n, \mathbf{c})} q_{1,j_1}^{\left(\frac{1}{M}-1\right)(r+1)} \cdots q_{M,j_M}^{\left(\frac{1}{M}-1\right)(r+1)} \\
&\quad \times \sum_{s \in \mathbb{S}_{j_1}} \left(\frac{p_s}{q_{1,j_1}}\right)^{\frac{r+1}{m}} \left(1 - \frac{p_s}{q_{1,j_1}}\right)^{c_{1,j_1}-r} \cdots \sum_{s \in \mathbb{S}_{j_M}} \left(\frac{p_s}{q_{M,j_M}}\right)^{\frac{r+1}{M}} \left(1 - \frac{p_s}{q_{M,j_M}}\right)^{c_{M,j_M}-r},
\end{aligned}$$

which completes the proof.

## E Estimation of the smoothing parameters: computational aspects

### E.1 The Dirichlet Process case

From the finite-dimensional laws of the Dirichlet process, it is easy to show that the sketch  $\mathbf{C}_J$  follows a Dirichlet-multinomial distribution with parameter  $(\theta/J, \dots, \theta/J)$ .

The log-likelihood is then

$$\ell(\theta; \mathbf{C}_J) \propto \log \Gamma(\theta) - \log \Gamma(\theta + n) - J \log \Gamma(\theta/J) + \sum_{j=1}^J \log \Gamma(\theta/J + c_j)$$

We choose  $\theta$  by maximizing  $\ell(\theta; \mathbf{C}_J)$  via the BFGS algorithm.

## E.2 The Normalized Generalized Gamma Process case

The finite-dimensional laws under the NGGP do not have closed-form expressions so that the likelihood of  $\mathbf{C}_J$  is not available. We consider then two strategies. The first one is more computationally efficient but applies only when we have access to a subsample of the  $X_i$ 's. This is the case, e.g., of streaming data whereby we decide to store the first  $m$  samples in memory before hashing them. Such a setting was recently considered in Sesia and Favaro (2022). The second one is more general but more demanding from the computational side.

In the first case, we estimate the parameters by maximizing the marginal likelihood of  $X_1, \dots, X_m$ . Its expression can be found in Lijoi et al. (2007) but it involves a sum of  $m$  terms (with alternating signs) involving incomplete Gamma functions. We found it essentially impossible to obtain a numerically stable procedure to evaluate such an expression for  $m > 50$ . Instead, we focus here on the alternative expression found in Proposition 3 of James et al. (2009). Denoting by  $X_1^*, \dots, X_{k_m}^*$  the  $k_m$  the unique values in  $X_1, \dots, X_m$  and by  $n_1, \dots, n_{k_m}$  their cardinalities, we have

$$\Pr[X_1 \in dx_1, \dots, X_n \in dx_n] = \frac{\theta^{k_m} e^{\beta}}{\Gamma(m)} \prod_{j=1}^{k_m} (1-\alpha)_{(n_j-1)} \int_{\mathbb{R}_+} u^{m-1} e^{-\frac{\theta}{\alpha}(\tau+u)^\alpha} (\tau+u)^{-m+k_m\alpha} du$$

where  $\beta = \theta/\alpha\tau^\alpha$  and  $(a)_{(b)}$  is the Pochhammer symbol.

For numerical stability reasons we work in the logarithmic scale so that the log-likelihood is

$$\ell(\theta; \mathbf{C}_J) \propto k_m \log \theta + \beta - k_m \log(1-\alpha) \sum_{j=1}^{k_m} \log \Gamma(n_j - \alpha) + \log (F_{m, k_m, \theta, \alpha, \tau}(u) du)$$

To evaluate the logarithm of the last integral we employ once again the log-sum-exp trick.

Given that the parameters  $\theta$  and  $\tau$  are redundant (i.e., if  $\mu \sim NGGP(\theta, \alpha, \tau, G_0)$  then for any  $q > 0$   $q\mu \sim NGGP(\theta q^\alpha, \alpha, \tau/q, G_0)$ ) we fix  $\tau = 1/2$  and optimize over  $\theta \in \mathbb{R}_+$  and  $\alpha \in (0, 1)$  using the BFGS algorithm.

If instead, we have access only to the sketch  $\mathbf{C}_J$ , we follow the approach proposed in Dolera et al. (2023) based on a minimum-distance estimator. Specifically, this consists in finding  $(\hat{\theta}, \hat{\alpha})$  that minimize

$$\mathbb{E} \left[ W_1(\mathbf{C}_J, \tilde{\mathbf{C}}_J(\theta, \alpha, m) \frac{n}{m}) \right] \quad (68)$$

where  $W_1$  is the 1-Wasserstein distance and the expectation is with respect  $\tilde{\mathbf{C}}_J(\theta, \alpha, m)$ , which is a synthetic sketch obtained by sampling  $\tilde{X}_1, \dots, \tilde{X}_m$  from the marginal distribution of an NGGP with parameter  $(\theta, \alpha, 1/2)$  and hashing them with another hash function. Note that the use of the Wasserstein distance is fundamental due to the arbitrariness of the labels attached to the  $X_i$ 's. In practice, (68) is approximated via Monte Carlo. To sample  $\tilde{X}_1, \dots, \tilde{X}_m$ , we use a generalized Pólya Urn scheme and sample  $\tilde{X}_1 \sim G_0$ ,  $\tilde{X}_2 \mid \tilde{X}_1$ , and so on. Explicit formulas for these conditional distributions are given in Eqs. (9)-(11) of Lijoi et al. (2007). However, as discussed above in the case of the marginal distribution, these involve sums of incomplete Gamma functions that are extremely prone to numerical instability. Instead, we use the generative scheme presented in Section 3.3 of James et al. (2009). We report it below.

- Sample  $\tilde{X}_1 \sim G_0$ , set  $X_1^* = \tilde{X}_1$ ,  $n_1 = 1$ ,  $k = 1$ .
- For  $i = 1, \dots, m - 1$ 
  1. Sample a latent variable  $U$  with density

$$f_U(u) \propto \frac{u^{i-1}}{(u + \tau)^{i-\alpha k}} e^{-\frac{\theta}{\alpha}((u+\tau)^\alpha - \tau^\alpha)}$$

2. Sample  $c$  from a categorical distribution over  $1, \dots, k + 1$  such that

$$\Pr[c = h \mid U = u] \propto \begin{cases} n_h - \alpha & \text{for } h = 1, \dots, k \\ \theta(u + \tau)^\alpha & \text{for } h = k + 1 \end{cases}$$

If  $c = k + 1$ , sample  $X_{k+1}^* \sim G_0$  and update  $k \mapsto k + 1$ . Set  $X_{i+1} = X_c^*$  and  $n_k \mapsto n_k + 1$ .

When sampling the latent variable  $U$ , it is more convenient to sample  $V = \log U$  whose density is

$$f_V(v) \propto \frac{e^{vi}}{(e^v + \tau)^{i-\alpha k_i}} e^{-\frac{\theta}{\alpha}((e^v + \tau)^\alpha - \tau^\alpha)}$$

which is log-concave. We employ the adaptive rejection sampling algorithm (Gilks and Wild, 1992) implemented in the Julia package `AdaptiveRejectionSampling.jl` (Tec, 2018).

## F Further Simulations

### F.1 The role on $J$ with a single hash function

We now assess the effect of the parameter  $J$ , that is the width of the hash function, letting  $J = 10, 100, 1000, 10000$  and simulating  $n = 100,000$  observations either from `PYP(100, 0.25)` or from `PYP(100, 0.75)`. Observe that in the first case, the expected numbers of distinct symbols in the sample is approximately 2200, so that when  $J = 10000$  we are likely occupying more memory than saving the original dataset

in memory. Figure 10 shows the MAEs for the frequency recovery problem as a function of  $J$ , averaged over 50 independent replications. For low frequency tokens, the MAE converges to zero as  $J$  increases, while for high frequency tokens (empirical frequency larger than 16) this does not happen even in the case of  $J = 10,000$ . Figure 11 shows the absolute error between the true number of distinct symbols and the estimated one, as a function of  $J$ , averaged over 50 independent replications. For both the frequency and cardinality estimation problems, the NGGP smoothing usually provides better estimates, with the notable exception of  $J = 10,000$  and data generated from a Pitman-Yor process with parameters  $(100, 0.75)$ , where the DP smoothing has a lower MAE for the frequency estimation problem and absolute error for the cardinality estimation problem.

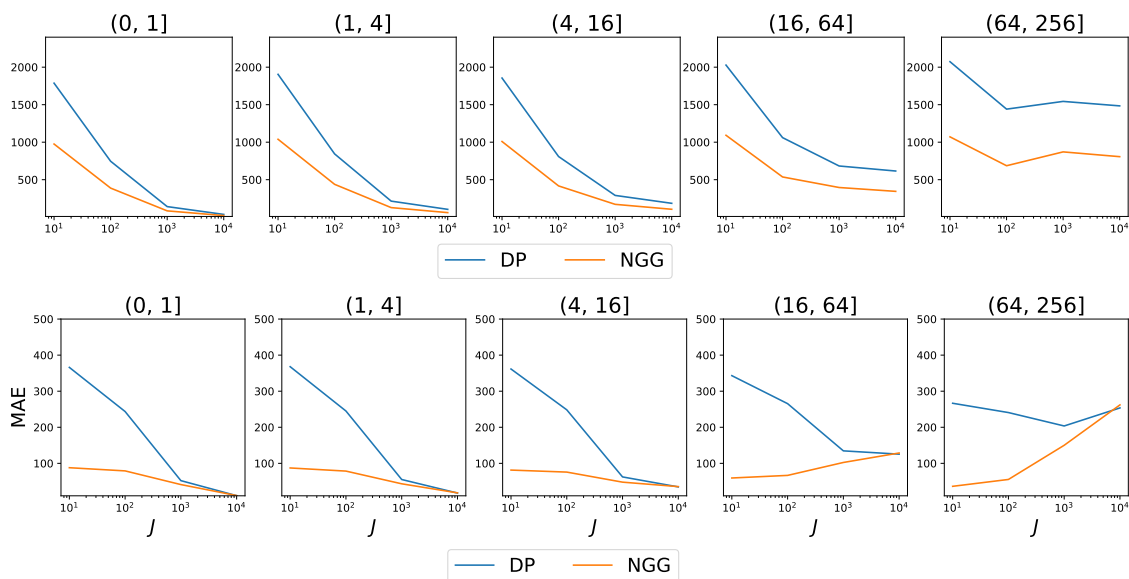


Figure 10: MAEs for the frequency estimators with DP and NGG smoothing. Data generated from a Pitman-Yor process with parameters  $(100, 0.25)$  (top row) and  $(100, 0.75)$  (bottom row). The width of the hash  $J$  varies across the  $x$ -axis.

## F.2 Further Tables and Plots

$\theta$	$\alpha$	Model	(0, 1]	(1, 4]	(4, 16]	(16, 64]	(64, 256]	(256, Inf]
1	0.00	DP	24.85	4.46	6.95	0.32	10.60	111.91
1	0.00	NGG	17.97	3.50	4.40	8.46	35.84	4644.27
1	0.25	DP	103.12	141.27	400.13	853.32	1749.00	1746.67
1	0.25	NGG	58.87	74.15	216.87	478.36	907.83	4225.67
1	0.50	DP	550.62	536.02	619.38	990.39	1402.58	2724.20
1	0.50	NGG	294.82	287.98	325.94	510.39	690.28	3418.29
1	0.75	DP	507.53	512.51	541.02	669.31	849.22	2111.93
1	0.75	NGG	240.19	242.07	270.94	306.70	375.30	1631.42
10	0.00	DP	45.61	198.41	915.70	2828.01	4471.81	9842.68
10	0.00	NGG	23.00	100.83	467.43	1439.54	2231.31	5096.32
10	0.25	DP	497.14	882.69	902.39	1282.83	3177.91	7977.46
10	0.25	NGG	259.17	459.68	466.99	653.48	1607.32	3921.58
10	0.50	DP	599.22	626.34	724.14	994.69	1758.74	4236.60
10	0.50	NGG	359.08	372.31	427.47	567.20	1003.07	2444.15
10	0.75	DP	458.63	468.30	486.77	643.85	860.62	1431.65
10	0.75	NGG	207.78	216.11	228.90	280.41	353.82	825.32
100	0.00	DP	746.32	821.35	1042.69	1479.36	2587.94	4133.92
100	0.00	NGG	378.60	409.30	518.76	729.82	1246.50	1807.36
100	0.25	DP	607.72	634.07	718.03	1043.62	1612.92	2528.17
100	0.25	NGG	317.57	332.77	374.05	535.96	802.53	1112.01
100	0.50	DP	453.52	459.22	514.10	637.53	900.43	1299.67
100	0.50	NGG	219.62	225.15	250.25	297.07	389.18	442.91
100	0.75	DP	243.98	248.98	253.64	285.24	305.41	285.03
100	0.75	NGG	79.33	79.10	77.36	70.62	69.61	326.54
1000	0.00	DP	291.86	296.77	315.70	352.96	411.05	312.08
1000	0.00	NGG	100.93	101.93	104.21	106.81	95.60	138.32
1000	0.25	DP	199.55	200.98	204.88	218.42	202.47	109.08
1000	0.25	NGG	83.90	83.46	81.73	75.22	52.85	169.91
1000	0.50	DP	110.68	110.57	108.81	96.99	59.97	131.87
1000	0.50	NGG	66.85	65.94	61.48	47.25	36.83	204.19
1000	0.75	DP	43.18	41.91	37.18	20.56	48.94	247.70
1000	0.75	NGG	53.69	52.59	48.07	30.42	40.62	201.60

Table 1: Mean Absolute Errors for the frequency recovery simulation setup in Section 6.2 for data generated from a PYP.

$\theta$	$\alpha$	Model	$n = 100$	$n = 1,000$	$n = 10,000$	$n = 10,0000$
1.00	0.00	DP	1.07	0.97	0.86	1.84
1.00	0.00	NGG	0.96	28.61	80.25	43.36
1.00	0.25	DP	2.47	17.01	35.29	67.68
1.00	0.25	NGG	2.19	20.72	189.59	610.90
1.00	0.50	DP	12.12	43.50	160.44	506.53
1.00	0.50	NGG	2.79	22.26	60.13	348.61
1.00	0.75	DP	38.78	263.71	1433.17	9158.79
1.00	0.75	NGG	28.46	249.30	1204.08	6608.67
10	0.00	DP	13.06	33.21	56.90	75.58
10	0.00	NGG	11.56	7.87	184.96	798.94
10	0.25	DP	27.71	83.23	185.06	349.92
10	0.25	NGG	28.05	71.80	89.69	908.58
10	0.50	DP	27.64	130.49	445.35	1392.30
10	0.50	NGG	24.96	115.52	165.33	264.86
10	0.75	DP	52.26	346.10	1847.56	12044.61
10	0.75	NGG	51.86	330.95	1645.83	8337.21
100	0.00	DP	58.00	215.85	408.23	623.73
100	0.00	NGG	59.20	192.26	161.97	1280.29
100	0.25	DP	65.52	290.13	783.18	1564.87
100	0.25	NGG	60.32	273.48	455.92	565.01
100	0.50	DP	69.44	415.64	1456.00	5638.79
100	0.50	NGG	70.75	393.27	1105.10	1970.70
100	0.75	DP	79.37	589.92	3210.12	21654.22
100	0.75	NGG	80.19	575.14	3049.16	16436.74
1000	0.00	DP	84.46	609.12	1642.72	3144.14
1000	0.00	NGG	87.86	588.69	1273.71	1285.24
1000	0.25	DP	82.48	665.54	2215.45	6546.01
1000	0.25	NGG	85.82	652.16	2137.90	1894.59
1000	0.50	DP	84.28	726.75	2997.70	14396.68
1000	0.50	NGG	87.34	711.04	3428.72	9739.97
1000	0.75	DP	84.91	803.67	3969.91	32892.45
1000	0.75	NGG	88.58	790.90	5456.84	30052.63

Table 2: Mean Absolute Errors for the cardinality recovery simulation setup in Section 6.2 for data generated from a PYP.

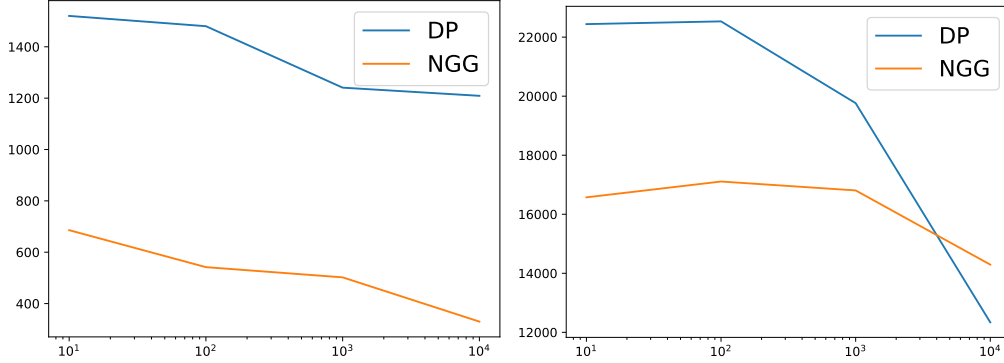


Figure 11: Absolute difference between the true number of distinct symbols and estimated cardinality. Data generated from a Pitman-Yor process with parameters  $(100, 0.25)$  (left plot) and  $(100, 0.75)$  (right plot). The width of the hash  $J$  varies across the  $x$ -axis.

Params	Model	100	1000	10000	100000
1.30	DP	36.14	244.64	1377.48	9203.69
1.30	NGG	NaN	236.01	1193.71	6623.06
1.60	DP	16.81	90.53	404.33	1645.03
1.60	NGG	NaN	55.57	141.33	295.76
1.90	DP	7.49	40.03	152.04	540.63
1.90	NGG	4.34	5.68	87.70	455.90
2.20	DP	3.34	20.99	71.63	224.75
2.20	NGG	3.96	15.86	133.26	553.39

Table 3: Mean Absolute Errors for the frequency recovery simulation setup in Section 6.2 for data generated from a Zipf distribution.



$\theta$	$\alpha$	J	Model	Rule	(0, 1]	(1, 4]	(4, 16]	(16, 64]	(64, 256]	(256, Inf]
10	0.25	50	CMS	CMS	41.25	97.07	343.96	1084.00	3320.19	14995.98
10	0.25	50	DP	MIN	18.67	43.76	129.42	387.30	1001.78	4944.18
10	0.25	50	DP	PoE	41.25	97.07	343.93	1083.98	3320.18	14995.98
10	0.25	50	NGG	MIN	0.88	2.37	14.11	56.02	202.01	3096.35
10	0.25	50	NGG	PoE	1.00	2.69	8.96	34.12	131.95	3664.00
10	0.75	50	CMS	CMS	1125.10	1135.56	1194.35	1527.37	2204.00	4882.84
10	0.75	50	DP	MIN	92.51	91.44	88.56	81.05	62.34	1074.53
10	0.75	50	DP	PoE	288.11	288.47	293.61	326.79	351.62	863.49
10	0.75	50	NGG	MIN	2.37	1.08	4.71	27.41	117.34	1364.42
10	0.75	50	NGG	PoE	1.00	2.53	8.23	31.20	121.97	1373.37
100	0.25	50	CMS	CMS	153.94	189.50	348.62	913.50	2194.03	5819.76
100	0.25	50	DP	MIN	42.96	47.17	64.57	113.54	170.26	572.81
100	0.25	50	DP	PoE	117.72	151.72	293.01	847.90	2064.75	5675.91
100	0.25	50	NGG	MIN	4.66	3.59	4.37	21.03	114.48	1024.91
100	0.25	50	NGG	PoE	1.00	2.70	8.91	33.19	133.37	1047.04
100	0.75	50	CMS	CMS	2283.32	2289.58	2332.17	2449.43	2843.48	3989.37
100	0.75	50	DP	MIN	46.13	44.77	39.63	20.12	66.97	666.53
100	0.75	50	DP	PoE	59.71	58.40	53.39	32.62	53.26	642.00
100	0.75	50	NGG	MIN	1.72	0.71	5.42	28.42	119.23	750.57
100	0.75	50	NGG	PoE	0.98	2.51	8.15	31.11	120.75	751.21
1000	0.25	50	CMS	CMS	2292.69	2299.25	2332.03	2463.42	2810.58	3373.22
1000	0.25	50	DP	MIN	29.56	27.96	22.06	10.86	87.93	370.95
1000	0.25	50	DP	PoE	34.40	32.82	26.96	12.19	81.95	364.12
1000	0.25	50	NGG	MIN	2.78	1.21	5.08	29.05	119.90	407.21
1000	0.25	50	NGG	PoE	1.00	2.69	8.84	33.00	124.25	412.00
1000	0.75	50	CMS	CMS	3794.05	3796.95	3804.92	3839.25	3947.88	4119.45
1000	0.75	50	DP	MIN	4.88	3.35	2.74	24.88	108.61	378.49
1000	0.75	50	DP	PoE	5.04	3.51	2.68	24.70	108.43	378.32
1000	0.75	50	NGG	MIN	0.72	0.82	6.47	29.03	112.81	383.24
1000	0.75	50	NGG	PoE	0.56	1.11	6.79	29.30	113.44	384.03

Table 4: Mean Absolute Errors for the frequency recovery simulation setup in Section 6.3 for data generated from a PYP,  $J = 50$ ,  $M = 20$

$\theta$	$\alpha$	$J$	Model	Rule	(0, 1]	(1, 4]	(4, 16]	(16, 64]	(64, 256]	(256, Inf]
10	0.25	100	CMS	CMS	41.25	97.07	343.96	1084.00	3320.19	14995.98
10	0.25	100	DP	MIN	29.61	67.93	230.57	723.42	2106.58	9701.60
10	0.25	100	DP	PoE	41.25	97.07	343.94	1084.00	3320.19	14995.98
10	0.25	100	NGG	MIN	1.65	4.26	28.21	132.02	365.16	2957.30
10	0.25	100	NGG	PoE	0.98	2.64	8.87	34.07	131.93	3663.73
10	0.75	100	CMS	CMS	526.18	533.93	596.90	914.96	1588.13	4144.42
10	0.75	100	DP	MIN	94.84	95.10	97.49	110.57	128.34	890.61
10	0.75	100	DP	PoE	300.24	304.49	341.90	535.87	925.71	2605.57
10	0.75	100	NGG	MIN	6.31	4.91	3.06	22.41	108.97	1351.34
10	0.75	100	NGG	PoE	0.95	2.47	8.14	31.15	121.71	1372.77
100	0.25	100	CMS	CMS	78.71	122.22	272.32	846.90	2110.25	5733.33
100	0.25	100	DP	MIN	30.92	42.51	82.06	213.45	444.65	884.52
100	0.25	100	DP	PoE	69.51	114.89	260.00	832.20	2084.65	5708.11
100	0.25	100	NGG	MIN	4.95	5.60	9.07	20.30	80.13	989.03
100	0.25	100	NGG	PoE	1.00	2.69	8.90	33.10	132.93	1047.06
100	0.75	100	CMS	CMS	1066.41	1070.32	1113.86	1237.86	1663.12	2822.22
100	0.75	100	DP	MIN	65.74	64.68	60.93	44.66	49.33	582.24
100	0.75	100	DP	PoE	97.97	97.15	94.41	81.48	51.73	509.93
100	0.75	100	NGG	MIN	4.98	3.49	2.93	24.93	114.06	740.63
100	0.75	100	NGG	PoE	0.65	1.80	6.90	30.13	120.91	753.23
1000	0.25	100	CMS	CMS	1010.65	1019.68	1058.87	1188.68	1567.41	2121.59
1000	0.25	100	DP	MIN	51.33	50.03	45.27	27.36	55.54	315.90
1000	0.25	100	DP	PoE	67.91	66.75	62.44	44.85	44.24	285.51
1000	0.25	100	NGG	MIN	7.58	5.95	3.10	23.10	111.75	396.16
1000	0.25	100	NGG	PoE	0.51	2.12	8.28	32.41	123.41	412.46
1000	0.75	100	CMS	CMS	1823.27	1825.91	1836.01	1868.75	1980.42	2143.21
1000	0.75	100	DP	MIN	10.34	8.83	4.05	19.23	102.13	370.61
1000	0.75	100	DP	PoE	10.89	9.37	4.42	18.66	101.46	369.95
1000	0.75	100	NGG	MIN	2.77	1.32	4.32	26.75	110.44	379.83
1000	0.75	100	NGG	PoE	1.76	0.73	5.41	27.90	111.53	380.32

Table 5: Mean Absolute Errors for the frequency recovery simulation setup in Section 6.3 for data generated from a PYP,  $J = 100$ ,  $M = 10$

$\theta$	$\alpha$	$J$	Model	Rule	(0, 1]	(1, 4]	(4, 16]	(16, 64]	(64, 256]	(256, Inf]
10	0.25	500	CMS	CMS	43.00	117.64	343.96	1084.00	3323.03	14995.98
10	0.25	500	DP	MIN	42.01	115.40	336.56	1062.52	3252.49	14706.44
10	0.25	500	DP	PoE	42.97	117.29	343.85	1083.06	3318.38	14995.29
10	0.25	500	NGG	MIN	12.56	34.93	72.10	197.38	382.21	2904.90
10	0.25	500	NGG	PoE	18.99	41.73	121.37	397.09	1177.96	5152.19
10	0.75	500	CMS	CMS	134.73	149.39	209.36	467.40	1221.68	3662.94
10	0.75	500	DP	MIN	73.30	80.06	104.81	217.93	552.55	1601.72
10	0.75	500	DP	PoE	91.74	102.16	142.72	332.15	914.40	2548.65
10	0.75	500	NGG	MIN	27.88	28.37	28.18	31.67	60.22	1291.65
10	0.75	500	NGG	PoE	23.91	23.39	22.14	24.53	58.23	1297.18
100	0.25	500	CMS	CMS	76.44	128.68	284.09	848.81	2085.51	5917.28
100	0.25	500	DP	MIN	57.82	97.25	209.62	623.53	1497.13	4094.27
100	0.25	500	DP	PoE	69.36	119.48	263.75	796.70	1991.72	5668.14
100	0.25	500	NGG	MIN	17.45	30.75	65.36	150.61	231.42	656.71
100	0.25	500	NGG	PoE	12.61	24.48	60.86	165.16	305.86	839.24
100	0.75	500	CMS	CMS	241.70	250.10	288.88	408.93	834.15	1983.84
100	0.75	500	DP	MIN	86.31	88.46	96.26	117.89	200.68	431.21
100	0.75	500	DP	PoE	105.62	109.40	121.73	158.32	292.72	564.81
100	0.75	500	NGG	MIN	27.46	26.62	22.96	16.65	71.01	698.03
100	0.75	500	NGG	PoE	23.95	22.96	19.27	15.21	69.13	686.43
1000	0.25	500	CMS	CMS	241.18	251.64	287.85	410.50	786.62	1336.97
1000	0.25	500	DP	MIN	88.68	91.06	98.22	123.28	200.41	225.23
1000	0.25	500	DP	PoE	107.09	110.62	122.70	163.23	284.70	385.02
1000	0.25	500	NGG	MIN	36.12	35.03	32.41	25.51	62.97	339.46
1000	0.25	500	NGG	PoE	33.08	32.34	28.43	21.29	60.65	336.40
1000	0.75	500	CMS	CMS	380.79	384.24	394.12	429.86	533.79	700.14
1000	0.75	500	DP	MIN	36.51	35.31	30.98	18.00	58.01	284.73
1000	0.75	500	DP	PoE	39.57	38.41	34.21	20.52	54.63	276.94
1000	0.75	500	NGG	MIN	19.84	18.61	13.55	11.70	81.73	333.80
1000	0.75	500	NGG	PoE	19.83	18.47	13.56	11.60	82.21	334.98

Table 6: Mean Absolute Errors for the frequency recovery simulation setup in Section 6.3 for data generated from a PYP,  $J = 500$ ,  $M = 2$

$\theta$	$\alpha$	J	Model	Rule	(0, 1]	(1, 4]	(4, 16]	(16, 64]	(64, 256]	(256, Inf]
10	0.25	1000	CMS	CMS	59.45	162.45	411.85	1130.47	4056.87	15035.28
10	0.25	1000	DP	MIN	59.11	161.54	409.40	1124.58	4036.21	14960.60
10	0.25	1000	DP	PoE	59.11	161.54	409.40	1124.58	4036.21	14960.60
10	0.25	1000	NGG	MIN	25.89	51.16	102.85	248.94	367.17	3041.74
10	0.25	1000	NGG	PoE	29.20	79.56	201.12	598.89	2086.05	7815.07
10	0.75	1000	CMS	CMS	256.98	259.38	341.71	570.53	1342.74	3710.03
10	0.75	1000	DP	MIN	168.66	165.42	219.89	360.93	882.13	2259.36
10	0.75	1000	DP	PoE	168.66	165.42	219.89	360.93	882.13	2259.36
10	0.75	1000	NGG	MIN	43.88	45.46	52.77	67.10	89.61	1229.09
10	0.75	1000	NGG	PoE	57.51	59.91	75.62	109.00	190.46	1023.42
100	0.25	1000	CMS	CMS	290.03	356.20	449.22	1074.69	2296.12	6206.38
100	0.25	1000	DP	MIN	254.66	311.50	392.33	932.73	1995.06	5383.13
100	0.25	1000	DP	PoE	254.66	311.50	392.33	932.73	1995.06	5383.13
100	0.25	1000	NGG	MIN	49.61	62.68	105.96	218.71	291.27	636.25
100	0.25	1000	NGG	PoE	153.42	182.34	231.03	520.43	1139.86	2548.97
100	0.75	1000	CMS	CMS	257.30	268.57	303.72	445.60	837.18	1967.26
100	0.75	1000	DP	MIN	131.45	135.05	151.14	210.71	372.15	699.64
100	0.75	1000	DP	PoE	131.45	135.05	151.14	210.71	372.15	699.64
100	0.75	1000	NGG	MIN	43.88	44.33	42.68	41.78	67.05	665.09
100	0.75	1000	NGG	PoE	48.03	48.57	48.45	49.38	60.60	596.49
1000	0.25	1000	CMS	CMS	255.72	264.14	299.17	429.16	796.21	1359.63
1000	0.25	1000	DP	MIN	139.89	144.02	161.81	220.43	394.43	586.98
1000	0.25	1000	DP	PoE	139.89	144.02	161.81	220.43	394.43	586.98
1000	0.25	1000	NGG	MIN	57.35	56.84	56.09	58.93	73.57	292.81
1000	0.25	1000	NGG	PoE	66.98	68.09	69.05	80.35	99.14	164.05
1000	0.75	1000	CMS	CMS	251.84	255.06	263.49	302.97	405.16	576.01
1000	0.75	1000	DP	MIN	55.26	54.67	51.81	44.84	52.95	178.27
1000	0.75	1000	DP	PoE	55.26	54.67	51.81	44.84	52.95	178.27
1000	0.75	1000	NGG	MIN	39.16	38.57	34.60	25.54	50.92	269.60
1000	0.75	1000	NGG	PoE	39.36	38.79	34.99	26.26	50.79	256.25

Table 7: Mean Absolute Errors for the frequency recovery simulation setup in Section 6.3 for data generated from a PYP,  $J = 1000$ ,  $M = 1$